Lehrstuhl für Genetik der
Technischen Universität München

The cellular polarity of ENHANCER OF PINOID: underlying factors and its role in the organogenesis of *Arabidopsis thaliana*

Michaela Matthes

Vollständiger Abdruck der von der Fakultät Wissenschaftszentrum Weihenstephan für Ernährung, Landnutzung und Umwelt der Technischen Universität München zur Erlangung des akademischen Grades eines

Doktors der Naturwissenschaften

genehmigten Dissertation.

Vorsitzender: Univ.- Prof. Dr. A. Gierl

Prüfer der Dissertation:

1. apl. Prof. Dr. R. A. Torres Ruiz
2. Univ.- Prof. Dr. E. Grill
3. Univ.- Prof. Dr. B. Poppenberger- Sieberer

Die Dissertation wurde am 30.9.13 bei der Technischen Universität München eingereicht und durch die Fakultät Wissenschaftszentrum Weihenstephan für Ernährung, Landnutzung und Umwelt am 29.11.13 angenommen.

Contents

Abbreviations v

Zusammenfassung 3

1 Introduction 5

1.1 Cell polarity in *Arabidopsis thaliana* . . . 5
1.2 Auxin . . . 6
1.2.1 Auxin signaling cascade . . . 6
1.2.2 Polar auxin transport (PAT) . . . 7
1.3 Auxin in embryogenesis . . . 9
1.4 The interplay of PID, PIN1 and ENP in cotyledon and flower organogenesis . . . 12
1.5 Aims of the work . . . 13

2 Material and Methods 15

2.1 Material . . . 15
2.1.1 Antibiotics and herbicides . . . 15
2.1.2 Plant material . . . 15
2.1.2.1 Wild type and mutant lines . . . 15
2.1.2.2 Transgenic lines . . . 15
2.1.2.3 Crossings . . . 16
2.1.3 Chemicals . . . 16
2.1.3.1 Chemicals for the pharmacological studies . . . 18
2.1.3.2 Chemicals for silique application . . . 18
2.1.4 Size markers . . . 18
2.1.5 Bacterial strains . . . 19
2.1.6 *S.cerevisiae* strains . . . 19
2.1.7 Primers . . . 20
2.1.8 Devices . . . 23
2.1.9 Software and databases . . . 24
2.1.10 Standard vectors . . . 24
2.1.11 *S.cerevisiae* control vectors . . . 25
2.1.12 Other materials and enzymes . . . 25
2.1.13 Media . . . 26
2.2 Methods . . . 27
2.2.1 Plant work . . . 27
2.2.1.1 Seed sterilization . . . 27
2.2.1.2 Growing of plants on soil . . . 27
2.2.1.3 Crossings . . . 27
2.2.1.4 Rescue experiments . . . 28

2.2.2 Molecular methods . . . 28
2.2.2.1 Preparation of competent *E.coli* cells . . . 29
2.2.2.2 Preparation of electrocompetent *A.tumefaciens* cells . . . 29
2.2.2.3 Isolation of DNA . . . 29
2.2.2.4 Isolation of total RNA . . . 29
2.2.2.5 Reverse transcription . . . 30
2.2.2.6 Polymerase chain reaction (PCR) . . . 30
2.2.2.7 Agarose gel electrophoresis . . . 32
2.2.2.8 Purification of DNA fragments . . . 32
2.2.2.9 Sequencing . . . 32
2.2.2.10 Gateway® cloning . . . 32
2.2.2.10.1 BP reaction . . . 32
2.2.2.10.2 LR reaction . . . 33
2.2.2.11 Transformation of plasmids into *E.coli* . . . 33
2.2.2.12 Electroporation of plasmids into *A. tumefaciens* . . . 34
2.2.2.13 Small scale transformation of plasmids into *S.cerevisiae* . . . 34
2.2.2.14 Plasmid mini- and midi preparation from *E.coli* . . . 34
2.2.2.15 Plasmid mini preparation from *A.tumefaciens* . . . 35
2.2.2.16 Plant transformation (floral dip) . . . 36
2.2.3 Yeast two-hybrid screening . . . 36
2.2.3.1 Primary screening . . . 37
2.2.3.1.1 Mating . . . 37
2.2.3.1.2 Replica plating . . . 37
2.2.3.1.3 Replica cleaning . . . 37
2.2.3.1.4 Primary positives . . . 37
2.2.3.2 Phenotyping . . . 38
2.2.3.2.1 Replica plating and cleaning . . . 38
2.2.3.2.2 Scoring . . . 38
2.2.3.2.3 Yeast lysis . . . 38
2.2.3.2.4 Yeast lysate PCR . . . 39
2.2.3.3 Verification . . . 39
2.2.4 Direct interaction testing with the ProQuest™ system (Gateway®) . . . 40
2.2.4.1 *HIS3* reporter activity . . . 41
2.2.4.2 *URA3* reporter activity . . . 41
2.2.4.3 *LacZ* reporter activity . . . 41
2.2.5 Transcriptomics . . . 42
2.2.5.1 Seed sterilization . . . 42
2.2.5.2 Total RNA isolation from seedlings . . . 42
2.2.5.3 Determination of the RNA quantity and quality . . . 42
2.2.5.4 Preparation of a labeling reaction . . . 42

2.2.5.5 cDNA synthesis . . . 43
2.2.5.6 cRNA synthesis . . . 43
2.2.5.7 Purification of the labeled amplified cRNA . . . 44
2.2.5.8 Determination of yield and specific activity of the labeling reaction . . . 44
2.2.5.9 Fragmentation and hybridization . . . 44
2.2.5.10 Washing . . . 44
2.2.5.11 Scan . . . 45
2.2.5.12 Data evaluation . . . 45
2.2.5.13 GO enrichment analysis . . . 45
2.2.5.14 Pathway mapping analysis . . . 45
2.2.5.15 Common transcription factor binding sites . . . 45
2.2.6 Confocal laser scanning microscopy . . . 46
2.2.7 Pharmacological studies . . . 46
2.2.8 Chemical treatment of siliques . . . 47

3 Results 48
3.1 Intrinsic and extrinsic factors controlling the cellular polarity of ENP . . . 48
3.1.1 Extrinsic factors . . . 48
3.1.1.1 The subcellular trafficking of ENP is actin dependent . . . 49
3.1.1.2 Tissue specific factors . . . 51
3.1.2 Intrinsic factors . . . 52
3.1.2.1 Analysis of deletion constructs . . . 53
3.1.2.2 Analysis of domain swap constructs . . . 54
3.1.2.3 Analysis of point mutation constructs . . . 55
3.1.3 Separation of full functionality and polarity . . . 58
3.1.3.1 Analysis of the deletion constructs . . . 59
3.1.3.2 Analysis of the domain swap constructs . . . 60
3.1.3.3 Analysis of point mutation constructs . . . 61
3.2 Global and targeted yeast two-hybrid screens to uncover ENP interactors . . . 63
3.3 The analysis of the cellular polarity of ENP and PIN1 in *rpk1-7* . . . 67
3.4 Transcriptomics of cotyledon-less seedlings . . . 69
3.5 The effect of boronic acids in signaling studies of different membrane proteins and in *in vivo* studies . . . 77
3.5.1 Phenylboronic acid (PBA) treatment of roots . . . 77
3.5.2 *In vivo* studies . . . 79
3.5.2.1 Application of PBA onto siliques causes *mp*-like seedling phenocopies . . . 79
3.5.3 Comparative analysis between *mp*, *bdl* and *mp*-like phenocopies . . . 85
3.5.3.1 Analysis of PBA effects in early embryogenesis . . . 85

3.5.3.2 Expresssion analysis of *TARGET OF MONOPTEROS* genes in *mp*, *bdl* and *mp*-like phenocopies 87
3.5.3.3 Analysis of auxin maxima in *mp*-like phenocopies 87

4 Discussion **89**
4.1 ENP's localization is dependent on extrinsic and intrinsic factors 89
4.1.1 Tissue specific factors determine an apical or basal localization of ENP 89
4.1.2 The subcellular targeting of ENP is actin, but not BFA dependent . . . 90
4.1.3 Intrinsic factors determine a lateral extension of ENP's localization . . 91
4.2 ENP's function can be separated from its polar localization 92
4.3 ENP is a potential target for phosphorylation 93
4.3.1 Functional importance of Y409 93
4.3.2 ENP might be substrate of AGCVIII kinases other than PID 94
4.3.3 ENP might be linked to a PDK1 associated signaling cascade 95
4.4 The function of ENP with respect to its BTB POZ domain 96
4.5 PIN1 polarity changes in *rpk1* are different to those in *pid enp* 98
4.6 Transcriptomics of cotyledon-less seedlings 100
4.7 Boronic acids in signaling studies 102

5 References **106**

Acknowledgements **120**

Appendix **121**

Abbreviations

Apart from those listed below, the abbreviations used throughout this thesis follow the recommendations of the IUPAC-IUB Joint Commission on Biochemical Nomenclature as outlined in the Biochemical Journal (1992), 281, 1-19

3-AT	3-aminotriazole
2,4-D	2,4-dichlorophenoxy acetic acid
5-FOA	5-fluoroorotic acid
ABA	abscisic acid
ABP1	AUXIN BINDING PROTEIN1
AFB	AUXIN SIGNALING F-BOX
AGCVIII	cAMP-dependent kinase, cGMP-dependent kinase, phospholipid-dependent protein kinase C
ARF	AUXIN RESPONSE FACTOR
ARF- GEF	guanine-nucleotide exchange factor for ADP-ribosylation factor-type G proteins
A.thaliana	*Arabidopsis thaliana*
A.tumefaciens	*Agrobacterium tumefaciens*
AUX1	AUXIN RESISTANT1
Aux/IAA	AUXIN/INDOLE-3-ACETIC ACID
BDL	BODENLOS
BES	benzoic acid
BFA	brefeldin A
bHLH	basic helix-loop-helix
CHX	cycloheximide
CLSM	confocal laser scanning microscope
CK	cytokinin
Cm	chloramphenicol
Col-0	Columbia-0
CTAB	Cetyl trimethylammonium bromide
CUC	CUP SHAPED COTYLEDON
cytD	cytochalasin D
dd	double distilled
DPb	DIMERIZATION PARTNERS OF E2Fs b
DTT	dithiothreitol

E.coli	*Escherichia coli*
E.hyemalis	*Eranthis hyemalis*
ENP	ENHANCER OF PINOID
FC	fold change
GA	gibberellin
GEF	GUANINE NUCLEOTIDE EXCHANGE FACTOR
Gen	gentamycin
GFP	green fluorescent protein
GO	Gene Ontology
GPI	glycosylphosphatidylinositol
GUS	β-glucoronidase
IAA	indole-3-acetic acid
KNOX	class I KNOTTED-like homeobox
lat	*laterne*
LAX	LIKE AUX1
L*er*	Landsberg *erecta*
MAB	MACCHI-BOU
MDR/PGP	MULTIDRUG RESISTANCE/P-GLYCOPROTEIN
MEL	MAB4/ENP/NPY1-like
MIPS	D- *MYO*-INOSITOL-3-PHOSPHATE SYNTHASE
MP	MONOPTEROS
mQ	milli-Q
NAA	naphthalene-1-acetic acid
NASC	Nottingham *Arabidopsis* Stock Center
NOA	1-naphtoxy-acetic acid
NPA	naphtylphtalamic acid
NPH3	NONPHOTOTROPIC HYPOCOTYL3
NPY	NAKED PINS IN YUC MUTANTS
OD	optical density
ORF	open reading frame
PAA	phenylacetic acid
PAT	polar auxin transport
PBA	phenylboronic acid
PCR	polymerase chain reaction
PDR	PLEIOTROPIC DRUG RESISTANCE

PID	PINOID
PIN	PIN-FORMED
PINHL	PIN hydrophilic loop
PM	plasma membrane
PO	Plant Ontology
PP2A	PROTEIN PHOSPHATASE 2A
QC	quiescent center
RAM	root apical meristem
RIC	ROP Interactive CRIP motif- containing proteins
RNase A	ribonuclease A
ROP	RHO GTPases OF PLANTS
RPK1	RECEPTOR-LIKE PROTEIN KINASE1
RT	room temperature
RT-PCR	reverse transcription-polymerase chain reaction
S.cerevisiae	*Saccharomyces cerevisiae*
SAM	shoot apical meristem
SC	synthetic complete
SCF	SKP-CULLIN-F-BOX PROTEIN
SDS	sodiumdodecylsulfate
SKP1	S-PHASE KINASE ASSOCIATED PROTEIN 1
STM	SHOOTMERISTEMLESS
TAIR	The *Arabidopsis* Information Resource
Taq- polymerase	*Thermus aquaticus* DNA polymerase
TIBA	triiodobenzoic acid
TIR1	TRANSPORT INHIBITOR RESPONSE1
TMO	TARGET OF MONOPTEROS
TOAD2	TOADSTOOL2
WRKY	WRKY DNA-BINDING PROTEIN
WUS	WUSCHEL homeobox protein
X-gal	5-bromo-4-chloro-3-indolyl-β-D-galactopyranoside
Y2H	yeast two-hybrid
YFP	yellow fluorescent protein

Summary

Cellular polarity is a pivotal feature for pattern formation and morphogenesis of *Arabidopsis thaliana*. Polarity is particularly important for auxin mediated patterning processes, since auxin has to be directionally transported. This active transport system generates gradients, eventually resulting in auxin maxima and minima, which are tissue and cell specifically translated into appropriate responses. In embryogenesis and in the shoot, the auxin transport is mainly guided through the cellular localization of the auxin efflux carrier PINFORMED1 (PIN1). It was shown to be localized at the apical site of the plasma membrane (PM) in the embryonic and shoot epidermis, leading to an auxin flux in direction of incipient primordia and the shoot meristem. In the vascular system PIN1 is localized at the basal site leading to a root-tip directed auxin flux necessary for the functioning of the root meristem.

The disturbance or abolishment of the cellular localization of PIN1 leads to severe phenotypes. One of them is the *laterne* phenotype, which is characterized by the complete loss of cotyledons and flowers due to the complete reversal of the apical PIN1 polarity in the epidermis. Molecular analysis had shown that *laterne* is caused by simultaneous mutations in the serine/threonine kinase *PINOID* (*PID*) gene and in the NPH3-like *ENHANCER OF PINOID* (*ENP*) gene. This revealed a synergistic effect of ENP and PID on the localization of PIN1.

It was shown that ENP colocalizes with PIN1 at the apical site of the PM in the epidermis of cotyledons and the question arose how the polarization of ENP is achieved. A main task of this work therefore was to analyse several deletion, point mutation and domain swap constructs. This revealed that ENP necessitates N-terminal regions for its localization at the apical site of the PM, whereas C-terminal regions seem to account for a lateral diffusion in the membrane. Further the study pointed at the importance of a specific tyrosine residue, whose phosphorylation status might be required for the subcellular localization of ENP. Additional rescue experiments revealed functionally important sites and domains of ENP.

The subcellular trafficking of ENP was studied with pharmacological approaches and it could be shown that ENP primarily needs intact actin filaments for its polar targeting to the PM and furthermore that ENP localization is independent from PIN1.

A global yeast two-hybrid screen detected novel interaction partners of ENP. Among them was the GTP cyclohydrolase1, whose interaction with ENP displayed auxin sensitivity and the AGC kinase PDK1, which is known to phosphorylate PID. This finding provides the first potential molecular connection in the ENP/PID/PIN1 chain.

Consequences of the loss of PIN1 polarity in the *laterne* mutant were assessed on the transcriptome level by doing a comparative microarray analysis with wild type and cotyledon-less seedlings. The study showed, that whereas the wild type needs genes for the regulation of the leave identity, to control fatty acid biosynthesis and to manage photosynthesis, the *laterne* seedling is enriched in genes, that specify the abaxial and adaxial polarity axis, as well as those accounting for abscission. Further, when analyzing genes, that fell into a specific cluster of Gene Ontology terms, it appeared that they are commonly regulated by a specific set of

transcription factors. Strikingly, the regulation of hormonal pathways was different in the two seedling types. Whereas the wild type seedling was enriched in genes related to auxin, ABA, brassinosteroid, ethylene and cytokinin signaling, the *laterne* seedling was enriched in genes conferring to gibberellic acid and jasmonic acid signaling.
With respect to cellular localization the question arose, whether the cellular localization of PIN1 and ENP might be means, by which the plant is able to influence cotyledon number. Therefore the cellular localization of both proteins were analyzed in another unique cotyledon mutant, named *rpk1-7*, a mutation in the *RECEPTOR LIKE PROTEIN KINASE1*, which segregates a monocotyledonous phenotype. The analyses could show that the mutation alters cell divisions as well as PIN1 and ENP polarity. The defects are stochastic and depend on the time point and position of the lapse of *RPK1* function.
As a spin-off project the pharmacological experiments were extended. This work showed that boronic acids can be used in signaling studies to effectively challenge the localization and stability of membrane and membrane associated proteins. This hints at a possible role of boron in the PM architecture and therefore at a potential contribution of boron in early signaling processes in embryo- and organogenesis.

Zusammenfassung

Zellpolarität spielt bei der Musterbildung und Morphogenese von *Arabidopsis thaliana* eine entscheidende Rolle, vor allem bei Auxin-vermittelten Prozessen, die of durch gerichteten Auxintransport gekennzeichnet sind. Der aktive Transport des Phytohormons erzeugt Gradienten, die zu lokalen Maxima und Minima führen. Diese wiederum werden von der Pflanze gewebe- und zellspezifisch in entsprechende Antworten umgesetzt. In der Embryogenese und im Spross wird der Auxinflux vor allem durch die polare Lokalisation des Auxineffluxtransporters PIN-FORMED1 (PIN1) gesteuert. Auf zellulärer Ebene weist PIN1 eine apikale bzw. ein basale Lokalisation an der Plasmamembran (PM) auf; erstere in Epidermiszellen im Embryo und im Spross; letztere in den vaskulären Elementen. Somit führt der Auxinfluss in Richtung der entstehenden Primordien und des Sprossmeristems bzw. in Richtung Wurzel.

Störungen der Lokalisation von PIN1 führen zu stark beschädigten Phänotypen. Ein besonders auffälliger Phänotyp ist *laterne*, eine Mutante, die den vollständigen Verlust der Keimblätter und der Blütenorgane aufweist. Die Deletion der Organe kann auf die vollständige Umkehr der apikalen Polarität von PIN1 im Embryo und im Spross zurückgeführt werden. Es zeigte sich, dass *laterne* eine Mutation im Gen der Serin/Threonin Kinase *PINOID (PID)*, sowie gleichzeitig eine Mutation im Gen des NPH3-ähnlichen Proteins *ENHANCER OF PINOID (ENP)* darstellt. Dies deutet auf einen synergistischen Effekt beider Proteine auf die polare Lokalisation von PIN1 hin.

ENP weist Kolokalisierung mit PIN1 auf und zwar an der apikalen Seite der PM in der Keimblattepidermis. Dies warf eine Kernfrage dieser Arbeit auf, nämlich wie ENP selbst polar lokalisiert wird. Die Analyse verschiedener Deletions-, Punktmutations- und Domänenaustauschkonstrukte zeigte, dass N-terminale Bereiche von ENP entscheidend für dessen Lokalisation an der apikalen Zellseite sind, wohingegen C-terminale Bereiche dessen laterale Diffusion in der Membran bedingen. Die Untersuchungen wiesen des Weiteren darauf hin, dass ein spezifischer phosphorilierbarer Tyrosinrest für die Lokalisation entscheidend ist. Rettungsexperimente zeigten zusätzlich die funktionale Wichtigkeit einzelner Domänen und Aminosäuren von ENP auf.

Mittels pharmakologischer Studien konnte gezeigt werden, dass der zelluläre Transport von ENP an die PM hauptsächlich stabile Aktinfilamente benötigt und dass die Lokalisation von ENP und PIN1 unabhängig ist.

Ein globaler Screen basierend auf dem Hefe-Zwei-Hybrid System lieferte neue mögliche Interaktionspartner von ENP. Einer war die GTP-Cylohydrolase1, deren Interaktion mit ENP Auxinsensitivität aufwies, ein anderer war die AGC kinase PDK1, von der bekannt ist, dass sie unter anderem PID phosphoryliert. Diese Befunde bringen neue Proteine ins Spiel und geben im Falle von PDK1 zum ersten mal einen möglichen molekularen Verbindungspunkt in der ENP/PID/PIN1 Kette an.

Mittels vergleichender Transkriptomanalysen von Wildtyp und *laterne* Keimlingen wurde der Frage nachgegangen, welche Konsequenzen der Polaritätsverlust von PIN1 mit sich bringt.

Diese differenzielle Analyse zeigte, dass in Keimblättern hauptsächlich Gene der Blattidentität, der Fettsäurebiosynthese und der Photosynthese reguliert werden. In *laterne*-Keimlingen werden Gene für abaxiale und adaxiale Polarität und Abszission angereichert. Promotoranalysen zeigten auf, dass Gene definierter Gene Ontology Kategorien von einem spezifischen Set an Transkriptionsfaktoren koreguliert werden könnten. Auffällig erschien zusätzlich die differenzielle Anreicherung von Genen unterschiedlicher Hormonprozesse. Im Wildtyp waren das hauptsächlich Gene für Auxin, Abszisinsäure, Brassinosteroide, Ethylen und Cytokinin; in *laterne* waren das Gene für Gibberellinsäure- und Jasmonsäure-relevante Prozesse.
Es stelle sich zudem die Frage, ob *Arabidopsis thaliana* mittels der zellulären Polarität von PIN1 und ENP eine Möglichlichkeit hat die Keimblattzahl zu beeinflussen. Darum wurde die Zellpolarität beider Proteine in einer weiteren Keimblattmutante, nämlich *rpk1-7*, untersucht. *rpk1-7* zeigt eine Mutation in der *RECEPTOR-LIKE PROTEIN KINASE1* (*RPK1*) auf und segregiert monokotyle Phänotypen. Die Analysen zeigten, dass die Mutante Zellteilungen und die Polarität von PIN1 und ENP verändert. Beide Defekte sind stochastisch und hängen ab vom Zeitpunkt und der Position der Fehlfunktion von *RPK1*.
Eine Ausweitung der pharmakologischen Experimente zeigte auf, dass Boronsäuren in der Untersuchung von Transportprozessen verwendet werden können, um Membran - und Membranassoziierte Proteine von der Membran zu lösen. Dies deutet zudem auf eine Funktion von Bor in endozytotischen Membranprozessen und/oder der Membranarchitektur hin. Dies impliziert, dass eine korrekte Bor-Homöostase der Zelle für Signalprozesse der Embryo- und Organogenese wichtig ist.

1 Introduction

1.1 Cell polarity in *Arabidopsis thaliana*

Cell polarity is a pivotal feature for the development, the growth and the morphogenesis of *Arabidopsis thaliana (A.thaliana)*. It can be referred to as the asymmetric distribution of cellular components along a particular axis. It is fundamental for processes like intercellular communication, cell division, cell morphogenesis and differentiation (Grebe et al., 2001). The nomenclature used for polarity domains in plants was suggested to follow the embryo-derived terminology of *A.thaliana* (Friml et al., 2006). This means on the longitudinal axis apical and basal, referring to the shoot and root apices respectively, as well as on the horizontal axis outer and inner, referring to epidermis and stele (Grebe, 2010). Polarization can be found at every step of the life cycle of *A.thaliana*. Apical/basal polarity can be found in the zygote (Lau et al., 2012 and references therein), is necessary for auxin mediated patterning processes (Berleth and Jürgens, 1993; Hardtke and Berleth, 1998; Hamann et al., 1999; Hamann et al., 2002; Dubrovsky et al., 2008; Benková et al., 2009; Tanaka et al., 2006), as well as for cell morphogenesis and cell division. The outer and inner polarity are important for the orientation of transporters involved in the exchange of nutrients between the root and the soil (Dettmer and Friml, 2011). Prominent examples are recently described transporters for boron, that are laterally localized (Dettmer and Friml., 2011). Boron is taken up by NIP1;5 and transported through the central vasculature by BOR1 (Takano et al., 2002; Takano et al., 2005; Takano et al., 2006; Takano et al., 2010). These transporters stress the significance of boron function, which was mainly associated to the cell wall, but various findings suggest a link to membrane function and signaling in embryogenesis as well (Robertson and Loughmann, 1974; Pollard et al., 1977; Tanada 1983; Goldbach, 1984; Jackson, 1989; Goldbach et al., 1990; Schon et al., 1990; Barr and Crane, 1991; Barr et al., 1993; Bennet et al., 1999; Lanoue et al., 2000). Clear cut proofs for these functions are nevertheless missing. Next to their importance in development specialized polar targeting pathways were shown to be important for pathogen defense (Dettmer and Friml, 2011).

Despite the ubiquity of polarity events little is known about the mechanisms involved in the establishment and maintenance of polar domains in plants. Thus far most insights come from the polar distribution of PIN- FORMED (PIN) proteins, which lead the auxin flux that in turn controls various aspects of plant development (Benková et al., 2003). Especially, the processes that establish and maintain PIN1 polarity are under intense investigation. After initial non-polar secretion PIN1 gets preferably localized to the basal site of the plasma membrane (PM) (Dhonukshe et al., 2008). For the targeting to the apical site PIN1 needs the antagonistic action of the kinase PINOID and the PROTEIN PHOSPHATASE 2A (PP2A) (Friml et al., 2004; Michniewicz et al., 2007). PID instructs PIN1 by phosphorylating the middle serine in three conserved TPRXS(N/S) motifs in its central hydrophilic loop (PINHL) (Huang et al., 2010; Dhonukshe et al., 2010). In order to target vesicles with non-phosphorylated PIN1 to the basal PM, the function of the Brefeldin A (BFA) (Nebenführ et al., 2002) sensitive endosomal

guanine-nucleotide exchange factor for ADP-ribosylation factor-type G proteins (ARF-GEF) GNOM is necessary (Geldner et al., 2003). PIN1 is maintained at the PM through permanent endocytotic recycling (Kleine-Vehn et al., 2011). Next to intrinsic mechanisms, like phosphorylation signals, specific transmembrane domains or cytosolic domains, external signals are important for the polarization of PIN proteins. One of this signals is auxin itself, thereby creating feedback loops to regulate the capacity and polarity of its own transport (Sachs, 1981). This was for example shown during the formation of the leave venation pattern (Scarpella et al., 2006) or during lateral bud activation (Balla et al., 2011). Whereas the exact mechanisms of this auxin-mediated PIN polarization are unclear, it was suggested to be mediated on the one hand by mechanical stress (Heisler et al., 2010), but also by inhibition of endocytosis (Robert et al., 2010). Further environmental signals, like light and gravity were shown to change PIN polarity (Friml et al., 2002a; Friml et al., 2002b; Harrison and Masson, 2008; Christie et al., 2006; Ding et al., 2011; Kleine-Vehn et al., 2010; Rakusová et al., 2011). The stability of the polar domains was shown to be maintained by constitutive recycling out of the polar domain, but also by PIN protein accumulation in distinct clusters of the polar domain, which are not defined, but depend on the sterol composition of the membranes (Kleine-Vehn et al., 2011). This points at a role for lipids in the formation of cell polarity. Recent findings link the RHO GTPases OF PLANTS (ROP) with the formation of cellular polarity (reviewed in Craddock et al., 2012). Apart of regulating F-acting dynamics and the organization of cortical microtubules, ROPs target polar exocytosis. It was further shown that interference with ROP function leads to the inhibition of PIN1 endocytosis, therefore linking ROP function to auxin (Craddock et al., 2012; Nagawa et al., 2012). This finding proposes an auxin-ROP signaling as general mechanism for the generation of cell polarity in plants. It additionally stresses the significance of the cytoskeleton for the polar transport of PIN vesicles.

1.2 Auxin

The phytohormone auxin has a crucial role in plant embryonic development and further regulates almost all aspects of a plant's growth and development (Vanneste and Friml, 2009). This includes postembryonic development and tropisms, such as the movement in relation to light and gravity. It acts on a cellular level influencing aspects of cell division, cell elongation and cell differentiation (Perrot-Rechenmann, 2010). Like other phytohormones auxin is active at low concentrations and it is endogenously produced. The most prominent auxin is indole-3-acetic acid (IAA), but there exist three additional endogenous auxins in some plant species, namely phenylacetic acid (PAA), 4-chloroindole-3-acetic acid and indole-3-butyric acid (Simon and Petrášek, 2010).

1.2.1 Auxin signaling cascade

Until today, there are one tryptophan independent and four tryptophane dependent pathways for the biosynthesis of IAA described (reviewed in Woodward and Bartel, 2005). In *A.thaliana,*

IAA is mainly produced in the shoot and the root apex, as well as in young leaves (Ljung et al., 2002; Ljung et al., 2005). From the three auxin receptor/co-receptor systems that have been identified the $SCF^{TIR1/AFB}$-auxin-AUX/IAA (SCF: SKP-CULLIN-F-Box; TIR/AFB: TRANSPORT INHIBITOR RESISTANT 1/AUXIN SIGNALLING F-BOX; AUX: auxin) co-receptor system is best described. It regulates auxin-dependent transcription and its place of action is the nucleus (Perry et al., 2009; Santner and Estelle, 2010; Calderon-Villalobos et al., 2012). AUX/IAA proteins function as negative regulators of gene expression by blocking AUXIN RESPONSE FACTORs (ARFs). At basal auxin levels, AUX/IAAs are more or less stable. They homo and heterodimerize with ARFs. The ARF bound AUX/IAAs block the transcription from auxin responsive promoters by controlling the amount of free ARF transcription factors to the promoters. An increase in auxin levels causes the $SCF^{TIR1/AFB}$ mediated proteasome degradation of AUX/IAAs. The degradation of AUX/IAAs gradually increases the number of functional active ARF proteins and the trascriptional activation of auxin responsive genes. An additional system that mediates auxin response on a transcriptional level is the S-PHASE KINASE-ASSOCIATED PROTEIN 2a. It is a component of the SCF complex. Upon binding of auxin it promotes the degradation of DIMERIZATION PARTNERS OF E2Fs b (DPb). DPb is a transcriptional repressor and its degradation allows cell cycle progression (Jurado et al., 2010). The third receptor/co-receptor system of auxin signaling consists of the AUXIN BINDING PROTEIN1 (ABP1). It mediates non-transcriptional auxin signaling in pavement cells, guard cells and in the root (reviewed in Murphy and Peer, 2012). ABP1 is anchored in the plasma membrane via the glycosylphosphatidylinositol- (GPI) anchored copper oxidase C-TERMINAL PEPTIDE-BINDING PROTEIN1, but binds extracellular auxin. Therefore it is hypothesized that a co-receptor exists. Auxin signaling mediated by ABP1 involves the ROP-GTPases and their associated ROP Interactive CRIP motif- containing proteins (RICs) (Xu et al., 2010). The ROP-RICs were shown to regulate clathrin-mediated endocytosis of PIN proteins on the PM (Lin et al., 2012). Further evidence links ABP1 also with transcriptional regulation of auxin signaling via ROPs (Tao et al., 2002; Zazímalová et al., 2010; Shi and Yang, 2011).

1.2.2 Polar auxin transport (PAT)

The rates of auxin synthesis as well as its conjugation are important for the overall auxin status of a plant. For the regulation of auxin dependent processes though, it is more important that auxin is transported from its place of synthesis to its place of action. Whereas in the apoplast (pH ~5.5) IAA enters cells via lipophilic diffusion (Rubery and Sheldrake, 1974; Raven, 1975) and anionic uptake mediated by the proton symporters of the AUXIN RESISTANT1/LIKE AUX1 (AUX1/LAX1) family (Bennett et al.,1996; Swarup et al.,2008; Yang et al., 2006), at a cytosolic neutral pH, it represents active transport.The active transport generates local auxin gradients and these auxin maxima (and minima) are translated by tissues and cells into respective responses (Benková et al., 2003). Along the axes of tissues this is referred to as polar auxin transport (PAT), a directed transport system of auxin. PAT is mediated by different influx and efflux transporter proteins. AUX1 and the related LAX1 proteins convey auxin influx (Ben-

nett et al.,1996; Marchant et al., 1999; Yang et al., 2006; Bainbridge et al., 2008; Swarup et al., 2008). Further members of the MULTIDRUG RESISTANCE/P-GLYCOPROTEIN family (MDRs/PGPs) are able to export auxin, as for instance PGP1 and PGP19 or they display auxin efflux and influx activity like PGP4 (Geisler et al., 2005; Terasaka et al., 2005; Geisler and Murphy, 2006; Petrášek et al., 2006; Cho et al., 2007). The main key players nevertheless belong to the PIN-FORMED family (PINs). In *A.thaliana* there are eight *PIN* genes. *PIN1, 2, 3, 4* and *7* (= *PIN1*- like) encode full length PINs and *PIN5, 6* and *8* encode short PINs. The short PINs don't contain the hydrophilic loop and whereas the PIN1-like group is mainly localized at the plasma membrane, the short PINs localize to endomembrane structures (Mravec et al., 2009). PIN1-like proteins have been shown to directly mediate auxin efflux (Chen et al., 1998; Geisler et al., 2005; Petrášek et al., 2006; Blakeslee et al., 2007; Yang and Murphy, 2009).

In the *A.thaliana* embryo, auxin is supplied through the outer layer and accumulates at the cotyledon primordia (Fig. 1A). From there it is drained into the interior of the primordium and transported downward through the central stele cells (Benková et al., 2003) (Fig. 1A). This model is referred to as reverse fountain model (Benková et al., 2003). In embryogenesis the auxin flow is mediated primarily, but not exclusively through PIN1 and its localization resembles the flux of IAA. In the epidermis cells, PIN1 localizes to the apical site of the PM and in the stele cells it is localized to the basal site of the PM, eventually leading to an auxin accumulation in the root apical meristem. PIN4 and PIN7 contribute to the auxin supply to the emerging root meristem (Friml et al., 2003). In the root, the PAT follows the so called fountain model (Fig. 1B). Auxin is transported from the shoot to the root tip in the vascular cylinder by PIN1 and PGP19 (Gälweiler et al., 1998; Friml et al., 2002a; Blilou et al., 2005; Blakeslee et al., 2007). From the quiescent center (QC) PIN4 transports auxin into the root cap (Friml et al., 2002a). PIN3 and PIN7 mediate efflux from the root columella cells and distribute auxin laterally (Friml et al., 2002b; Blilou et al., 2005). Whereas PGP1 and PGP19 exclude auxin from the columella cells, PIN2 and PGP4 channel auxin shootward in cortical and epidermal cells (Friml et al., 2003; Geisler et al., 2005; Santelia et al., 2005; Terasaka et al., 2005; Blakeslee et al., 2007; Lewis et al., 2007; Wu et al., 2007; Mravec et al., 2008). Cortically expressed PIN2, PIN3 and PIN7 redirect shootward auxin flow into the rootward transport system in the elongation zone (Benkova et al., 2003; Blilou et al., 2005).

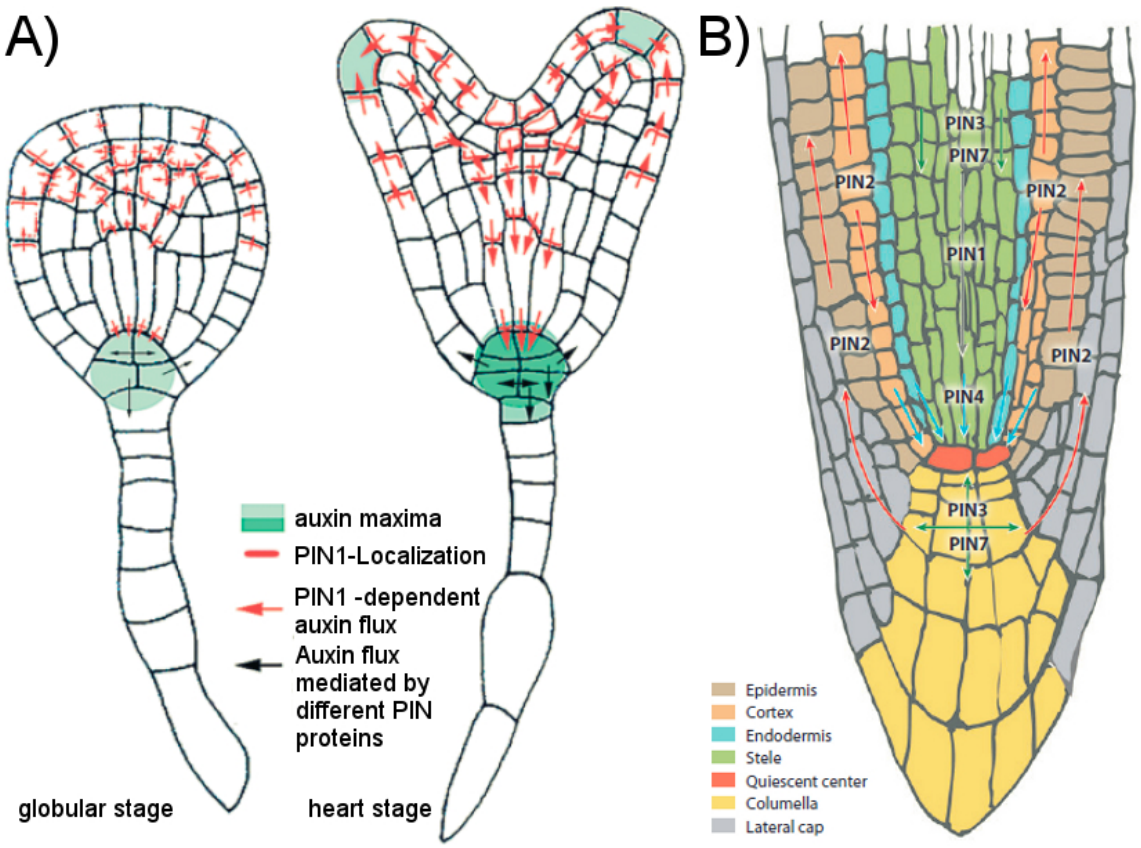

Figure 1 – Polar auxin transport in the embryo and the root apical meristem of *A.thaliana* A) taken from Matthes and Torres Ruiz (2012) B) taken from Kleine-Vehn and Friml (2008)

1.3 Auxin in embryogenesis

The life span of *A.thaliana* starts with embryogenesis (Fig. 2). During this developmental phase the basic body plan of this plant is established, resulting in a stereotyped seedling. It consists of an apically located shoot meristem (SAM), two cotyledons, a basally located root meristem (RAM), a hypocotyl and a seedling root (Jürgens et al., 1991; Torres-Ruiz, 2004). On the radial axis concentrically arranged tissue layers are formed, namely the outermost epidermis, the ground tissue and the centrally located vascular tissue.The embryogenesis of *A.thaliana* consists of a well defined cell division pattern. Out of the fertilized zygote the 2-cell, 4-cell, octant-, dermatogen-, early globular-, late globular-, the heart- and torpedo stage develop (Fig. 2).

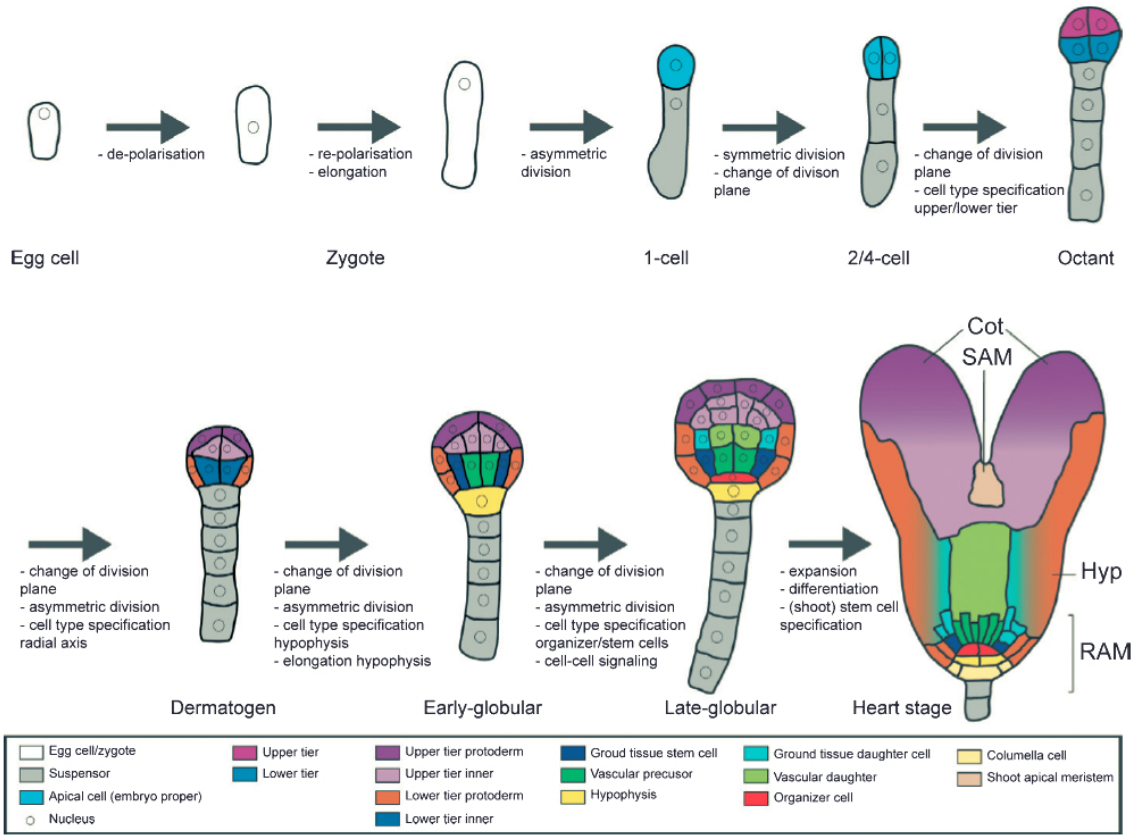

Figure 2 – Morphogenetic processes during the embryogenesis of *A.thaliana*. Schematic overview of the embryogenesis of *A.thaliana* from the egg cell to the heart stage embryo, highlighting the morphogenetic processes required for progress from one stage to the next. The colors represent cells of (essentially) the same type (see color legend), based on marker gene expression and lineage analysis. Cot, cotyledon; SAM, shoot apical meristem; Hyp, hypophysis; RAM, root apical meristem (taken from Wendrich and Weijers, 2013); © New Phytologist, with kind permission

The effect of IAA on embryogenesis, as for any other auxin dependent process, is primarily achieved through the already mentioned PAT (Fig. 1). It is extensively shown that auxin has pivotal roles in different steps of embryogenesis, for example primary root initiation. This is drastically seen by mutants that affect directional auxin transport (Friml et al., 2003), auxin response (Berleth and Jürgens, 1993; Hamann et al., 1999; Hobbie et al., 2000; Dharmasiri et al., 2003; Dharmasiri et al., 2005; Dharmasiri et al., 2007) or auxin biosynthesis (Stepanova et al., 2008; Cheng et al., 2007b). Severe cases even lead to the abolishment of the whole organs as it is the case for the pattern mutants *monopteros* (*mp*) (Berleth and Jürgens, 1993; Hardtke and Berleth, 1998) and *bodenlos* (*bdl*) (Hamann et al., 1999), which lack the embryonic root. MP is a transcription factor belonging to the class of ARFs (Hardtke and Berleth, 1998). With basal auxin concentrations MP is inhibited by BDL, which belongs to the class of IAA proteins (Hamann et al., 2002). MP and BDL are both expressed in the apical cell lineage and their action is confined to this region (Hardtke and Berleth, 1998; Hamann et al., 2002). Initial transport of auxin to the apical cells of the proembryo is maintained by PIN7, which is initially localized at the apical site of the suspensor cells, and basally from 32-cell stage onwards (Friml et al., 2003). Auxin targets BDL for degradation, which results in the derepression of MP via release of the transcriptional co-repressor TOPLESS (Dharmasiri et al., 2005; Szemenyei et al.,

2008). MP starts activation of the transcriptional targets PIN1 and TMO7, in the provascular cells (Schlereth et al., 2010). These are signals for hypophysis specification as root meristem precursors. The primary function of MP in embryo patterning is to facilitate the establishment of apical to basal auxin transport, by promoting PIN1 expression (Weijers et al., 2006), which in turn leads to an auxin accumulation in the hypophysis and hypophysis derivatives (Fig. 1). In addition, MP activates TMO7, which accumulates in the basal proembryo and is transported to the hypophysis. TMO7 therefore is mobile and is considered as a second signal for hypophysis specification (Schlereth et al., 2010). At present, TMO7 abundance in the hypophysis as well as auxin accumulation are the only known triggers for the correct division of the hypophysis, which is the pivotal step in correct root initiation (Schlereth et al., 2010). From the hypophysis, auxin is in part basally transported to the suspensor through an overal reversal of the basal to apical auxin flow from the dermatogen stage on, which is accomplished by a change in localization of PIN7 from the apical to the basal site of suspensor cells, but also by a localization of the initally nonpolar distributed PIN1 to the basal side of the lower inner cells (Friml et al., 2003; Steinmann et al., 1999) as well as the promotion of PIN1 expression in provascular cells by MP (Schlereth et al., 2010). Notably, loss of *MP* or auxin insensitive alleles of its repressor *BDL* lead to incorrect divsions of the hypophysis, which results in rootless seedlings (Berleth and Jürgens, 1993; Hamann et al., 1999).

Auxin and the proper auxin flux (Fig. 1) further play important roles in cotyledon development. In the inner cells of the provascular system the flux of IAA is rootwards, but in the protodermal cells it is directed towards the incipient cotyledon primordia (Steinmann et al., 1999; Benková et al., 2003; Treml et al., 2005). Because auxin maxima correlate directly with the sites of cotyledon initiation it is assumed that auxin causes their initiation (Benková et al., 2003). Similarly important nevertheless is the exclusion of specific transcripts/ proteins, like SHOOT MERISTEMLESS (STM) and *CUP SHAPED COTYLEDON (CUC)* genes or the competence of cells to respond to these transcription factors (Furutani et al., 2004; Treml et al., 2005). STM plays a crucial role for the initiation of the SAM (Barton and Poethig, 1993; Long et al., 1996; Lenhard et al., 2002) and its expression depends on the putatitve transcription factors CUC1-3 (Aida et al, 1997; Aida et al., 1999; Takada et al., 2001; Vroemen et al., 2003; Hibara et al., 2006). At the late globular and heart stage of embryogenesis the auxin flux is dominated by the polar localization of PIN1 (Fig. 1). For the development of cotyledons primarily the apical localization of PIN1 in protodermal cells is important. Notably, disturbances of this apical PIN1 localization lead to various cotyledons defects ranging from reduction (Berleth and Jürgens, 1993; Hamann et al., 1999) and addition of cotyledons (Bennet et al., 1995) to the complete loss of those organs (Furutani et al., 2004; Treml et al., 2005; Furutani et al., 2007; Cheng et al., 2008). One example of a mutant with no cotyledons is the *laterne* mutant (Treml et al., 2005; Treml, 2008; Furutani et al., 2007). The cotyledon-less seedling of the *laterne* mutant develops rosette leaves. It further fails to initiate flowers, resulting in adult flowers with blind ending stems (Treml et al., 2005; Furutani et al., 2008). Molecular analyses revealed that the *laterne* phenotype is due to simultaneous mutations in the serine/threonine kinase *PINOID* (*PID*) gene

as well as in the NONPHOTOTROPIC HYPOCOTYL3 (NPH3)-like protein *ENHANCER OF PINOID* (*ENP*) gene. PIN1, which is apically localized in the epidermal cells of the *A.thaliana* wild type embryo (Fig. 1), displays a completely reversed localization in the *laterne* embryo (Treml et al., 2005; Treml, 2008). These analyses showed that PID and ENP have synergistic effects upon the polarity and the functioning of PIN1.

1.4 The interplay of PID, PIN1 and ENP in cotyledon and flower organogenesis

PID belongs to the cAMP-dependent kinase, cGMP-dependent kinase, phospholipid-dependent protein kinase C VIII (AGCVIII) family of serine/threonine kinases (Christensen et al., 2000). It is expressed in the cotyledon primordia of embryos, in young leaves and in young floral organs (Christensen et al., 2000; Benjamins et al., 2001). Further it is detected in seedlings mainly in the vascular tissue in regions of vascular differentiation proximal to the meristems and lateral root primordia (Benjamins et al., 2001), but also in the root epidermis (Michniewicz et al., 2007; Dhonukshe et al., 2010). According to this expression pattern, PID is involved in determining the position and outgrowth of cotyledon, leaf and floral organ primordia (Benjamins et al., 2001). The subcellular localization of PID is apolar around the membrane in epidermal cells of cotyledons (Benjamins et al., 2001; Michniewicz et al., 2007; Dhonukshe et al., 2010). In the root epidermis PID is found at the basal and the apical site, but not at the lateral sites (Michniewicz et al., 2007;Dhonukshe et al., 2010). PID is phosphorylated by the 3 PHOSPHOINOSITOL DEPENDENT PROTEIN KINASE 1 (PDK1) (Zegzouti et al., 2006). Upon its own phosphorylation PID is enabled to phosphorylate PIN1 in the middle serine in three conserved TPRXS(N/S) motifs in its central hydrophilic loop (Wisniewska et al., 2006; Huang et al., 2010; Dhonukshe et al., 2010). PID was shown to act redundantly with at least three other AGCVIII kinases, namely PID2, WAG1 and WAG2 in cotyledon and flower formation. This is seen by the mutant phenotypes. Whereas *pid* single mutations don't abolish cotyledons, but lead to supernumerary ones (Bennet et al., 1995) the quadruple mutants *pid pid2 wag1 wag2* lead to a complete loss of cotyledons (Cheng et al., 2008). This phosphorylation in concert with permanent recycling, for which the BFA sensitive endosomal ARF GEF GNOM is necessary (Geldner et al., 2003), clustering and endocytosis are important to target and maintain PIN1 at the apical site of the PM (Kleine-Vehn et al., 2011). Further factors influencing the localization of PIN1 are tissue determinants (Friml et al., 2002a; Friml et al., 2002b), the actin cytoskeleton (Geldner et al., 2001), the sterol composition of the PM (Willemsen et al., 2003), auxin transport itself (Geldner et al., 2001) and the action of PP2A (Michniewicz et al., 2007).

Molecular analysis further revealed the importance of the NPH3-like protein *ENP* gene in the maintenance of the apical PIN1 polarity in cotyledon organogenesis (see above; Treml et al., 2005; Furutani et al., 2007; Cheng et al., 2008). ENP is a soluble protein, associated to the PM with a molecular mass of 66.4kDa (Treml, 2008; Furutani et al., 2011; Zweigardt, 2010). ENP is expressed in the protodermal cell layer of the embryo and in the meristem L1 layer

at the site of organ initiation. In the course of embryology *ENP* expression gets restricted to the tip of cotyledon primordia, including several inner cells, radicles and to the presumptive SAM. In postembryonic development *ENP* is expressed in the organ primordia and the SAM (Treml, 2008; Furutani et al., 2011). On a subcellular scale ENP localizes to the apical site of the PM in epidermal cells of cotyledons (Treml, 2008; Zweigardt, 2010; Furutani et al., 2011). The localization at the apical site of the PM in the epidermis of cotyledons is very similar to that of PIN1 (Zweigardt, 2010; Furutani et al., 2011). Protoplast studies also showed an intracellular, yet unidentified, accumulation of vesicles with ENP, which shows a partial overlap with PID intracellular vesicle accumulation (Furutani et al., 2007). ENP constitutes a subgroup of the NPH3 family consisting of five members, namely ENP, also known as MACCHI-BOU 4 or NAKED PINS IN YUC MUTANTS 1 (MAB4/NPY1) (Cheng et al., 2007a) and NPY2/MEL3 (MAB4/ENP/NPY1-LIKE 3) -NPY5/MEL1 respectively. From heart stage embryos onwards they show unique and overlapping expressions, which hints at their redundant, but also unique, most likely tissue specific, functions (Furutani et al., 2007; Treml, 2008; Cheng et al., 2007a; Cheng et al., 2008). In the globular-heart stage embryo *ENP* shows coexpression with *NPY3/MEL2*, *NPY4/MEL4* and *NPY5/MEL1*, whereas in later embryonic stages *NPY2/MEL3* and *NPY4/MEL4* have unique expression domains. In the seedling root promoter::GUS fusions showed a partial coexpression of pENP::GUS with pNPY4::GUS in the stele, the root epidermis and root cap and the meristem region. Notably the other pNPY::GUS expressions were not detected in the root epidermis (Li et al., 2011). Interestingly, although quintuple mutations of the NPY genes have not been reported to have a striking embryonic phenotype, they display a defect in flower organogenesis, depicting a blind ending stem, as seen in the *laterne* adult phenotype (Cheng et al., 2008).

1.5 Aims of the work

Whereas the interplay of PID and PIN1 is well understood, the molecular link between ENP and PIN1 and PID respectively remains elusive. The striking *enp pid* (=*laterne*) phenotype undoubtedly assigns an important role for *ENP* in PIN1 polarity and in turn *A.thaliana* organogenesis. However, in spite of the (combined) efforts of different groups, unraveling the role of ENP has turned out to be a special challenge. For instance, a direct interaction of ENP and PIN1 (or PID) has not been found so far. Therefore, our lab has begun to dissect the complete process into three different steps. The first considers that factors (intrinsic and extrinsic) are required for the polar localization of ENP at the plasma membrane. This includes the question, whether ENP's localization depends on PIN1 or vice versa. The second step assumes that ENP's impact on PIN1 is mediated through other molecules, possibly also required for association at the plasma membrane. The third considers interactions of ENP with unknown factors and PID in order to achieve PIN1 apical polarity.

This in mind, the presented work first analyzed domains and possible amino acid sequence signals of the ENP protein required for its polarity and full functionality.

Pharmacological studies with inhibitors targeting different cellular processes and structures

aimed to analyze extrinsic factors of ENP's polarity. This work addressed questions such as whether actin and or microtubules are required for ENP's polarity or whether ENP depends on PIN1 or vice versa respectively. These experiments also intended to explore a potential new tool, namely phenylboronic acid (PBA), for these analyses.
Global and direct interaction screens with recently developed yeast two-hybrid systems (Y2H) planned to detect and validate ENP interactors (including potential extrinsic factors) and to address whether these would provide insight into the molecular mechanisms involving ENP.
Considering the aspects of PIN1 and ENP epidermal polarity, mutants of *RECEPTOR LIKE PROTEIN KINASE 1 (RPK1)* came into focus, because they display the loss of one cotyledon. This forced to analyze whether this phenotype could be linked to the loss of both cotyledons (i.e. *laterne*) and thus to the activity of the PID/ENP/PIN1 chain.
Comparative transcriptomics of wild type and *laterne* seedlings should provide information on downstream targets of correct auxin homeostasis in the cotyledons.
During the course of the pharmacological studies, the results with PBA increasingly suggested that boronic acids might be of general use to analyze the subcellular trafficking and the architecture of membranes and associated proteins respectively. The potential importance of this finding caused a spin-off project, which was followed to some extent.

2 Material and Methods

2.1 Material

2.1.1 Antibiotics and herbicides

Table 1 lists the antibiotic and herbicide stock solutions used in this thesis. Working solutions were 1/1000 dilutions of the given stock solutions. Hygromycin was used as a working solution of 13 mg/l.

Antibiotic	**Concentration**
Ampicillin	100 mg/ml in H_20
Genatmycin	25 mg/ml in H_20
Kanamycin	50 mg/ml in H_20
Phosphinotricine	25 mg/ml in H_20
Rifampicin	35 mg/ml in methanol
Streptomycin	25 mg/ml in H_20
Tetracyclin	25 mg/ml in ethanol
Timentin	13 mg/ml in H_20

Table 1 – List of employed stock solutions of antibiotics and herbicides

2.1.2 Plant material

2.1.2.1 Wild type and mutant lines

For all described experiments with plants the ecotypes Landsberg *erecta* (L*er*) (obtained from the Nottingham *Arabidopsis* Stock Center, NASC) and Columbia-0 (obtained from NASC) of *A.thaliana* were used.
The mutant lines used in this study are described in table 2.

Name	**Described in**
enp pid / *enp pid* (*laterne*)	Treml et al., 2005
enp pid/*enp* + (III-2-A "*spirrig*")	Treml et al., 2005
rpk1-7/*rpk1-7*	Luichtl et al., 2013
rpk1-6/*rpk1-6*	Luichtl et al., 2013

Table 2 – *A.thaliana* mutant lines used in this study

2.1.2.2 Transgenic lines

The transgenic lines used and created in this study are depicted in table 3. All constructs generated in this study were transformed into L*er* background, if not otherwise mentioned.

Name	Described in
pPIN1:PIN1::GFP (Col-0 background)	Benkova et al., 2003
DR5rev::GFP (Col-0 background)	Friml et al., 2003
p35S:EGFP::ENP1-4	Treml, 2008
p35S:EGFP::ENP3-4	Treml, 2008
pPIN2:PIN2::GFP (Col-0 background)	Abas et al., 2006
p35S:NPY4::YFP	this work
p35S:ENPdeltaNPH3_All::GFP	this work
p35S:ENPdeltaNPH3_2+3::GFP	this work
p35S:ENPdeltaNPH3_3::GFP	this work
p35S:ENPdeltaCterm::GFP	this work
p35S:enpY409A::GFP	this work
p35S:enpL144D::GFP	this work
p35S:enpP46T::GFP	this work
p35S:enpY409E::GFP	this work
p35S:NPY4_ENPCtermShort::GFP	this work
p35S:NPY4_ENPCtermLong::GFP	this work

Table 3 – Transgenic lines used and created in this study

2.1.2.3 Crossings

For the functional analysis of ENP all transgenic lines of ENP and NPY4 (see table 3) were crossed to *enp pid/enp + (spirrig)* plants. Further crossings used in this study are listed in table 4.

Name	Used for
rpk1-7 x pPIN1:PIN1::GFP	Localization studies of PIN1 in *rpk1-7*
rpk1-7 x p35S:EGFP::ENP1-4	Localization studies of ENP in *rpk1-7*
rpk1-6 (N2995) x pPIN1:PIN1::GFP	Localization studies of PIN1 in *rpk1-6*

Table 4 – Crossings used in this study

2.1.3 Chemicals

Name	Company
Acetic acid	Merck, Darmstadt
Agar-agar	Merck, Darmstadt
Agarose	Biozym, Eldendorf
Ampicillin sodiumsalt	Serva, Heidelberg
β- mercaptoethanol	Sigma, Steinheim
Benzoic acid	Sigma-Aldrich, Munich
Brefeldin A	Fischer-Scientific, Schwerte
Bromophenolblue	Serva, Heidelberg
Chlorophorm	Merck, Darmstadt
Colchizin	Merck, Darmstadt

Cycloheximid	Applichem, Darmstadt
CytochalasinD	Sigma-Aldrich, Munich
Desoxyribonucleoside- triphosphates (dNTPS)	Fermentas, St. Leon Roth
Dimethylsulfoxid (DMSO)	Merck, Darmstadt
Di-sodium hydrogenphosphate	Merck Darmstadt
EDTA	Sigma, Steinheim
Ethanol	Merck, Darmstadt
Ethidiumbromide	Roth, Karlsruhe
Gentamycin sulfate	Duchefa, Haarlem, Netherlands
Glucose	Merck, Darmstadt
Glycerine	Merck, Darmstadt
Glycine	Serva, Heidelberg
Hydrochloric acid	Merck, Darmstadt
Hygromycin B	Duchefa, Haarlem, Netherlands
Indol -3- acetic acid	Sigma, Steinheim
Isopropyl alcohol	Merck, Darmstadt
Isopropyl-β-D-thiogalactopyranosid (IPTG)	Duchefa, Haarlem, Netherlands
Kanamycin sulfate	Duchefa, Haarlem, Netherlands
Latrunculin B	Sigma-Aldrich, Munich
Magnesium chloride	Merck, Darmstadt
Methanol	VWR, Darmstadt
Murashige and Skoog medium and B5 vitamins	Duchefa, Haarlem, Netherlands
Oryzalin	Sigma -Aldrich, Munich
Peptone	Serva, Heidelberg
Phenol	Merck, Darmstadt
Phenylacetic acid	Sigma-Aldrich, Munich
Phenylboronic acid	Merck, Darmstadt
Potassium chloride	Merck, Darmstadt
Potassium dihydrogenphosphate	Merck, Darmstadt
Potassium hydroxide	Merck, Darmstadt
Rifampicin	Duchefa, Haarlem, Netherlands
Saccharose	Serva, Heidelberg
Silwet-77	Witco Europe, Genf, Switzerland
Sodium acetate	Merck, Darmstadt
Sodium chloride	Merck, Darmstadt
Sodium dihydrogenphosphate	Merck, Darmstadt
Sodium hydroxide	Merck, Darmstadt
Sodium laurylsulfate (SDS)	Serva, Heidelberg
Tris(hydroxymethyl)-aminomethan (Tris)	Merck, Darmstadt
Triton X-100	Applichen, Darmstadt

Trypton	Serva, Heidelberg
Tween 20	Merck, Darmstadt
Yeast extract	Roth, Karlsruhe

Table 5 - General chemicals used in this study

2.1.3.1 Chemicals for the pharmacological studies

In order to study the extrinsic factors necessary for the polarity of ENP the chemicals listed in table 6 were used.

Chemical	Concentration (embryo)	Concentration (root)
Phenylboronic acid	25 mM	5 mM
Oryzalin	10 µM, 20 µM, 40 µM	-
LatrunculinB	20 µM	-
Brefeldin A	50 µM	-
Cytochalasin D	20 µM, 40 µM	-
Colchicine	10 µM	-

Table 6 – Chemicals used for the pharmacological studies

2.1.3.2 Chemicals for silique application

The chemicals applied on siliques of Col-0 and L*er* are given in table 7.

Chemical	Concentration
Phenylboronic acid (PBA)	50 mM
Benzoic acid (BES)	50 mM
Phenylacetic acid (PAA)	50 mM

Table 7 – Chemicals applied onto *A.thaliana* siliques

2.1.4 Size markers

For usual size discrimination on agarose gels 1kb+ GeneRuler (Fermentas, St. Leon Roth) was used. In order to obtain DNA concentration information from agarose gels, the lambda Hind marker was used. In order to use this marker lambda DNA (Fermentas, St. Leon Roth) was digested with HindIII for several hours at 37°C.

2.1.5 Bacterial strains

Name	Genotype	Application	Described in
E.coli XL1 Blue (Stratagene)	supE44, hsdR17, recA1, endA1, gyrA46, thi,relA1 lac-lac [F' proAB+ lacIq lacZ ΔM15 Tn10 (tetR)]	Standard Cloning	Bullock et al., 1987
E.coli One Shot® Omni Max ^{TM}2-T1^{R} (Invitrogen)	F' {proAB+ lacIq lacZΔM15 Tn10(TetR)Δ(ccdAB)} mcrA Δ(mrrhsdRMS- mcrBC) φ80 (lacZ) ΔM15 Δ(lacZYA-argF)U169 endA1 recA1 supE44 thi-1 gyrA96 relA1 tonA panD	Gateway ® cloning	Blumenthal, 1989
E.coli One Shot® Omni Max ^{TM} *ccdB* Survival ^{TM} T1^{R} Competent Cells (Invitrogen)	F^{-} mcrA Δ(mrr-hsdRMS -mcrBC) Φ80lacZΔM15 ΔlacX74 recA1 araΔ139 Δ(ara-leu)7697 galU galK rpsL (Str^{R}) endA1 nupG fhuA::IS2	Gateway® cloning	Bernard and Couturier, 1992
A.tumefaciens GV3101 pMP90	Gentamycin^{R}, Rifampicin^{R}, Ti-Plasmid ohne T-DNA	Plant Transformations	Koncz and Schell, 1986

Table 8 – Bacterial strains used in this work

2.1.6 *S.cerevisiae* strains

Name	Genotype	Application	Described in
MaV203	MAT, leu2-3,112,trp1-901,his3200, ade2-101, gal4, gal80, SPAL10::URA3, GAL1::lacZ, HIS3$_{UAS\ GAL1}$::HIS3@LYS2, can1^{R},cyh2^{R}	ProQuest^{TM} Y2H	Invitrogen (2002)
Y8800	Mat a, leu2-3,112 trp1-901 his3-200 ura3-52 gal4Δ gal80Δ GAL2-ADE2 LYS2::GAL1-HIS3 MET2::GAL7-lacZ cyh2^{R}	Y2H screening	Dreze et al., 2010
Y8930	Matα, leu2-3,112 trp1-901 his3-200 ura3-52 gal4Δ gal80Δ GAL2-ADE2 LYS2::GAL1-HIS3 MET2::GAL7-lacZ cyh2^{R}	Y2H screening	Dreze et al., 210

Table 9 – *S.cerevisiae* strains used in this thesis

2.1.7 Primers

Name	Sequence
GFP_to_ENP_rev	AAA GTT CTT CTC CTT TAC TCA
ENPLinkerREV	ATC TTT CGG AAT CAC ATT CTC
ENPCterm_FW	CAG AAC GAG AGA CTT CCA CTA
ENP_NPH3_1_FW	GTT GCA AGG TGG TTA CCA GAA
35S_ENP_FW	AGGAAGTTCATTTCATTTGG
35SLinker_ENP_FW	TATCTCCGGTCTGGTAAGCA

Table 10 – Primers used for sequencing assessment of ENP derived constructs in transgenic *A.thaliana* plants

Name	Sequence	Sequening of
pDest 32 FW	AACCGAAGTGCGCCAAGTGTCTG	Bait plasmids ProQuest^{TM}
pDest 32/22 REV	AGCCGACAACCTTGATTGGAGAC	Bait/Prey plasmids ProQuest^{TM}
pDest 22 FW	TATAACGCGTTTGGAATCACT	Prey plasmids ProQuest^{TM}
AD	CGCGTTTGGAATCACTACAGGG	Y2H screening AD constructs
DB	GGCTTCAGTGGAGACTGATATGCCTC	Y2H screening DB constructs
Term	GGAGACTTGACCAAACCTCTGGCG	Y2H screening AD/DB constructs

Table 11 – Sequencing primers for the assessment of generated clones

Name	Sequence
TMO5 FW	ATGTACGCAATGAAAGAAGA
TMO5 REV	ATTATAACATCGATTCACCA
TMO7 FW	ATGTCGGGAAGAAGATCACG
TMO7 REV	TTGGGTAAGTAAGCTTCTGA
MP FW	TGACACAAGCACACATGGAGG
MP REV	TGAGCAGCAGCAGCAAGAAC
BDL FW	ACGCTCTGCTGAATCTTCC
BDL REV	TCCAATCCCCTTCCTTATCTTC

Table 12 – Primers for the PCR analysis of *MP*, *BDL*, *TMO5* and *TMO7* in *mp*-like phenocopies and mutant *mp* seedlings

Name	Sequence	Application
ENP	GGGGACAAGTTTGTACAAAAAAGCAGG	Localization
FW	CTTCATGAAGTTCAT GAAGCTAGGGTC	study; Y2H
ENPΔNPH3_All	GGGGACCACTTTGTACAAGAAAGCTG	Localization
REV	GGTTAATCACATTCTCTTCTCTCTTCTC	study; Y2H
ENPΔNPH3_2+3	GGGGACCACTTTGTACAAGAAAGCTG	Localization
REV	GGTTATCTTTGTTTGAAGAAGCTTCTGA	study; Y2H
ENPΔNPH3_3	GGGGACCACTTTGTACAAGAAAGCTG	Localization
REV	GGTTCAACAAAATTCCATTTCCTAAAAC	study; Y2H
ENPΔCterm	GGGGACCACTTTGTACAAGAAAGCTG	Localization

REV	GGTTGAGCTGCTCAAAGTAGAGAAC	study; Y2H
ENP Cterm	GGGGACAAGTTTGTACAAAAAAGCAGG	Localization
FW	CTTCATGCACAGCCCCGTGGCGTCT	study; Y2H
NPY4	GGGGACAAGTTTGTACAAAAAAGCAGG	Localization
FW	CTTCATGAAGTTTATGAAACTTGGAA	study; Y2H
ENP	GGGGACCACTTTGTACAAGAAAGCTG	Localization
REV	GGTCCGATATCGAATG TCTGCGGCG	study; Y2H
NPY4_ENPCterm	CGAAGCCGCAACAGACGCCACGGGGCTGTGATT	Localization
Long REV	GGCTCTAATCTGTTCAAAGAAGAGAAC	study; Y2H
NPY4_ENPCterm	GCTTCCTCTGCTTTTCTTGCTCAGCTCCACAAA	Localization
Short REV	CTCTTTCTCATGGTCCCATTCATCATCCTC	study; Y2H
ENP Cterm	CACAGCCCCGTCGCGTCTGTTGCGGCTTCG	Localization
Long FW	TCACACTCGCCGGTTGAGAAG	study; Y2H
ENP Cterm	GTGGAGCTGAGCAAGAAAAGCAGAGGA	Localization
Short FW	AGCAAGAGCACGAGGAGTGGT	study; Y2H

Table 13- Primers for generating the plasmids that were used in the localization study and in the yeast two-hybrid screening

Name	**Sequence**	**Overexpressed in**
At3g05730 FW	ACAACCCCCA TGGAGTAGTA	wild type
At3g05730 REV	GAAGCAGAGA GAAGCCGTCA	
AT5G26000 FW	ATGAAGCTTC TTATGCTCGC	wild type
AT5G26000 REV	ATCTGCAAGA CTCTTCCGAT	
AT4G28780 FW	ATGTCCACAT TTCTCCTAAC	wild type
AT4G28780 REV	ATTCTGGAGTCTAAAGCCAT	
AT1G12940 FW	ATGGAGGTCG AAGGCAAAGG	wild type
AT1G12940 REV	GGGATGAGTCGTTGTGGCTC	
AT1G32900 FW	ATGGCAACTG TGACTGCTTC	wild type
AT1G32900 REV	TGGCCAGAGG AGCTATCTCT	
AT5G59750 FW	CTGCTTTATA TCATCCTCGA	wild type
AT5G59750 REV	CTGATCGTTG TTATCAGAGA	
AT4G37150 FW	ATGAAGCATT ATGTGCTAGT	*laterne*
AT4G37150 REV	CGATCACGA GTTCATGAGG	
AT3G08860 FW	ATGCGGAAGT TAACGGCGGT	*laterne*
AT3G08860 REV	CTTGGACATG GCGTGATCCA	
AT2G39310 FW	ATGGCGAAGA TGTACCGGAA	*laterne*
AT2G39310 REV	AGTGACTCCG ATGCTGTGAA	
AT1G62500 FW	ATGGGTTCGA GAGTTTTGGC	*laterne*
AT1G62500 REV	GTGAGAGGAG GGCAGACAAA	
AT2G05440 FW	ATGGCTTCCA AGGCTTTGAT	*laterne*

AT2G05440 REV	AGTCTGAACA GGTTCGTTTA	
AT5G42580 FW	ATGGCAGAAC TCATCATCGT	*laterne*
AT5G42580 REV	AAAGGGTCGA ACCGAACAAC	
AT4G17810 FW	ATG AAC GGT GGT GCA TGG ATG	WT
At4g17810 REV	TCA CGG TGG ATG GTG CCC TAG	
STP1 FW	ATG CCT GCC GGT GGA TTC GTC	WT
STP1 REV	TCA AAC ATG CTT CGT TCC AGC	
WRKY22 FW	ATG GCC GAC GAT TGG GAT CTC	WT
WRKY22 REV	TCA TAT TCC TCC GGT GGT AGT	
AT1G33811 FW	ATG GGC ATT CTC CGT TTT GTA	WT
AT1G33811 REV	TCA AAG ATT GGC TAG TTC TTG	
AT2G32550 FW	ATG TCG GAA AAC ATG GTG AAT	WT
AT2G32550 REV	TTA GTT GTC CAG ATT CTG AAG	
APT2 FW	ATG TTT GCC GTG GAG AAT GGG	*laterne*
APT2 REV	TTA TAA GGT TAA TTC ATC AAA C	
AT5G25840 FW	ATG GCC CCC CTT CAA CGC ACC	WT
AT5G25840 REV	CTA ATT AAC CAA GGT ACG ATC	
IAA29 FW	ATG GAG TTG GAT CTT GGT CTA	WT
IAA29 REV	CAA ACA TCT TGT ATA TGC ACA	
LTP2 FW	ATG GCT GGA GTG ATG AAG TTG	*laterne*
LTP2 REV	TCA CCT CAC GGT GTT GCA GTT	
At4g15400 FW	ATG GAA GCG AAG CTA GAG GTG	*laterne*
At4g15400 REV	TTA TGC CAC GAC CGG GGG ATT	
Ext4 FW	ATG GGG GCA CCA ATG GCC TCT	*laterne*
Ext4 REV	CAA TTC TCC CGT CAA CGA TCT	

Table 14 - Primers used for the assessment of the transcriptomics results between wild type and cotyledon less seedlings

2.1.8 Devices

Description	Detail	Manufacturer
Axiophot		Zeiss, Jena
Incubators		Memmert, Schwabach; Heraeus Vötsch, Reiskirchen
Balances	Precision Balances, Analytical Balances	Sartorius, Goettingen
Gelexamination	UV- Transilluminator	Bachhofer
	Bioprintsystem	Fröbel
	Videokamera, Computer and Videoprinter	Mitsubishi
Climate Chamber		Haraeus Vötsch, Reiskirchen
FV1000/IX81	CLSM	Olympus, Hamburg
Fridge and freezer	4, -20, -70°C	Bosch, Stuttgart
Laminar Flow	LaminAir HB 2448	Heraeus Vötsch, Reiskirchen
Freedom Evo	liquid handling robot	Tecan, Maennedorf, Switzerland
Lightsources	KL 1500 Electronic	Zeiss, Hamburg
Microwave		NEFF, Munich
Nanophotometer		Implen, Munich
PCR Machine	DNA Engine Tetrad	MJ Research, Massachusetts, USA
	TGradient	Biometra, Goettingen
	Thermocycler	Biometra, Goettingen
Photometer	SpectroPhotometer U 1100	Hitachi
Voltage Generators (Gelelectrophoresis)	Phero- stab500 Electrophoresis Power Supply	Biotec Fischer, Reiskirchen
Thermomixer	T5436	Eppendorf, Hamburg
Variopipettes	10, 20, 100, 200, 1000µl	Gilson, Wisconsin, USA
Vortexer		Janke und Kunkel, Staufen
Water Baths		GFL, Burgwedel
Centrifuges	Standing Centrifuge J2-H6	Beckman Coulter, Krefeld
	Table- Centrifuge CS- 15R	Beckman Coulter, Krefeld
	Table Centrifuge A14	Jouan, Unterhaching
Speed Vac		Sauer Laborbedarf, Reutlingen
Walk in growth chamber	HEMZ 20/240/S	Heareus Vötsch, Reiskirchen

Table 15 – Devices used for the molecular analysis

2.1.9 Software and databases

Name	Distributor/citation
MS Office	Microsoft, Unterschleißheim
Fluoview	Olympus, Hamburg
GIMP	www.gimp.org
R package	http://cran.r-project.org
Bioconductor	www.bioconductor.org
limma	Smyth, 2004
Blast	Altschul et al., 1990
TAIR	www.arabidopsis.org
MapMan	Thimm et al., 2004; Usadel et al., 2005
Cytoscape	Shannon et al., 2003
ClueGo	Bindea et al., 2009
Genomatix Software Suit	www.genomatix.de; vers.3.0
PredictProtein	https://predictprotein.org

Table 16 – List of the applied software and databases

2.1.10 Standard vectors

Standard vectors used in this study are given in table 17.

Vector	Resistance/ auxotrophy	Source	Application
pDONR207	*ccdB*	Invitrogen	Cloning of PCR fragments
	E.coli: Gen, Cm		containing attB sites
pMDC83	*ccdB*		plant expression vector,
	E.coli: Kan	ABRC	containing GFP
	A.thaliana: Hygromycin		
pEarlyGate101	*ccdB*		plant expression vector,
	E.coli: Kan	ABRC	containing YFP
	A.thaliana: BASTA		
pDest-32	*ccdB*		yeast expression vector;
	E.coli: Gen	Invitrogen	Bait (ProQuest^{TM})
	S.cerevisiae: -Leu		
pDest- 22	*ccdB*		yeast expression vector;
	E.coli: Amp	Invitrogen	Prey (ProQuest ^{TM})
	S.cerevisiae: -Trp		
pDest_DB	*ccdB*	Pascal	yeast expression vector;
	E.coli: Amp	Braun	Bait (Y2H screening)
	S.cerevisiae: - Leu	TU München	
pDest_AD	*ccdB*	Pascal	yeast expression vector;
	E.coli: Amp	Braun	Prey (Y2H screening)
	S.cerevisiae: -Trp	TU München	

Table 17 – Standard vectors used in this study

2.1.11 *S.cerevisiae* control vectors

Name	Resistance/ auxotrophy	Application	Source
pEXTTmM32/Krev1	*E.coli*: Gen *S. cerevisiae*: -Trp	ProQuest ™	Invitrogen (2002)
pEXPTM22/RalGDS-m1	*E.coli*: Amp *S.cerevisiae*: -Leu	ProQuest ™	Invitrogen (2002)
pEXPTM22/RalGDS-m2	*E.coli*: Amp *S.cerevisiae*:-Leu	ProQuest ™	Invitrogen (2002)
pDest-DB-*CHY2*-pRB	*E.coli*: Amp *S.cerevisiae*: -Leu	Y2H screen	Dreze et al., 2010
pDest-DB-Fos	*E.coli:* Amp *S. cerevisiae*: -Leu	Y2H screen	Dreze et al., 2010
pDest-DB-Gal4	*E.coli*: Amp *S.cerevisiae*: -Leu	Y2H screen	Dreze et al., 2010
pDest-DB-dDP	*E.coli*: Amp *S.cerevisiae*: -Leu	Y2H screen	Dreze et al., 2010
pDest-AD-E2F1	*E.coli:* Amp *S.cerevisiae*: -Trp	Y2H screen	Dreze et al., 2010
pDest-AD-Jun	*E.coli*: Amp *S.cerevisiae*: -Trp	Y2H screen	Dreze et al., 2010
pDest-AD-dE2F1	*E.coli*: Amp *S.cerevisiae*: -Trp	Y2H screen	Dreze et al., 2010
pDest-AD-*CYH2*-dE2F1	*E.coli*: Amp *S.cerevisiae*: -Trp	Y2H screen	Dreze et al., 2010

Table 18 – *S.cerevisiae* control vectors for the ProQuest™ direct interaction test and the global Y2H screening

2.1.12 Other materials and enzymes

Name	Producer
Bio-Rad Protein Assay	Bio-Rad Laboratories, Munich
BP clonase II Enzyme Mix	Invitrogen, Darmstadt
GeneRuler 1kb+ DNA ladder	Fermentas, St. Leon Roth
LR clonase II Enzyme Mix	Invitrogen, Darmstadt
Reverse transcriptase	Roche, Penzberg
Nucleo Spin RNA Plant	Macherey-Nagel, Düren
One*Taq*	Promega, Mannheim
ProofStart Polymerase	Quiagen, Hilden
rDNase	Macherey-Nagel, Düren
Restriction enzymes (diverse)	New England Biolabs, Frankfurt
RNase A	Macherey-Nagel, Düren
T4 DNA Ligase	Roche, Penzberg
GFX™ kit	GE Healthcare, Munich
Promega RNA isolation kit	Promega, Mannheim
Quiagen isolation kit	Quiagen, Hilden
X-Gal	Peqlab, Erlangen

Table 19 – Other materials and enzymes used in this study

2.1.13 Media

dYT

16g peptone, 10g yeast extract, 5g NaCl and 15g agar (in case of solid medium) were filled with ddH_2O up to 1l, mixed and autoclaved.

Lysogeny Broth (LB)

10g peptone, 5g yeast extract, 10g NaCl and 15g agar (in case for solid medium) were mixed with ddH_2O up to 1l. The pH was adjusted with NaOH to 7.0 and the medium was autoclaved.

Super optimal broth with catabolite repression (SOC)

20g tryptone, 5g yeast extract, 0.5g NaCl and 10 ml KCl (250 mM) were mixed with 1l ddH_2O and the pH was adjusted to 7.0 with NaOH. The medium was autoclaved. Prior use $MgCl_2$ and glucose were added to final concentrations of and 10 mM and 20 mM respectively.

Amino acid powder mix (ProQuest^{TM})

Equal weights of adenine sulfate, alanine, arginine, aspartic acid, asparagine, cysteine, glutamic acid, glutamine, glycine , isoleucine, lysine, methionine, phenylalanine, proline, serine, threonine, tyrosine and valine were mixed.

Amino acid powder mix (Y2H screening)

The amino acid mix was done as in the ProQuest ^{TM} system, but adenine sulfate was left out and uracil added.

Yeast extract-peptone-dextrose medium + adenine (YPAD)

10g of yeast extract, 20g of peptone, 20g of dextrose, 100mg of adenine sulfate were filled with ddH_2O to 1l. Prior autoclaving the pH was adjusted with HCl to 6.0.

Synthetic Complete (SC) medium

For the synthetic complete medium 6.7g yeast nitrogen base without amino acids and 1.35g of amino acid powder mix were dissolved in 500 ml ddH_2O. After adjusting the pH to 5.9 with NaOH the media was autoclaved. 20g of agar agar were dissolved in 450 ml ddH_2O and autoclaved. After autoclaving SC medium was mixed with the agar agar and 50 ml of 40% sterile glucose was added. Depending on the auxotrophies to be tested, 8 ml of the appropriate amino acids were added respectively (uracil, histidine-HCL, leucine, tryptophane).

In case of the Y2H screening per liter SC medium 7.5 ml adenine were added, since this amino acid was not included in the amino acid powder mix.

H_2O Agar

4g agar-agar were dissolved in 400 ml ddH_2O and autoclaved.

1/2 Murashige Skoog (MS)

2.2g Murashige and Skoog medium (Sigma-Aldrich, Munich) were dissolved in 500 ml ddH_2O, the pH adjusted to 5.8 with KOH and autoclaved. 20g saccharose were dissolved in 500 ml ddH_2O and 9g agar agar were added and autoclaved. After autclaving, the Murashige and Skoog medium and the saccharose were united and 1 ml of 1000x MS-vitamins (Sigma-Aldrich, Munich) was added. In case of selection for transgene *A.thaliana* plants the respective antibiotic or herbicide was added (see table 1) and the media was poured into petri dishes.

2.2 Methods

2.2.1 Plant work

2.2.1.1 Seed sterilization

For growing of plants under sterile conditions seeds were collected in a 1.5 ml Eppendorf tube. 500 µl of ddH_2O were added. Afterwards the water was replaced with 500 µl 70% ethanol and incubated for 2 to 3 minutes. The ethanol was removed and the seeds were washed three times with 500 µl ddH_2O. While permanently shaking, the seeds were incubated in 500 µl seed sterilization solution (5% hypochlorite, 0.05% Triton X-100) for 20 minutes. The seeds were washed four times with 500 µl ddH_2O respectively. After the last washing step the H_2O was kept in the Eppendorf to facilitate transferring the seeds onto 1/2 MS plates or H_2O agar plates respectively. The petri dishes with the surface sterilized seeds were sealed with parafilm. After stratification for 2 days at four degrees, the petri dishes were put into a light chamber with 20°C and permanent light.

2.2.1.2 Growing of plants on soil

For growing *A.thaliana* seeds on soil “Pikiererde type T” (Bayerische Gärtnerei Genossenschaft) was used, which was sieved, mixed 2:1 with quartz sand and autoclaved. The trays with the seed pots were covered with autoclaving bags to prevent dry out. After a stratification period of two days at 8°C, the trays were transferred into a walk in growth chamber (Heraeus) with 18°C and permanent light. The developing plants were regularly watered until the ripening of the seeds.

2.2.1.3 Crossings

In order to cross *A.thaliana* plants in a controlled manner prior to crossing all flowers with ripe petals, already fertilized flowers and the siliques of the acceptor plant were removed. The oldest remaining flowers of the inflorescences were emasculated and all others removed. The stigmata/gynocea of the emasculated flowers were pollinated with the pollen of ripe anthers of the donor plant either immediately or on the following day. All crossed flowers were marked.

2.2.1.4 Rescue experiments

Different analyses showed that when a *pid enp* double mutant is made transgenic for an ENP wild type copy it is even by pyrosequencing difficult to show that the plant is indeed *enp/enp/ ENP*^{transgenic} and not *enp/ENP/ ENP*^{transgenic}. Therefore our lab has developed a special strategy to verify the functionality of an ENP-derived construct in an *enp pid* homozygous background. The rationale of these rescue experiments with ENP-derived constructs is based on two facts: first, on the stage dependent activity of the 35S promoter and second, on the late requirement of flower development for ENP activity. It has been demonstrated that homozygous *enp pid* (L*er* ecotype) plants do neither develop cotyledons nor flowers, thus generating blind ending stems (Treml et al., 2005).

In the embryo the onset of activity of the 35S promoter is late (heart stages and beyond). A 35S-full length ENP construct is therefore not capable to rescue the cotyledon-less embryo phenotype of homozygous *enp pid* (*laterne*). However, such constructs are fully functional during flower development due to the activity of p35S in adult stages. Such *enp pid _/enp pid ENP*^{transgenic} plants have a *pid/pid* phenotype and develop abnormal but fertile *pid*-flowers. As a corollary of p35S´ late embryo activity, these plants produce mostly 100% *laterne* seedlings (very rare exceptions with abnormal cotyledons). Among these again plants with *pid*-flowers grow. Thus, the functionality of ENP-derived constructs can be assessed by transformation of plants, which are crossed to *pid enp* segregating acceptors (or directly to the latter). In the next but one generation (herbicide resistant) *laterne* plants, which are undoubtedly homozygous *enp pid* are assessed for a possible flower rescue (Fig. 3).

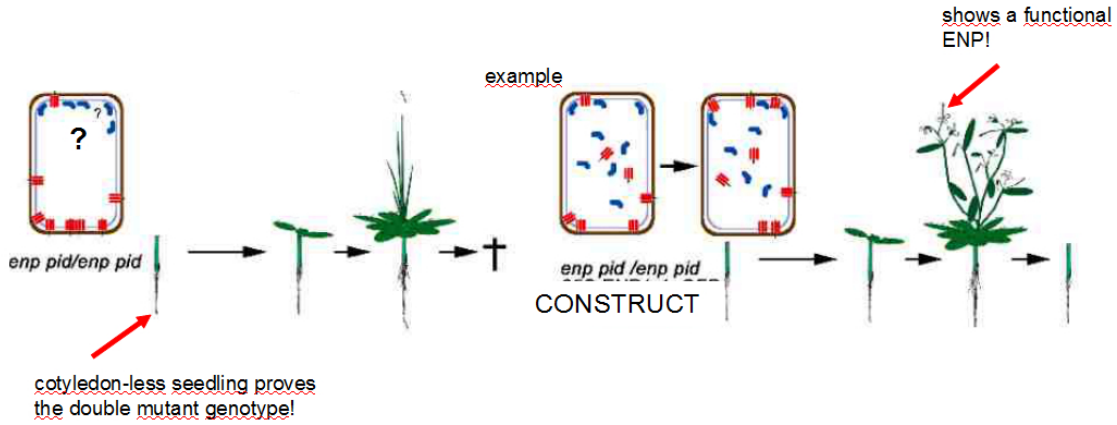

Figure 3 – Strategy for the rescue experiments of the adult *laterne* phenotype

2.2.2 Molecular methods

If not otherwise mentioned, routine lab methods followed the laboratory manual of Sambrook and Russel (2001).

2.2.2.1 Preparation of competent *E.coli* cells

For the preparation of chemical competent *E.coli* cells the rubidium chloride method was used. A 5 ml overnight culture of *E.coli* XL1 Blue cells were inoculated in 100 ml LB media containing 15 mg/l tetracycline. The cells were grown to an $OD_{600} < 0.5$ and then pelleted by centrifugation for 20 minutes at 4°C with 4500 rpm. The supernatant was discarded and the pellet resuspended in cold TBF1 buffer [100 mM $RbCl_2$, 30 mM KAc, 10 mM $CaCl_2$, 50 mM $MnCl_2$, 15% (v/v) glycerine; sterile filtrated]. After incubation on ice for 20 minutes the cells were centrifuged again at 4°C with 4000 rpm for 5 minutes. The pellet was resuspended in 3.6 ml cold TBF 2 buffer [10 mM NaMOPS (pH 7.0), 10 mM $RbCl_2$, 15 mM $CaCl_2$, 15% (v/v) glycerine; sterile filtrated]. After resuspension, the cells were aliquoted in 100 µl aliquots, snap frozen in liquid nitrogen and stored at -70°C.

2.2.2.2 Preparation of electrocompetent *A.tumefaciens* cells

500 ml of LB media was inoculated with 5 ml of a saturated culture of *A.tumefaciens* (strain: GV3101::pMP90). The culture was incubated at 28°C with vigorous agitation. At log phase (OD_{550} 0.5 - 0.8) the culture was chilled on ice and the cells were pelleted by centrifugation with 4000 rpm for 10 minutes at 4°C. The cells were washed three times by resuspending in 500 ml, 250 ml and 50 ml of ice cold ddH_2O respectively. After the washing steps, the pellet was finally resuspended in 5 ml of 10% (v/v) ice - cold, sterile glycerol. 50 µl aliquots were snap frozen in liquid nitrogen and stored at -70°C.

2.2.2.3 Isolation of DNA

For the isolation of genomic DNA from plant material the cationic surfactant cetyltrimethylammmoniumbromide (CTAB) was used. The fresh plant material of interest was transferred into 2 ml Eppendorf tubes with two steel balls and snap frozen into liquid nitrogen. The plant material was afterwards homogenized by the help of a steel ball mill (Retsch). 600 µl of CTAB buffer [1% (w/v) PVP MG400, 1.4 M NaCl, 100 mM Tris-HCl (pH 8.0), 20 mM EDTA (pH 8.0), 2% (w/v) CTAB] were added, the sample vortexed and incubated for 30 minutes at 65°C. Afterwards 750 µl of chloroform:isoamylalcohol (24:1) were added. 15 seconds of vortexing followed. After a 5 minute centrifugation at 14000 rpm at room temperature 450 µl of the sample were transferred into a new 1.5 ml Eppendorf tube and the DNA was precipitated with isopropyl alcohol.

2.2.2.4 Isolation of total RNA

For the isolation of total RNA different kits were purchased and used depending on the application. For the transcriptomics analysis the RNeasy Plant Mini kit (Quiagen) was used. For all other applications the total RNA kit from Macherey and Nagel was used. RNA isolations were performed according to the manual of the respective company.

2.2.2.5 Reverse transcription

For transcribing RNA into cDNA the Reverse Transcription kit from Applied Biosystems/Roche was used. The procedure was done according to the manufacturer's description. Generally oligo dTs were used. A general pipetting scheme is listed in table 20. The programme listed in table 21 was performed in a thermocycler. In general 7.7 µl of RNA were used. In case of the verification of the transcriptomics experiments, equal amounts of RNA between L*er* and *laterne* (*enp pid*) seedling tissue was used. The volume was filled up to 20 µl with nuclease free H_20, as supplied by the different kits.

Pipetting scheme for a 20µl reaction	
10x TaqMan RT® Puffer	2 µl
dNTPS (2.5 mM respectively)	4 µl
Oligo-d(T)s (50 µM)	1 µl
$MgCl_2$ (25 mM)	4.4 µl
RNase Inhibitor (20 U/µl)	0.4 µl
MultiScribe^{TM} RT	50 U/µl
RNA	7.7 µl

Table 20 – Pipetting scheme for a general reverse transcription reaction

Temperature [°C]	**Time [minutes]**
25	20
48	45
95	5

Table 21 – Programme for the reverse transcription

2.2.2.6 Polymerase chain reaction (PCR)

The polymerase chain reaction was used for the enzymatic *in vitro* amplification of a specific DNA segment of interest. For genotyping transgenic plants, as well as the verification of differentially expressed genes from the transcriptomics analysis as well as yeast lysate PCR and the TMO5/7 PCR a standard *Taq* was used. Table 22 list a standard pipetting scheme and table 23 lists the programme used. A mixture of One*Taq* (New England Biolabs) and Proofstart*Taq* (Quiagen) was used for cloning. Table 24 list the general pipetting scheme (One*Taq*/ProofStart*Taq*) and table 25 the programme, that was used.

Pipetting scheme for a 20 µl reaction	
5x Buffer	4 µl
10 mM dNTPs	0.2 mM
Fw Primer	20 pmol
Rev Primer	20 pmol
template	10 ng - 100 ng
Taq	0.3 µl
H_2O	up to 20 µl

Table 22 – Pipetting scheme for a PCR reaction (20 µl) with a standard *Taq*

Temperature [°C]		**Time [min]**	**Comment**
1	94	2	Initial denaturation
2	94	0.5	Denaturation
3	primer specific	0.75	Annealing
4	68	1min/kb	Extension; go back to 2; repeat 39 times
5	68	5	Final extension
6	4	∞	Hold

Table 23 – Thermocycler Programme for PCR reaction with standard *Taq*

Pipetting scheme for a 50 µl reaction	
5x Buffer	10 µl
dNTPs	0.2 mM
Betain	1 M
Fw Primer	25 pmol
Rev Primer	25 pmol
template	10 ng - 100 ng
One*Taq*	5 U
ProofStart *Taq*	0.5 U
H_2O	up to 50 µl

Table 24 – Pipetting scheme for a PCR reaction (50 µl) with the One*Taq*/ProofStart*Taq* mixture

Temperature [°C]		**Time [min]**	**Comment**
1	95°C	2	Initial denaturation
2	94°C	0.5	Denaturation
3	primer specific	0.75	Annealing
4	68	1min/kb	Extension; go back to 2; repeat 39 times
5	68	5	Final Eextension
6	4	∞	Hold

Table 25 – Pipetting scheme and thermocylcer programme for a PCR reaction with the One*Taq*/Proofstart *Taq* mixture

2.2.2.7 Agarose gel electrophoresis

DNA isolation and PCR products were subjected to 1% (w/v) agarose gels containing ethidium bromide at a final concentration of 0.5 µg/ml. Gels were cast and run in 1x TAE Buffer (40 mM Tris, 20 mM acetic acid, 1 mM EDTA). Standard size markers were the lambda Hind marker (Fermentas) and the GeneRuler 1kb + marker (Fermentas). Prior loading onto the gel, the samples were mixed with 10x loading buffer [50 mM EDTA, 0.25% (w/v) bromophenol blue and 25% (w/v) Ficoll].

2.2.2.8 Purification of DNA fragments

For isolation and concentration of DNA fragments (50 bp up to 10 kb) out of PCRs, agarose gels and restriction digests the GFX™ DNA and Gel Band Purification kit (GE Healthcare) was used. The purification was done according to the company's instructions.

2.2.2.9 Sequencing

Plasmids were purified using the phenol chloroform extraction, whereas PCR products were purified using the GFX™ DNA and Gel Band Purification kit (GE Healthcare) prior to sequencing through Eurofins MGW Operon services (Ebersberg).

2.2.2.10 Gateway® cloning

In comparison to standard cloning techniques the Gateway® cloning system (Invitrogen) is based upon a sequence specific recombination system of the bacteriophage lambda. It uses four recognition sequences, which are in a specific way recombined. *att*B sites can recombine with *att*P sites, creating *att*L sites. *att*L sites itself recombine with *att*R sites. Therefore it is initially important to create PCR products containing *att*B sites. The PCR products are recombined with *att*P sites in the donor vector with a BP reaction. Positive entry clones contain *att*L sites and are subjected to another recombination reaction with *att*R sites in different destination vectors. This recombination is done in the so called LR reaction.

2.2.2.10.1 BP reaction

The BP reaction was used for creating entry clones. Out of this entry clones it was possible by a single LR reaction to create destination clones, which were used for different downstream applications. In general the pDONR207 vector was used for creating entry clones. Table 26 shows the pipetting scheme for a BP reaction.

Compound	**Amount**
pDONR 207	50 fmol
*att*B PCR product	50 fmol
TE	up to 4 µl
BP clonase	1 µl

Table 26 – Pipetting scheme for a BP reaction

The calculations for fmol was done according to the following formula:
(x) ng = (fmol to be used) * (base pairs of *att*B product) * $\frac{660fg}{fmol} * \frac{1ng}{10\text{^}6fg}$
The BP reaction was incubated overnight at room temperature and afterwards stopped with 0.5 µl proteinase K for 10 minutes at 37°C. The BP reaction was typically transformed into Omni Max^{TM} 2-T1^{R} cells (Invitrogen). After plasmid mini- or midi preparations (see 2.2.2.14) and sequencing the correct entry clones were subjected to LR reactions.

2.2.2.10.2 LR reaction

The LR reaction was used to create destination clones for different downstream applications. In this study the destination vector pMDC83 was used for GFP fusions in the localization studies, pDest-DB and pDest-AD (Pascal Braun) were used for the Y2H screening, pDest-32 and pDest -22 (Invitrogen) were used for the ProQuest^{TM} Y2H system. Table 27 list the pipetting scheme for a typical LR reaction.

Compound	**Amount**
Destination vector	150 ng
Entry clone	150 ng
TE	up to 4 µl
LR clonase	1 µl

Table 27 – Pipetting scheme of a LR reaction

The LR reaction was incubated overnight at room temperature and afterwards stopped with 0.5 µl proteinase K for 10 minutes at 37°C. LR reactions were transformed into Omni Max^{TM} 2-T1^{R} cells (Invitrogen). After mini- or midi preparations (see 2.2.2.14) and sequencing the correct destination clones were used for their respective downstream applications.

2.2.2.11 Transformation of plasmids into *E.coli*

The transformation of plasmids into *E.coli* was done according to the heat shock method. 10 ng plasmid were added to 25 µl (Omni Max^{TM} 2-T1^{R} cells) or to 100 µl (XL1 Blue cells) of chemical competent *E.coli* cells. The sample was incubated on ice for 30 minutes. The heatshock was performed at 42°C for 2 minutes (in case of XL1 Blue cells) or 30 seconds (in case of Omni Max^{TM} 2-T1^{R} cells and Omni Max^{TM} ccdB survival cells). Afterwards 900 µl of dyT media (in case of XL1 Blue cells) or 250 µl of SOC media (in case of Omni Max^{TM} 2-T1^{R} or Omni Max^{TM}ccdB survival cells) were added. The sample was incubated in a shaker at 37°C for one hour. Afterwards the transformations were plated onto LB plates containing the construct specific antibiotic. The plates were incubated overnight at 37°C.

2.2.2.12 Electroporation of plasmids into *A. tumefaciens*

For the electroporation of *A. tumefaciens* typically the strain GV3101::pMP 90 (see 2.1.5.) was used. 30-50 ng of the plasmid to be electroporated were mixed with 100 µl electrocompetent *A. tumefaciens* cells and incubated on ice for 5 minutes. After electroporation in a BIO-RAD Gene Pulser with 25 µF, 400 Ω and 2.5 V 1 ml of precooled LB media was added and the cells were incubated at 28°C for 2 hours, while shaking. 50 µl of this culture was plated onto LB plates containing 35 µg/ml rifampicin and the respective antibiotic for plasmid selection. The plates were incubated for two to four days at 28°C.

2.2.2.13 Small scale transformation of plasmids into *S.cerevisiae*

The small scale *S.cerevisiae* transformation was done according to the ProQuest^{TM} two hybrid system manual (Invitrogen, 2002) with slight alterations according to a protocol from the guide to yeast genetics (Dreze et al., 2010).
10 ml of YPAD were inoculated with a colony of MaV203 and grown overnight with vigourous shaking (160 rpm) at 30°C. The next morning the OD600 was determined and the cells were diluted with YPAD medium to an OD_{600} of 0.4. The cells were grown an additional two to four hours at 30°C with vigorous shaking (160 rpm). The *S.cerevisiae* cells were pelleted at 2500 rpm for 5 min at room temperature and the pellet was resuspended into 10 ml of ddH_2O. The aforementioned centrifugation step was repeated and the cells were resuspended in 10 ml TE/LiAc [10 mM Tris-HCL (pH 8.0), 1 mM EDTA, 0.1 M LiAc]. After another centrifugation step the *S.cerevisiae* cells were resuspended into 2 ml of TE/LiAc and 10 ml of TE/LiAc/PEG [10 mM Tris-HCL (pH 8.0), 1 mM EDTA, 0.1 M LiAc, 35.2% (v/v) PEG] solution supplemented with 200 µl of boiled carrier DNA (salmon sperm DNA) were added. The solution was mixed by inversion. For each transformation 120 µl of the *S.cerevisiae* suspension was mixed with 1 µg of plasmid DNA. The solution was incubated for 30 minutes at 30°C. Afterwards the cells were heat-shocked at 42°C for 7 minutes. The cells were centrifuged at 800 g for 5 minutes and then resuspended in 100 µl of sterile ddH_2O. After a centrifugation step, as the one before, the cells were resuspended in 50 µl sterile ddH_2O, were plated onto SC-Leu-Trp plates and incubated for two to three days at 30°C.

2.2.2.14 Plasmid mini- and midi preparation from *E.coli*

The isolation of plasmid DNA from *E. coli* in small scale (mini preparation) or intermediate scale (midi preparation) was done according to the principle of the alkaline lysis. For this 1.5 ml or 50 ml of LB media containing the construct specific antibiotic were inoculated with a single colony of *E.coli* containing the plasmid of desire and incubated overnight at 37°C and 140 rpm. The liquid culture was transferred into either an 2 ml Eppendorf tube or a 50 ml falcon. The culture was centrifuged for five minutes at 14000 rpm or 4500 rpm. The supernatant was completely removed and the pellet resuspended into either 100 µl or 1.5 ml of solution 1 [25 mM Tris-HCl (pH 8.0), 10 mM EDTA, 50 mM glucose, 5 mg/ml lysozyme].

The sample was incubated for 10 minutes on ice. Afterwards 200 µl or 3 ml freshly prepared solution 2 [0.2 M NaOH, 1% (w/v) SDS] were added and another incubation for 10 minutes on ice followed. Finally 150 µl or 2.25 ml of solution 3 [3 M NaAc; pH4.8] were added and again the preparations were incubated on ice for 10 minutes. The sample was centrifuged at 14000 rpm for 10 or 20 minutes at 4°C. The supernatant was transferred into a new Eppendorf tube or centrifugation tube and precipitated with 0.7 V isopropyl alcohol. The DNA pellet was resuspended into 100 µl or 0.8 ml TE [10 mM Tris-HCl (pH 8.0),1 mM EDTA . Na_2(pH 8.0)] and mixed with 1 V 5 M LiCl and incubated on ice for 10 minutes. The sample was centrifuged for 10 minutes at 14000 rpm and 4°C. The supernatant was transferred into a new Eppendorf tube and precipitated with isopropyl alcohol. The resulting pellet was resuspended in 100 µl or 200 µl T0.1E [10 mM Tris-HCl (pH 8.0), 0.1 mM EDTA . Na_2(pH 8.0)] and afterwards the remaining RNA was removed with a RNase digest (10 µg RNase/ml DNA) for 30 minutes at 37°C. The RNase was stopped and removed with a phenol chloroform extraction and a following isopropyl alcohol precipitation. The final pellet was resuspended in 50 µl or 200 µl T0.1E [10 mM Tris-HCl (pH 8.0),0.1 mM EDTA . Na_2(pH 8.0)]. The concentration of the isolated plasmid DNA was determined with a nanophotometer (Implen) and the purity of the isolated plasmid DNA was checked on an agarose gel (see 2.2.2.7). The correctness of the inserted DNA sequence was checked by sequencing (see 2.2.2.9).

2.2.2.15 Plasmid mini preparation from *A.tumefaciens*

This plasmid isolation was done in order to control for constructs that were transferred into *A.tumefaciens*. 10 ml of LB media containing rifampicin and kanamycin were inoculated with a single colony of transformed *A.tumefaciens* and incubated for two to three days at 28°C in a shaker. 2 ml of the culture were transferred into a 2 ml Eppendorf tube and centrifuged for 5 minutes at 14000 rpm. Afterwards the supernatant was removed. Another 2 ml of the liquid culture was added to the same Eppendorf tube and again centrifuged at 14000 rpm for 5 minutes. The procedure was repeated another 2 times. The pellet was resuspended in 150 µl solution 1 [25 mM Tris-HCl (pH 8.0), 10 mM EDTA, 50 mM glucose]. 300 µl of freshly prepared solution 2 [0.2 M NaOH and 1% (w/v) SDS] were added, the Eppendorf tube inverted and incubated for 5 minutes on ice. Afterwards 225 µl of 7.5 M ammonium acetate were added to the Eppendorf tube and 5 minutes incubated on ice. The lysed cells were centrifuged for 10 minutes at 4°C. 600 µl of the supernatant were transferred into a new 1.5 ml Eppendorf tube and digested with RNase (20 µg/ml) for 30 minutes at 37°C. The RNase was stopped and removed with a phenol chloroform extraction. Afterwards an isopropyl alcohol precipitation was done and the resulting pellet was resuspended in 20 µl TE [10 mM Tris-HCl (pH 8.0), 1 mM EDTA . Na_2(pH 8.0)]. For checking the correctness of the isolated plasmid the plasmid was used as template in a PCR (see 2.2.2.6).

2.2.2.16 Plant transformation (floral dip)

For generating stable *A.thaliana* transformants the floral dip method after Clough and Bent (1998) was used. In order to increase the transformation efficiency, the main stem of the *A.thaliana* plants was cut one to two weeks prior transformation. This induces the formation of side stems and will lead to more inflorescences in turn. Right before transformation the existing siliques were removed.
A single *A.tumefaciens* colony, which was tested for the correct insert, was inoculated into 10 ml LB media containing rifampicin and the construct-specific antibiotic and incubated for two to three days at 28°C. This starting culture was transferred into 200 ml LB media containing the same antibiotics and again incubated at 28°C at 160 rpm for another two to three days. The cells were centrifuged for 20 minutes at 3600 rpm and at 4°C. The pellet was resuspended in 200 ml transformation buffer [10 mM $MgCl_2$, 5% saccharose, 0.05% (v/v) silwet-77]. Four to seven plants to be transformed were dipped into the *A.tumefaciens* suspension for 20 seconds. The transformed plants were put onto a tray, watered and covered with a plastic bag, which was blown up and tightly sealed in order to increase the CO_2 content and the humidity. The trays were put into a walk-in growth chamber with 18°C and a day/night light rhythm for two to three days. Afterwards the plastic bag was removed and the plants were watered regularly until the ripening of the seeds. In order to increase the transformation efficiency the floral dip was applied to the same plants a second time one week after the initial transformation.

2.2.3 Yeast two-hybrid screening

In order to find candidates interacting with ENP and with NPY4/MEL4 the Y2H pipeline initially described by Dreze et al. (2010) was used. This system consists of three steps, namely primary screening, phenotyping and retesting, which ensure a high-throughput and a reliable removal of artifacts. In this thesis different site directed mutagenesis constructs of ENP, as well as deletion constructs of ENP and NPY4/MEL4 and domain swap constructs of these proteins were subjected to screening. Existing pDONR207 vectors were recombined into the destination vector pDest DB (see 2.1.10) with the help of the LR reaction (see 2.2.2.10.2), which in the following are named DB constructs. Clones were sequenced for a correct insert and afterwards transformed into Y8800 *S.cerevisiae* strain (see 2.1.6). The correctness of the transformation into *S.cerevisiae* was ensured by yeast lysate PCR (see 2.2.3.2.4). Positive *S.cerevisiae* colonies were inoculated into SC-Leu media and after being grown for two to three days at 28°C were mixed with an equal amount of 40% (v/v) glycerol and stored at -70°C. The prepared glycerol stocks represented the initial material for the Y2H screening against an AD-pool of 12000 open reading frames (ORFs), which sums up to about 40% of the whole *A.thaliana* genome.

2.2.3.1 Primary screening

2.2.3.1.1 Mating

All glycerol stocks of DB constructs, the six controls (see 2.1.11.) and the empty AD construct as auto activator control, as well as the glycerol stock of the AD master pool plate were thawed. 200 µl of each DB construct respectively were inoculated in 20 ml SC-Leu media. 5 µl of each well of the AD master pool plate were inoculated in 160 µl SC-Trp media on a 96-well plate. 5 µl of the empty AD construct respectively were inoculated in 160 µl SC-Trp on the same 96-well plate on positions A-H11. In order to allow for gas exchange while growing, the 96-well plate was covered with a membrane. 50 µl of all controls respectively were inoculated in 10 ml SC-Leu-Trp media. All cultures were incubated at 30°C for three days on a shaker. For each DB construct to be tested, 5 µl of each well of the AD pool master plate was spotted on a single YEPD plate using a liquid handling robot (TECAN). Spots were allowed to dry for 5-10 minutes and afterwards 5 µl of the DB construct to be tested were spotted on top of the AD pool spots of the respective YEPD plate. The six Y2H controls (see 2.1.11) were spotted onto every plate and afterwards all mating plates were incubated at 30°C for 14-18 hours.

2.2.3.1.2 Replica plating

Mated yeast cells were replica-plated onto SC-Leu-Trp-His + 1 mM 3-Amino-1,2,4-triazole (3AT) and to detect *de novo* autoactivators onto SC-Leu-His +1 mM 3AT + 1 mg/l cycloheximide (CHX) plates with the help of a replica-plating block. All screening plates were incubated at 30°C for 14-18 hours.

2.2.3.1.3 Replica cleaning

All screening plates were replica cleaned to reduce background. This was done by placing each plate on a piece of velvet stretched over a replica-plating block and pushing evenly on the plate to remove excess *S.cerevisiae* cells. All replica cleaned plates were incubated at 30°C for five days.

2.2.3.1.4 Primary positives

Primary positive colonies from the screening plates were picked and resuspended in a 96-well plate containing 160 µl of liquid SC-Leu-Trp/well. Primary positive colonies were those colonies that grew better than control 1, which depicts the background growth and where the corresponding spot on the respective CHX plate was negative. It is possible to obtain different interactions per spot. That is why at most three colonies per spot were picked. The culture plates were incubated at 30°C for 72 hours.

2.2.3.2 Phenotyping

The culture plates with the primary positives were directly used for the phenotyping. For this 5 µl/well of each culture plate was spotted on a SC-Leu-Trp plate. Onto each plate the six Y2H controls were added. All plates were incubated for 48 hours at 30°C.

2.2.3.2.1 Replica plating and cleaning

Each SC-Leu-Trp plate was replica plated onto four phenotyping plates, namely SC-Leu-Trp-His + 1 mM 3AT, SC-Leu-Trp-Ade, SC-Leu-His + 1 mM 3AT + 1 mg/l CHX and onto SC-Leu-Ade + 1 mg/l CHX. The first two plates were used for the assessment of Y2H reporter activity, whereas the two CHX plates allow the detection of autoactivators. All phenotyping plates were replica cleaned immediately after replica plating and incubated at 30°C for 72 hours.

2.2.3.2.2 Scoring

The phenotyping plates containing CHX were used to assess *de novo* autoactivators. Any *S.cerevisiae* spot showing growth on these plates were not considered for further processing. Candidate interactions were identified by *S.cerevisiae* spots that activated both reporter genes, meaning that they showed growth on the -His plates as well as on the -Ade plates. All secondary positives were patched onto fresh SC-Leu-Trp plates and incubated for 48 hours at 30°C.

2.2.3.2.3 Yeast lysis

The yeast lysis was done by resuspending a small amount of *S.cerevisiae* cells into 15 µl yeast lysis buffer [2.5 mg/ml zymolase in 0.1 M sodium phosphate buffer; pH 7.4]. The mixture was put into the thermocycler and subjected to the programme given in table 28.

Temperature [°C]	**Time [min]**
37	15
95	5
10	∞

Table 28 – Thermocycler programme for *S.cerevisiae* cell lysis

To each sample 100 µl of filter-sterilized H_2O was added. Afterwards the sample was centrifuged at 800 g for 10 minutes and stored at -20°C.

2.2.3.2.4 Yeast lysate PCR

For the yeast lysate PCR the general PCR pipetting scheme (see 2.2.2.6) and a 30 µl reaction was used. 3 µl of yeast cell lysate was added. Table 29 depicts the programme that was used for the yeast lysate PCR.

	Temperature [°C]	**Time [minutes]**	**Comment**
1	94	4	Initial denaturation
2	94	0.5	Denaturation
3	58	0.5	Annealing
4	68	3-7	Elongation go back to 2; repeat 34 times
5	68	10	Final elongation
6	10	∞	

Table 29 – Yeast lysate PCR programme

2.2.3.3 Verification

Whereas in the initial screening spontaneous autoactivators are identified in every step, the verification step protects for example from mutations elsewhere in the yeast genome and ensures robust high quality data. The verification step was performed four times independently by five researchers (Michaela Matthes, Ottilie Peis, Moritz Jakab and Xiaomeng Yang/Ramon Angel Torres-Ruiz). The individual steps of the verification process consisted of mating and phenotyping according to the initial screening processes. Initially the *S.cerevisiae* clones were rearrayed corresponding to the candidate Y2H interacting pairs.
The individual glycerol stocks of DB and AD constructs were thawed and 5 µl of each were inoculated in 160 µl SC-Leu (for DB) and SC-Trp (for AD) media into 96-well plates. All plates were incubated for 72 hours at 30°C on a shaker. 5 µl of each well of the AD plates was spotted onto YEPD plates with the help of a liquid handling robot (TECAN). The spots were let to dry for five to ten minutes. Afterwards 5 µl of each well of the corresponding DB plates were spotted on top of the AD spot. All six Y2H controls were added to each mating plate, which were afterwards incubated for 14 to 18 hours at 30°C. In order to select for diploids the mating plates were replica plated onto SC-Leu-Trp plates, which were then incubated at 30°C for 14 to 18 hours. The phenotyping of the diploid *S.cerevisiae* cells was done by replica plating the SC-Leu-Trp plates onto SC-Leu-Trp-His + 1 mM 3AT, SC-Leu-His + 1 mM 3AT + 1 mg/l CHX, SC-Leu-Trp-Ade and SC-Leu-Ade + 1 mg/l CHX plates. The phenotyping plates were replica cleaned immediately after replica plating and incubated at 30°C for 3 days. The scoring was done as described in 2.2.3.2.2. Verified interactions were those, which scored positive in at least three out of the four plates and which were never scored as autoactivators.

2.2.4 Direct interaction testing with the ProQuest™ system (Gateway®)

Having obtained possible interaction partners for ENP from a previous global screening (Treml, 2008) and from the global screening done in this thesis possible candidates were directly tested using the ProQuest™ System (Invitrogen). The possible interaction partners were cloned into the vectors pDest-32 (see 2.1.10) and pDest-22 (see 2.1.10) respectively. The obtained clones were transformed into the *S.cerevisiae* strain MaV203 (see 2.1.6) and positive diploid *S.cerevisiae* colonies were subjected to different reporter activation tests. The tested interaction pairs are listed in table 30.

pDest-32 Construct	**pDest-22 Construct**
NPY4 (At2g23050)	NPY4 (At2g23050)
NPY4 (At2g23050)	ENP
ENP	NPY4(At2g23050)
ENP	ENP
ENP BTB POZ	ENP BTB POZ
ENP BTB POZ	NPY4 BTB POZ
NPY4 BTB POZ	ENP BTB POZ
NPY4 BTB POZ	NPY4 BTB POZ
ENP	PDK1
ENP	VOZ1

Table 30 – Tested interaction pairs with the ProQuest™ System (Invitrogen)

To reduce false positives the ProQuest ™ sytem uses three reporter genes to test for positive interactors, where the promoter regions of these three reporter genes are unrelated (except for the presence of Gal4 binding sites) (Invitrogen, 2002). In order to test for reporter activity of possible protein interactions after *S.cerevisiae* transformation and selection for diploid *S.cerevisiae* cells, a masterplate, containing all Y2H controls (see 2.1.11) as well as at least four different colonies of the interactions to be tested. They were streaked onto a fresh SC-Leu-Trp plate and incubated for 18 hours at 30°C. An example of a masterplate is given in figure 4.

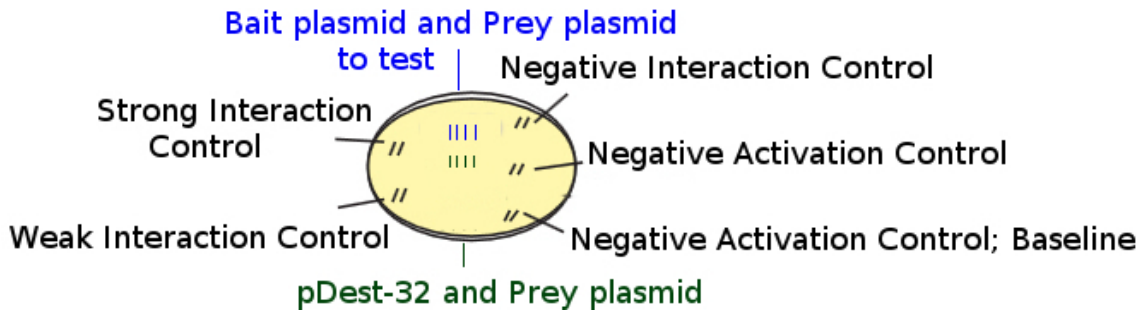

Figure 4 – Example of a masterplate, which was used for testing reporter gene activity in the ProQuest™ system (Invitrogen)

2.2.4.1 *HIS3* reporter activity

The induction of the *HIS3* reporter gene by two hybrid dependent transcriptional activation allows cell growth on plates lacking histidine. *HIS3* can be specifically inhibited in a dose dependent manner by 3AT. By determining the threshold of resistance to 3AT and including that concentration of 3AT in plates lacking histidine, even slight increases in *HIS3* reporter gene expression are detected. In order to assay *HIS3* reporter gene activity, the masterplate was replica plated onto SC-Leu-Trp-His + 3AT (10 mM, 25 mM, 50 mM, 100 mM) plates and immediately replica cleaned. Afterwards, the plates were incubated for 24 hours at 30°C and again replica cleaned. After two days incubation at 30°C the phenotypes were determined.

2.2.4.2 *URA3* reporter activity

Similarly to the induction of *HIS3*, the induction of the *URA3* reporter gene by a two hybrid dependent transcriptional activation allows cell growth on plates lacking uracil. At the same time, a second phenotype can be assayed here with the addition of 5-fluoroorotic acid (5-FOA). In case of a two hybrid dependent induction of *URA3* 5-FOA is converted into 5-fluorouracil, which is toxic (Boeke et al., 1987). Therefore cells containing interacting proteins grow when plated on medium lacking uracil, but do not grow, when plated on medium containing 5-FOA. The masterplate was replica plated on SC-Leu-Trp-Ura plates and onto SC-Leu-Trp + 0.2% (w/v) 5-FOA. The 5-FOA plates were immediately replica cleaned and afterwards all plates were incubated for 24 hours at 30°C. Following incubation, the plates lacking uracil and the plates containing 5-FOA were replica cleaned. After incubation for another two days at 30°C the phenotypes were determined.

2.2.4.3 *LacZ* reporter activity

The induction of the *lacZ* gene was assayed with an 5-bromo-4-chloro-3-indolyl-β-D-galactopyranoside (X-gal) assay resulting in a blue colour for positve interactors. For the X-gal assay the masterplate was replica plated onto a nitrocellulose membrane on a YPAD plate and colonies were grown for 24 hours at 30°C. After incubation the membrane was shock frozen in liquid nitrogen and put onto two Whatmann papers soacked with X-gal assay buffer (Invitrogen, 2002). The assay was put into 37°C and incubated for 24 hours. Blue color development was documented after 1, 3, 5 and 24 hours.

2.2.5 Transcriptomics

2.2.5.1 Seed sterilization

In order to adjust the plant handling and experimental setup with a previous done metabolomics analysis (Gülersonmez, 2011) the seed sterilization method and the growing of the seedlings was conform to the mentioned study. Seed material of L*er* and *laterne* (manually segregated out of a seed pool from *enp pid/enp* + plants) were collected in 1.5 ml Eppendorf tubes and covered with 1 ml of ddH_2O. The tubes were briefly vortexed and centrifuged for 20 seconds at 2000 rpm. The ddH_2O was afterwards removed and replaced with seed sterilization solution (50% (v/v) ethanol, 0.5% (v/v) sodium hypochlorite, 0.1% (v/v) Triton-X). The seeds were incubated in sterilization solution for exactly 2 minutes, which was then removed and replaced by ddH_2O. The seeds were washed four times with 1 ml ddH_2O respectively and then plated onto H_2O agar + 100 mg/ml Amp plates. The seeds were let to stratify for 2 days in the cold room (8°C) and transferred onto a metabolomics stand in a walk-in growth chamber, where the roots could grow vertically along the agar plates, facilitating the harvest of the seedling material. The plates were rotated randomly on the metabolomics stand daily in order to adjust for possible light differences at different positions on the metabolomics stand. The seedlings were grown for exactly four days in the walk-in growth chamber with continuous light and were then immediately shock frozen in liquid nitrogen.

2.2.5.2 Total RNA isolation from seedlings

For the isolation of RNA for the performed transcriptomics analysis four independent pools of L*er* and *laterne* seedlings were used. Total RNA was isolated using the Quiagen RNeasy Plant Mini Kit following the manufacturer's instructions.

2.2.5.3 Determination of the RNA quantity and quality

In order to determine the RNA quantity and quality of the isolated RNA samples to be used for the transcriptomics analysis the Bioanalyzer (Agilent) was used. Next to the concentration of the RNA to be analyzed the Bioanalyzer gives a RNA Integration Number (RIN), which gives the quality of the isolated RNA. Only samples with a RIN higher than 8 were taken for further analysis.

2.2.5.4 Preparation of a labeling reaction

As internal standards spike-in dilutions were used. Spike A was used for Cy3 labeled samples, whereas Spike B was used for Cy5 labeled samples. For the spike in dilutions initially a 1:20 dilution of the stock spike in solutions was done. Out of this initial dilution a 1:20 dilution was made, which was subjected to a final 1:4 dilution. This 3rd dilution was taken into the labeling reaction. The pipetting scheme for one labeling reaction is shown in table 31.

Compound	Amount
RNA	913 ng
H_2O	to 8.3 µl
T7 Promoter	1.2 µl
Spike A or B (3rd)	2 µl

Table 31 – Pipetting scheme for a labeling reaction

The samples were put into a thermal cycler and subjected to the following programme: 65°C for 10 minutes and 4°C for 5 minutes. Afterwards a cDNA synthesis was performed.

2.2.5.5 cDNA synthesis

The pipetting scheme for one cDNA synthesis reaction is given in table 32.

Compound	Amount
5x First Strand Buffer	4 µl
0.1 M DTT	2 µl
10 mM dNTP	1 µl
MML V-RT	1 µl
RNase Out	0.5 µl
RNA/Spike-in sample	11.5 µl

Table 32 – Pipetting scheme for the cDNA synthesis as done for the transcriptomics analysis

The samples were put into a thermal cycler, performing the following programme: 40°C for 2 hours, 65°C for 15 minutes and 4°C for five minutes.

2.2.5.6 cRNA synthesis

Table 33 depicts the pipetting scheme for one cRNA synthesis of the transcriptomics analysis.

Compound	Amount
Nuclease free H_2O	15.3 µl
4x Transcription Buffer	20 µl
0.1 M DTT	6 µl
NTP mix	8 µl
50% PEG	6.4 µl
RNase out	0.5 µl
Inorganic Pyrophosphatase	0.6 µl
T7 RNA Polymerase	0.8 µl
Cy3-CTP or Cy5-CTP	2.4 µl

Table 33 – Pipetting scheme for one cRNA synthesis for the transcriptomics analysis

60 µl cRNA synthesis mix was added to each sample tube and incubated for 2 hours at 40°C. Afterwards the labeled RNA was purified.

2.2.5.7 Purification of the labeled amplified cRNA

The labeled and amplified cRNA was purified with the RNeasy mini spin kit (Quiagen) according to the manufacturer's instructions.

2.2.5.8 Determination of yield and specific activity of the labeling reaction

The yield and the specific activity of a labeling reaction was determined using the following formulas:

1) (Concentration of cRNA) * (elution volume) / 1000 = µg of cRNA

2) (Concentration of incorporated Cy3 or Cy5) / (Concentration of cRNA) * 1000 = pmol Cy3 or Cy5 per µg of cRNA

The concentrations of cRNA as well as of incorporated Cy3 or Cy5 were measured using an Implen spectrophotometer. Samples with a specific activity of greater than eight were taken for further analysis.

2.2.5.9 Fragmentation and hybridization

The pipetting scheme for one fragmentation reaction is given in table 34.

Compound	**Amount**
Cy3 labeled sample	825 ng
Cy5 labeled sample	825 ng
10x Blocking agent	11 µl
Nuclease free H_2O	to 52.8 µl
25x Fragmentation Buffer	10 µl

Table 34 – The pipetting scheme for one fragmentation reaction

Each reaction was put to 60°C for 30 minutes. Afterwards 55 µl of GEX Hyb Buffer were added and the samples were hybridized with Agilent microarrays.

2.2.5.10 Washing

After hybridization, the chamber + gasket + slide were dismounted and the slide was washed for 1 minute in wash buffer 1 (Agilent). Afterwards the slide was transferred into prewarmed (37°C) wash buffer 2 (Agilent) and washed exactly for 1 minute. Another wash in acetonitrile for one minute and in stabilizing and drying solution (Agilent) for another minute followed. After drying in darkness for about 15 minutes, the slide was put into a plastic holder, wrapped into aluminum foil and brought for scanning.

2.2.5.11 Scan

The scanning of Agilent microarrays was performed by IMGM services (Martinsried). The scanning parameters given in table 35 were used.

Parameter	Setting
Scan region	Scan area (61 x 21.6 mm)
Scan resolution	5 µm
Sum scanning mode	Singe Pass
Dye Channel	Red and Green
Green PMT	XDR Hi 100%; XDR Lo 10%
Red PMT	XDR Hi 100%; XDR Lo 10%

Table 35 – Scanning parameters for scanning the Agilent microarrays

2.2.5.12 Data evaluation

The transcriptomics data was analysed using the Bioconductor software (www.bioconductor.org) from the R package (http://cran.r-project.org). For differential gene expression analysis the limma package (Smyth, 2004) was used.

2.2.5.13 GO enrichment analysis

For the Gene Ontology (GO) enrichment analysis the software ClueGo was used (Bindea et al., 2009). The analysis was based on a two-sided (enrichment/depletion) test. A kappa score of 0.5, representing a medium stringency, was used. Further, the Bonferroni method for adjusted p-values was applied and the network specificity was set to be medium. The restriction on GO terms was set to have a minimum level of three and a maximum level of eight, whereas a grouping of functional terms was made in case at least eight genes or at least 5% of genes were represented in the group. The p-value cutoff was set to be 0.05 and the leading term of a functional group was determined to be the term with the highest percentage of genes/term. The created networks were visualized using Cytoscape 3.0.2 (Shannon et al., 2003).

2.2.5.14 Pathway mapping analysis

For the display of the transcriptomics data onto diagrams of metabolic pathways, the software MapMan, version 3.6.9 (Thimm et al., 2004; Usadel et al., 2005) was used. As input set all statistically significant and differentially expressed genes (p-value < 0.05; log fold change (FC) < -1 and log FC >1) were used.

2.2.5.15 Common transcription factor binding sites

The *in silico* promoter analysis for common transcription factor binding sites was performed with the program Common TFs out of the Genomatix software suit (www.genomatix.de; vers. 3.0). The software takes a set of input genes, searches for their promoter regions and detects

transcription factor binding sites, which are common to a set of promoter regions. A subset of genes from the transcriptomics results was used as input set, which referred to the GO cluster leaf morphogenesis.

2.2.6 Confocal laser scanning microscopy

For the subcellular localization of GFP, YFP and FM4-64 in transgenic *A.thaliana* embryos and roots the confocal laser scanning microscope (CLSM) LSM FV100 (Olympus) and its specific software FluoView was used.
Siliques of transgenic *A.thaliana* were opened and the ovules were transferred into a drop of water on an object slide. The slide was covered with a cover slip. In order to get the embryos out of the ovule the cover slip was slightly pressed on the slide. For the documentation of the subcellular localization of the fluorophores the settings depicted in table 36 were used. The laser intensity was kept at 12 to 15%. Further, a resolution of 512 x 512 was chosen for saving a picture, which was captured as mono-directional xyz scan (one to two µm steps; Calman Filter; four repetitions per scanned line).

Device	**Setting**
Objective	UPLSAPO 60xW(NA1,2) and 10x
GFP	Laser: 488 nm
	wavelength: 500 nm - 550 nm
YFP	Laser: 488 nm
	wavelength: 500 nm - 550 nm
FM4 - 64	Laser: 561 nm

Table 36 – Settings for the Olympus Fluoview laser scanning microscope

2.2.7 Pharmacological studies

In order to study the signaling of ENP in embryos different inhibitors and chemicals were applied to ovules. Table 6 lists the chemicals and concentrations used. The general procedure of the pharmacological studies with embryos was as follows: Ovules of 10-15 siliques from pPIN1:PIN1::GFP (heart stage) or p35S:GFP::ENP1-4 (mid-torpedo stage) transgenic *A.thaliana* plants were collected in a 1.5 ml Eppendorf tube with 500 µl H_2O mQ. Most of the collected ovules were transferred to a new 1.5 ml Eppendorf tube containing 500 µl of a 25 mM PBA (ENP) or 30 mM PBA (PIN1) solution and incubated for 15 (ENP) or 10 minutes (PIN1) respectively. An aliquot remained in H_2O as control. An aliquot of the PBA incubation was checked on the CLSM, by transferring the ovules to an object slide and squeezing the embryos out of the ovules by the help of a cover slip. Embryos prepared in that way were analyzed with the CLSM. The remaining ovules were washed three times with H_20 by transferring them three times into new Eppendorf tubes with each of them containing 500 µl H_2O mQ. After the third wash the ovules were aliquoted into new 1.5 ml Eppendorf tubes

containing different inhibitors or H_2O mQ for two hours. After incubation the ovules were transferred on object slides, where the embryos were squeezed out by the help of a cover slip and then subjected to CLSM analysis. After all analyses were done the control embryos, which were incubate for the whole time of the experiment in H_2O mQ were analyzed with the CLSM. This work also dealt with the effect of PBA on ENP in the root. For this usually 24 roots of either 10 day old p35S:GFP::ENP1-4 seedlings or pPIN2:PIN2::GFP seedlings were collected in 1/2 MS media without sugar. 16 seedlings were transferred into a 5 mM PBA solution and incubated for 15 minutes. Eight of them were analyzed using the CLSM. The remaining eight seedlings were washed three times in 1/2 MS media without sugar, afterwards incubated for two hours in 1/2 MS media without sugar and then subjected to CLSM. Following these steps, control seedlings, which were incubated in 1/2 MS without sugar for the entire time of the experiment were checked with the CLSM.

2.2.8 Chemical treatment of siliques

In order to assess the effect of PBA and different analogues siliques of Col-0 and L*er* plants were brushed with the respective chemical (see table 7) once and then put into the walk-in growth chamber until the ripening of the seeds. The seeds of the individual siliques were harvested. The seeds of each silique were put separately onto H_2O agar + 100 mg/ml Amp plates, stratified for two days at 4°C and afterwards put onto continuous light until the seedling phenotype could be assessed.

3 Results

3.1 Intrinsic and extrinsic factors controlling the cellular polarity of ENP

ENP is a soluble protein, associated to the PM with a molecular mass of 66.4kDa (Furutani et al., 2007; Treml, 2008; Zweigardt, 2010; Furutani et al., 2011). ENP is primarily expressed in the epidermal cell layer of the embryo, in particular the L1 layer at the site of organ initiation (Furutani et al., 2007). On a subcellular scale ENP localizes to the apical site of the PM in epidermal cells of cotyledons (Treml, 2008; Zweigardt, 2010; Furutani et al., 2011), where it colocalizes with PIN1 (Furutani et al., 2007; Zweigardt, 2010). Sequence-based polarity signals in ENP, as well as extrinsic factors important for the establishment or maintenance of its cellular polarity were almost not known (Treml, 2008; Zweigardt, 2010).

3.1.1 Extrinsic factors

Extrinsic factors, which could be important for the cellular polarity were so far elusive, since ENP showed a robust and strong association to the PM. Previous studies showed an insensitivity of ENP to BFA (Zweigardt, 2010), which was shown to relocate PIN1 from the PM into BFA compartments (Geldner et al., 2001; Geldner et al., 2003). Further, synthetic auxins (NAA, 2,4D) and toxins, inhibiting protein translation (CHX), interfering with the correct establishment of the cytoskeleton (oryzalin, cytochalasin D; cytD), influencing the endocytosis of vesicles (wortmannin) and PM proteins (fillipin) or those impeding auxin in- or efflux (triiodobenzoic acid; TIBA, naphthoxyacetic acid; NOA, 1-N-naphthylphthalamic acid; NPA) were not able to detach ENP from the PM into the cytosol (Zweigardt, 2010). This would have given the opportunity to analyze factors required for the subcellular targeting of ENP to the PM. Recent work (Bassil et al., 2004) and preliminary observations (R.A.Torres-Ruiz personal communication) indicated that boronic acids, especially PBA could be used to challenge the association of proteins to the membrane. Therefore an experimental system was established, which allowed the use of PBA to study the subcellular targeting of ENP to the PM in torpedo stage embryos, harbouring a transgenic p35S:GFP::ENP. Initial steps were the determination of efficient working concentrations. By incubating ovules harboring the embryos, relatively high concentrations (mM range) had to be applied. It further appeared that the higher the concentration the less time for the incubation was needed in order to see an effect on the localization of ENP. Nevertheless, there was a negative correlation between high concentrations and an effective washout of PBA. Series of different concentrations and incubation times ranging from 5 mM to 30 mM and 10 minutes to 1 hr revealed the best concentration to be 25 mM with an incubation time of 15 minutes. This condition allowed an effective detachment of ENP from the PM leading to an accumulation in the cytosol (Fig. 5A). It further allowed a retargeting to the PM by a subsequent 2 hour washout (Fig. 5B). With this tool in hand it was possible to study the effect of different inhibitors on the subcellular targeting of ENP as similarly done by

Geldner et al. (2001) with PIN1.

3.1.1.1 The subcellular trafficking of ENP is actin dependent

First, cytoskeletal requirements for the relocation of ENP to the PM after PBA treatment were assessed. Therefore, cytD, which is generally known to inhibit actin polymerization and oryzalin, which depolymerizes microtubules were applied after PBA pre-treatment. The application of 20 µm cytD impaired the relocalization of ENP to the PM. Instead of accumulating at the PM again, ENP was predominantly found in small intracellular patches (Fig. 5D). On the contrary, oryzalin treatment (10 µm and 20 µm) after PBA incubation did not block the relocalization of ENP with comparable strength. The protein was mainly found at the PM again (Fig. 5E), but with increasing concentrations of oryzalin (40 µm) the retargetting of ENP to the PM was also impaired (n = 23; see statistics in Fig. 6). Second, the involvement of BFA-sensitive ARF-GEFs in the delivery of ENP to the PM was investigated by applying BFA after the PBA treatment. Blocking the trafficking from recycling endosomes to the PM with BFA did not alter the delivery of ENP from the PBA induced intracellular compartements to the PM (Fig. 5F).

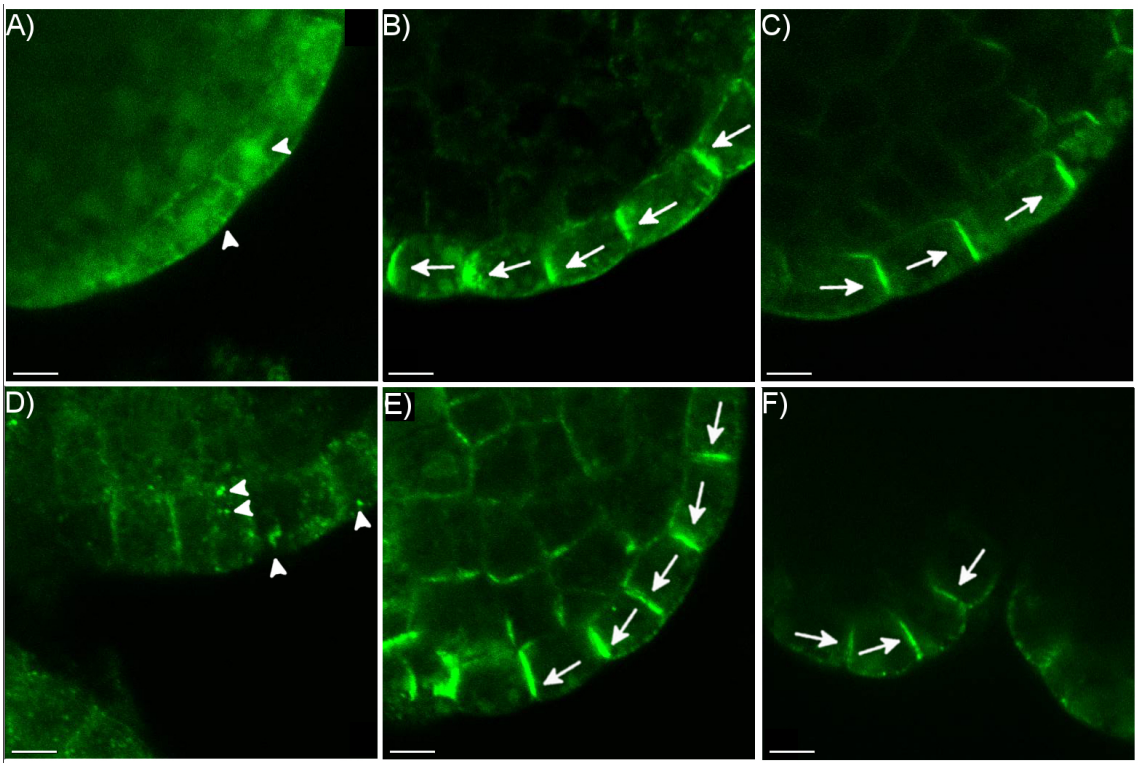

Figure 5 – PBA application studies in *A.thaliana* embryos carrying p35S:GFP::ENP. A) PBA treatment (25 mM) for 15 minutes. B) Washout of PBA with H_2O for 2 hr. C) H_2O control incubation for 2hr. D) 25 mM PBA for 15min, three times washout with H_2O and afterwards incubation in 20 µM cytD for 2hr. E) 25 mM PBA for 15 min, three times washout with H_2O and afterwards incubation in 10 µM oryzalin for 2hr. F) 25 mM PBA for 15 min, three times washout with H_2O and afterwards incubation in 50 µM BFA for 2hr. White arrows depict localization; white arrowheads depict intracellular vesicles; scale bars: 5 µm

The observations of depletion and relocalization were quantified by assessing the percentage of detached/relocalized ENP within a studied embryo. Each analysed embryo was assigned into

one of four categories, namely 100% localization, >50% localization, < 50% localization and 0% localization. For the assessment of localization versus no localization the first and the last two groups were combined (Fig. 6). For reduction of redundancy only the localization category is depicted in figure 6.

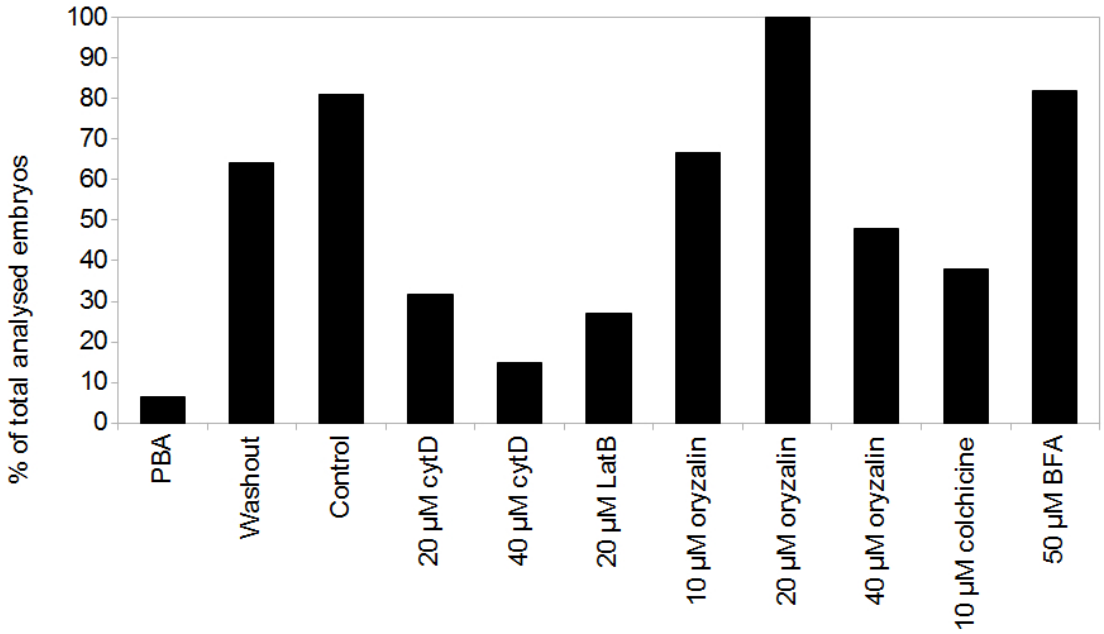

Figure 6 – Application of substances and toxins on *A.thaliana* embryos carrying p35S:GFP::ENP. 25 mM PBA n = 94 (9 experiments); Washout in H_2O mQ n = 67 (9 experiments); Control (H_2O mQ) n = 74 (9 experiments); 20 µM cytD n = 19 (3 experiments); 40 µM cytD n = 27 (4 experiments); 20 µM LatB n = 26 (2 experiments); 10 µM oryzalin n = 9 (1 experiment); 20 µM oryzalin n = 4 (1 experiment); 40 µM oryzalin n = 23 (2 experiments); 10 µM colchizin n = 28 (2 experiments); 50 µM BFA n = 11 (2 experiments). n = analysed embryos.

In order to confirm the found cytoskeletal impact on the subcellular targetting of ENP the effect of 20 µm latrunculin B (LatB), which also inhibits actin polymerization (Collings et al., 2006) was additionally tested. LatB impaired the retargeting of ENP to the PM like cytD (n = 26; Fig. 6). Further incubation with 10 µm colchicine, which is known to bind to the free subunits of microtubules disturbed the relocalization of ENP to the PM (n = 28; Fig. 6).

Subsequently, the general power of PBA in studying signaling processes of transmembrane proteins was adressed by incubating ovules of transgenic pPIN1:PIN1::GFP *A.thaliana* plants harboring heart stage embryos in PBA (Fig. 7). PIN1 accumulated in the cytosol, but also in distinct vesicles, possibly BFA compartments (Fig. 7A). The PBA effect was reversible and washout of this substance led to relocalization of PIN1 to the PM (Fig. 7B). Notably, after washout some internal vesicles of PIN1 were retained, whereas the cytosolic PIN1 completely relocalized. In accordance with previous studies (Geldner et al., 2001) blocking the trafficking of recycling endosomes to the PM with BFA resulted in agglomeration of PIN1 in BFA vesicles (Fig. 7C).

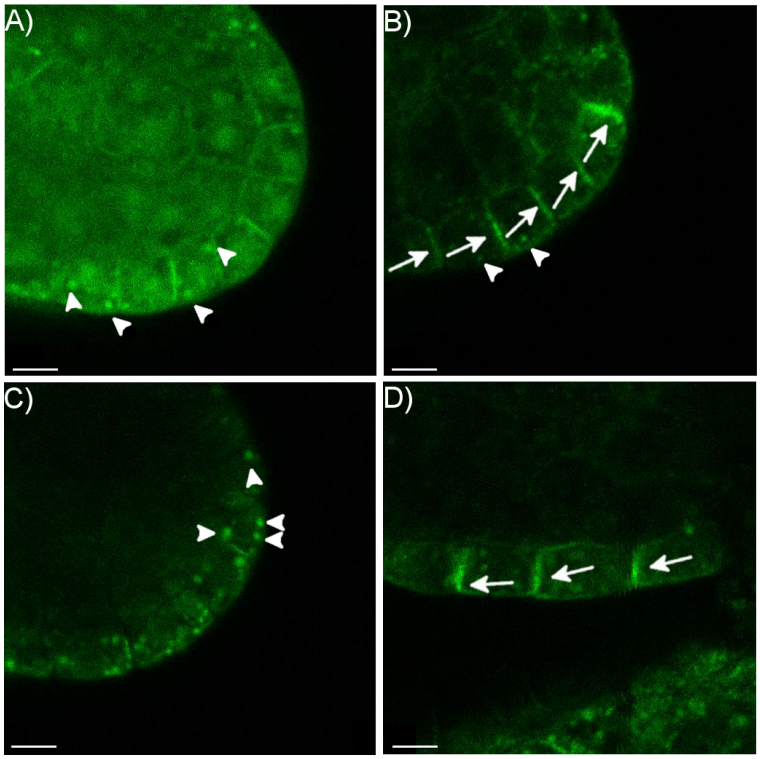

Figure 7 – PBA application studies in *A.thaliana* embryos carrying transgenic pPIN1:PIN1::GFP. A) Incubation in 30 mM PBA for 10 minutes. B) 30 mM PBA for 10 min and subsequent H_2O washout for 2 hrs C) 30 mM PBA for 10 min, three times washout with H_2O and subsequent incubation in 50 µM BFA for 2 hrs D) H_2O control for 2 hrs. White arrows indicate localization; white arrowheads indicate intracellular vesicles; scale bars: 5 µm

A comparison of the dynamics of PIN1 and ENP translocation in response to PBA revealed that the effective detachment of the respective protein from the PM was concentration and time dependent (ENP = 25 mM for 15 minutes; PIN1 = 30 mM for 10 minutes). Exchanging the conditions for the respective other lead in the case of ENP to a decrease in retargetting to the PM upon washout. In the case of PIN1 no reliable detachment was observed. Further, the effectivity in relocalization of both proteins in the standard conditions differed, i.e. ENP 25 mM for 15 minutes and PIN1 30 mM for 10 minutes. Whereas ENP fully relocalized within a two hour washout, PIN1's relocalization was reduced and the protein remained to some extent in intracellular vesicles (Fig. 7B; note white arrowheads).

3.1.1.2 Tissue specific factors

When analyzing the constitutive expression of p35S:GFP::ENP in comparison with the constitutive expression of p35S:NPY4::YFP it appeared that cellular polarity might be subject to a tissue specific factor. ENP is apically localized in the epidermis cells in cotyledons and its endogenous expression is restricted to these cells in the embryo. Its ectopic expression in the vasculature was found to be basal (Fig. 8A). Strikingly NPY4 (At2g23050), a homologue of ENP, shows a similar behaviour. Its endogenous expression is restricted to the vasculature, where it displays a basal localization. With the constitutive p35S promotor its expression is forced in epidermal cells of cotyledons and it displays an apical localization (Fig. 8C). These

parallels were already pointed out by Zweigardt (2010). To confirm this finding, the seedling root was analyzed in respect to the localization of these two proteins (Fig. 8B and 8D). The analysis of ENP showed an apical localization with lateral extension (apical/lateral) in the epidermal cells. Further, a basal localization was detected in the stele and cortex cells (Fig. 8B; note white arrows). Strikingly, some columella cells even depicted a lateral localization (Fig. 8B). NPY4 also showed a basal localization in the stele cells with a profound lateral extension (Fig. 8D). Notably in epidermal cells its localization was mainly apical, although some cells showed a lateral extension (Fig. 8D).

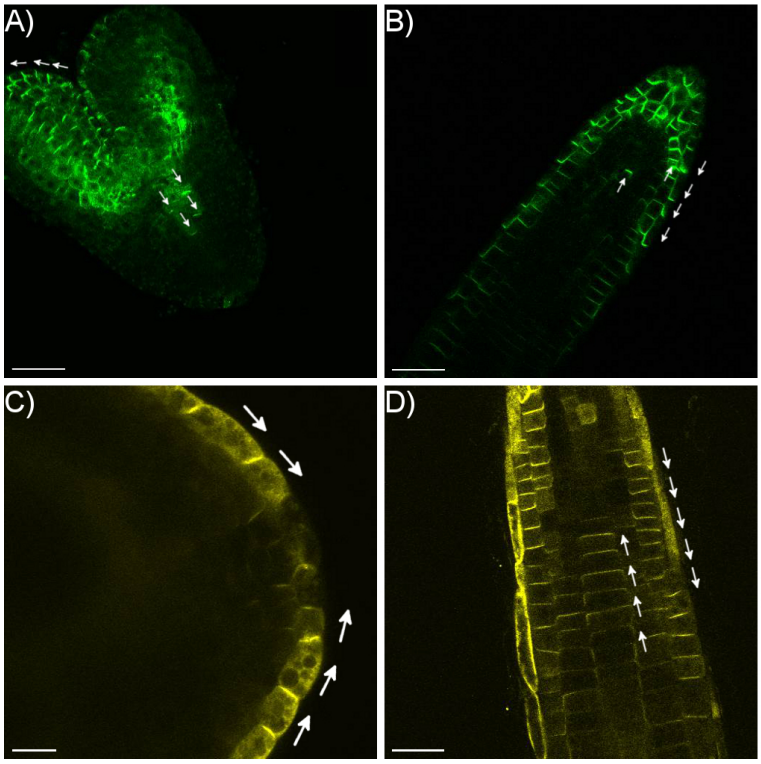

Figure 8 – Tissue specificity of the cellular polarity of ENP and NPY4 in the seedling root and in the embryo of *A.thaliana*. A) p35S:GFP::ENP in the embryo. B) p35S:GFP::ENP in the root. C) p35S:NPY4::YFP in the embryo. D) p35S:NPY4::YFP in the root. White arrows indicate localization; scale bars in A), B) and D) 30 µm and in C) 5 µm

3.1.2 Intrinsic factors

As a further approach, sequence-based polarity signals in ENP were adressed. On a structural level ENP has a N-terminal BTB POZ domain (Fig. 9), which is known to be a versatile protein protein interaction motif (Stogios et al., 2005). It further has a NPH3 domain (Fig. 9), whose function is up to now not known. It consists of three highly homologous regions, which are interrupted by non-homologous parts (Fig. 9; small linker 1 and 2). The NPH3 domain therefore can be subdivided into three domains, in the following designated NPH3_1, NPH3_2 and NPH3_3, respectively (Fig. 9). The C-terminus of ENP was shown to harbour functional elements, since mutations that delete this region cause with *pid* the *laterne* phenotype (Treml et al., 2005; Treml, 2008; Zweigardt, 2010; Chen et al., 2010). Next to its domains, ENP reveals some highly homologous amino acid residues, among them a proline in the BTB POZ domain

(Fig. 9; P46), a leucine in the large linker region (Fig. 9; L144) and a tyrosine at position 409 (Fig. 9; Y409). P46 is a residue in a small, highly conserved region and known, in non-plant BTB POZ domains, to be a contact site for protein interactions (Stogios et al., 2005).

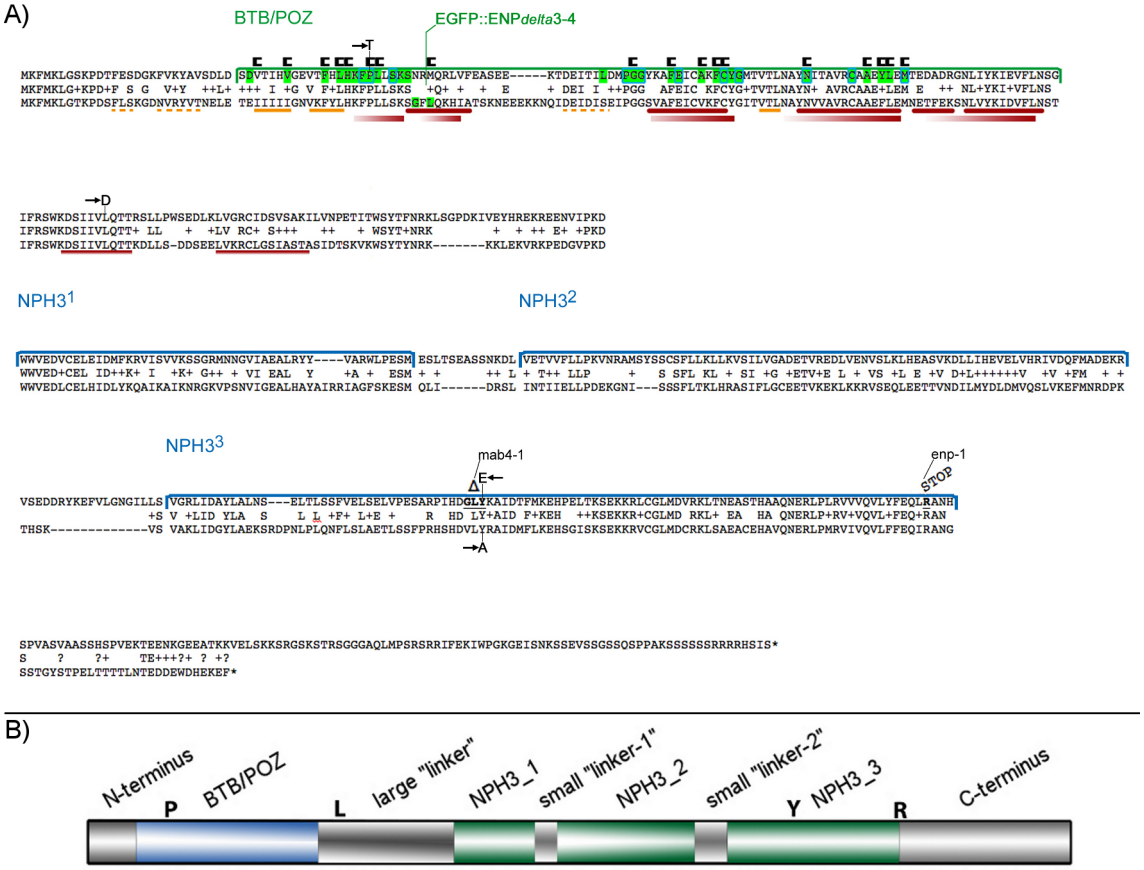

Figure 9 – ENP protein sequence and domain structure A) ENP protein sequence aligned with the protein sequence of close homolog NPY4 B) Domain structure of ENP with the indication of some highly conserved amino acids. Features of the BTB POZ domain (only) are highlighted in A). Green horizontal line: BTB POZ-domain of NPH3(-like) proteins. Letters with green shading: highly conserved NPH3 (-like) BTB POZ amino acid residues, most of which constitute the "signature sequence" of plant NPH3 (-like) BTB POZ. Bold C's: residue position burried in the core of the BTB POZ fold. Yellow underlining: predicted potential beta-sheets. Red underlining: predicted/potential alpha-helices. Some highly conserved residues D30, H43, ~~K44~~, ~~F45~~, P46, L47, ~~S49~~ and ~~K50~~ (crossed through = only dimerization) have been shown in other non-plant BTB POZ domains to be contact sites for Di- and Tetramerization. Modified after Stogios et al., 2005.

3.1.2.1 Analysis of deletion constructs

In order to understand the importance of the specific domains in ENP for its polar localization, ENP was systematically dissected into the single domains (Fig. 9 and Fig. 10). GFP-fusion constructs under the control of p35S harboring the BTB POZ domain and the large linker region (Fig. 10; ENPdeltaNPH3_All), the BTB POZ domain with the large linker region and the first NPH3 domain (Fig. 10; ENPdeltaNPH3_2+3), the BTB POZ domain with the large linker region and two NPH3 domains (Fig. 10; ENPdeltaNPH3_3), as well as the BTB POZ domain with all three NPH3 domains (Fig. 10; ENPdeltaCterm) were analysed with the CLSM in epidermal cells of *A.thaliana* ecotype L*er* torpedo stage embryos and roots of ten days old

seedlings (Fig. 13A-I and Fig. 13N).

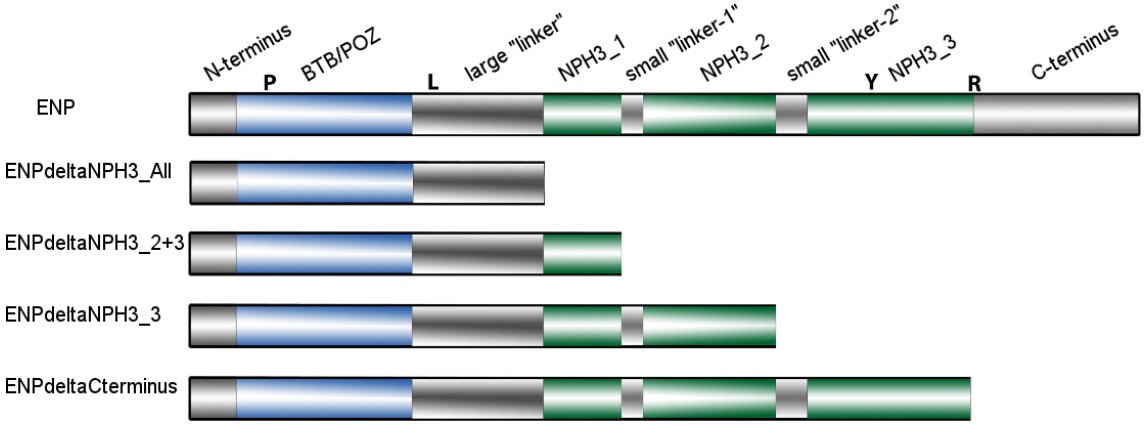

Figure 10 – Structural overview of the generated deletion constructs of ENP

The ENPdeltaNPH3_All construct, which comprised the BTB POZ domain and the large linker region was not able to localize to the PM. It was rather found throughout the cytosol and in distinct so far unknown intracellular compartments. This held true for roots (Fig. 13B) as well as for embryos (Fig. 13F). Similar results were seen for the constructs comprising the BTB POZ domain and either one (ENPdeltaNPH3_2+3) or two (ENPdeltaNPH3_3) NPH3 domains. Their subcellular localization was primarily cytosolic, sometimes accumulating in distinct intracellular compartements (Fig. 13C and Fig. 13G; ENPdeltaNPH3_2+3, Fig. 13D and Fig. 13H; ENPdeltaNPH3_3) in embryo and root tissues. The construct lacking the C-terminus of ENP (ENPdeltaCterm) was still able to localize to the apical site of the PM (Fig. 13I (root) and Fig. 13N (embryo); note white arrows). In comparison to the full-length ENP localization domain, which extended from the apical site of the PM to lateral sites in the embryo and root epidermal tissue (Fig. 13A (root) and Fig. 13E (embryo); note white arrowheads), the ENPdeltaCterm construct missed this lateral extension (compare Fig. 13A and Fig. 13E (full-lenght ENP) with Fig. 13I and Fig. 13N (ENPdeltaCterm)). Notably, in the root stele the ENPdeltaCterm construct showed the same basal localization pattern as the full-length ENP construct including the lateral extension (compare Fig. 13A and 13I; note white arrowheads).

3.1.2.2 Analysis of domain swap constructs

The localization of the ENPdeltaCterm construct, displayed similarities to the localization of NPY4, a close homologue of ENP, initially analyzed by Zweigardt (2010). The localization of NPY4, when ectopically expressed with p35S is strictly limited to the apical site of the PM in the epidermis of cotyledons (Fig. 13O), with no extension to the lateral sites. The same was observed with the ENPdeltaCterm construct (Fig. 13N). Notably, on the sequence level NPY4 depicts a much shorter C-terminus compared to ENP. To address the question, whether the different C-termini of ENP and NPY4 cause different localization patterns, domain swap constructs were created (Fig. 11). One construct replaced the entire C-terminus of NPY4 with that of ENP (Fig. 11; NPY4_ENPCtermLong) and with another construct the additional part of ENP's C- terminus was added to the shorter C-terminus of NPY4 (Fig. 11; NPY4_ENPCtermShort).

The constructs were analysed as GFP-fusions under the control of p35S in the epidermis of L*er* torpedo stage embryos and roots of ten days old seedlings with a CLSM (Fig. 13L-M and Fig. 13P-Q).

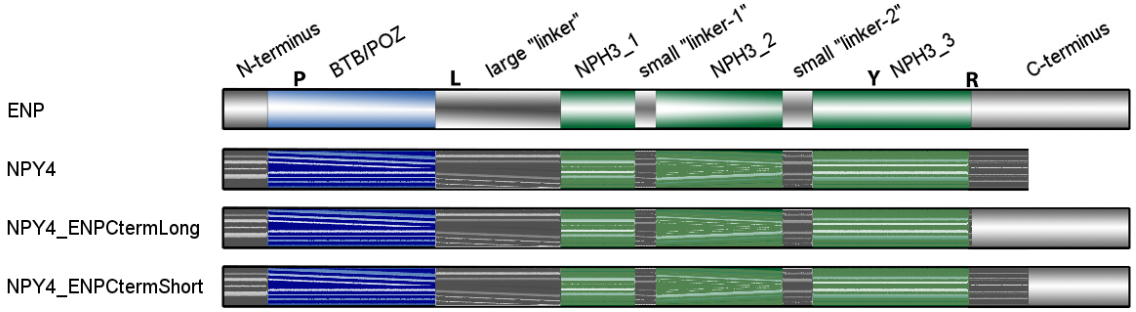

Figure 11 – Structural overview of the generated domain swap constructs between ENP and NPY4

The addition of either the full length or parts of the C-terminus of ENP to NPY4 did only in some cases extend the apical localization of NPY4 in the epidermal cells of cotyledons (Fig. 13P (NPY4_ENPCtermShort); note the white arrowhead). In the root tissue only the lateral extension in the stele cells was observed, which was similar to the unmodified NPY4 localization (compare Fig.13K (NPY4) with Fig. 13L (NPY4_ENPCtermShort) and Fig. 13M (NPY4_ENPCtermLong)).

3.1.2.3 Analysis of point mutation constructs

Subsequently the effect of specific point mutations in ENP was analyzed with respect to their influence on ENP's cellular polarity and functionality (Fig. 12). The highly conserved residues P46, located in the BTB POZ domain and L144, situated in the large linker region were point mutated. For site directed mutagenesis structurally diverse amino acids compared to the wild type residue were chosen, resulting in an amino acid change from P->T (Fig. 12; ENP_P46T) and from L->D (Fig. 12; ENP_L144D). Further the tyrosine residue at position 409 was point mutated into alanine (Fig. 12; ENP_Y409A) and glutamate (Fig. 12; ENP_Y409E). This residue is known to be a functional and potential phosphorylation site in NPH3 (Liscum and Briggs, 1995), which is highly homologous to ENP. The introduced point mutations lead to a loss of phosphorylation (Y409A) as well as to a possible phospho-mimick (Y409E) (Fig. 12). The constructs were analyzed as GFP-fusions under the control of p35S in the epidermis of L*er* torpedo stage embryos and roots of ten days old seedlings with a CLSM (Fig. 13R-Y).

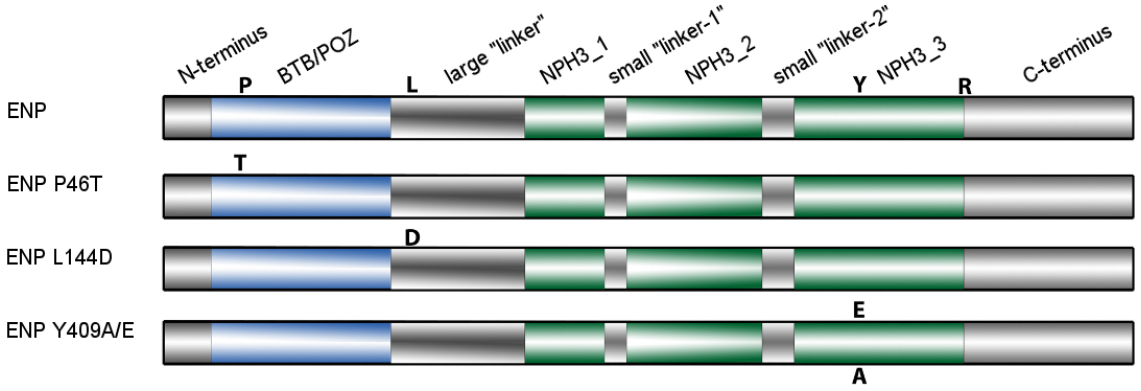

Figure 12 – Structural overview of the introduced point mutations in ENP. Letters in bold were targets of site specific mutagenesis.

The mutation in the BTB POZ domain (P46T) did not alter the localization of ENP. In the embryo it was localized to the apical site of the PM, even showing a weak lateral extension (Fig. 13V; note white arrowheads). In the root ENP_P46T displayed the apical/lateral localization in the epidermis and the basal/lateral localization in the stele and cortex cells as found for the full-length ENP as well (compare Fig. 13R with 13A; note white arrowheads). The construct with the point mutation in the large linker region was found predominantly in the cytosol and only a weak localization at the apical site of the PM was detected in the embryo (Fig. 13W; note white arrows). In the root, apart of a cytosolic accumulation of ENP_L144D, the apical localization in the epidermis was almost completely missing, whereas a weak basal localization in the stele cells was randomly observed (Fig. 13S; note white arrows). The potential phospho-mimick construct of Y409 was not able to localize ENP at the PM and was predominantly found in the cytosol in unidentified intracellular aggregates in both the root and the embryo tissue (Fig. 13U and Fig. 13Y). In comparison the destruction of the phosphorylation site (Y409A) did not impede ENP's ability to localize to the apical site of the PM in the embryo, but the lateral extension was obsolete (Fig. 13X). In the root, predominantly apical localization was observed in the epidermis and basal localizations in the stele and cortex cells. The latter ones also randomly showed a lateral extension (Fig. 13T).

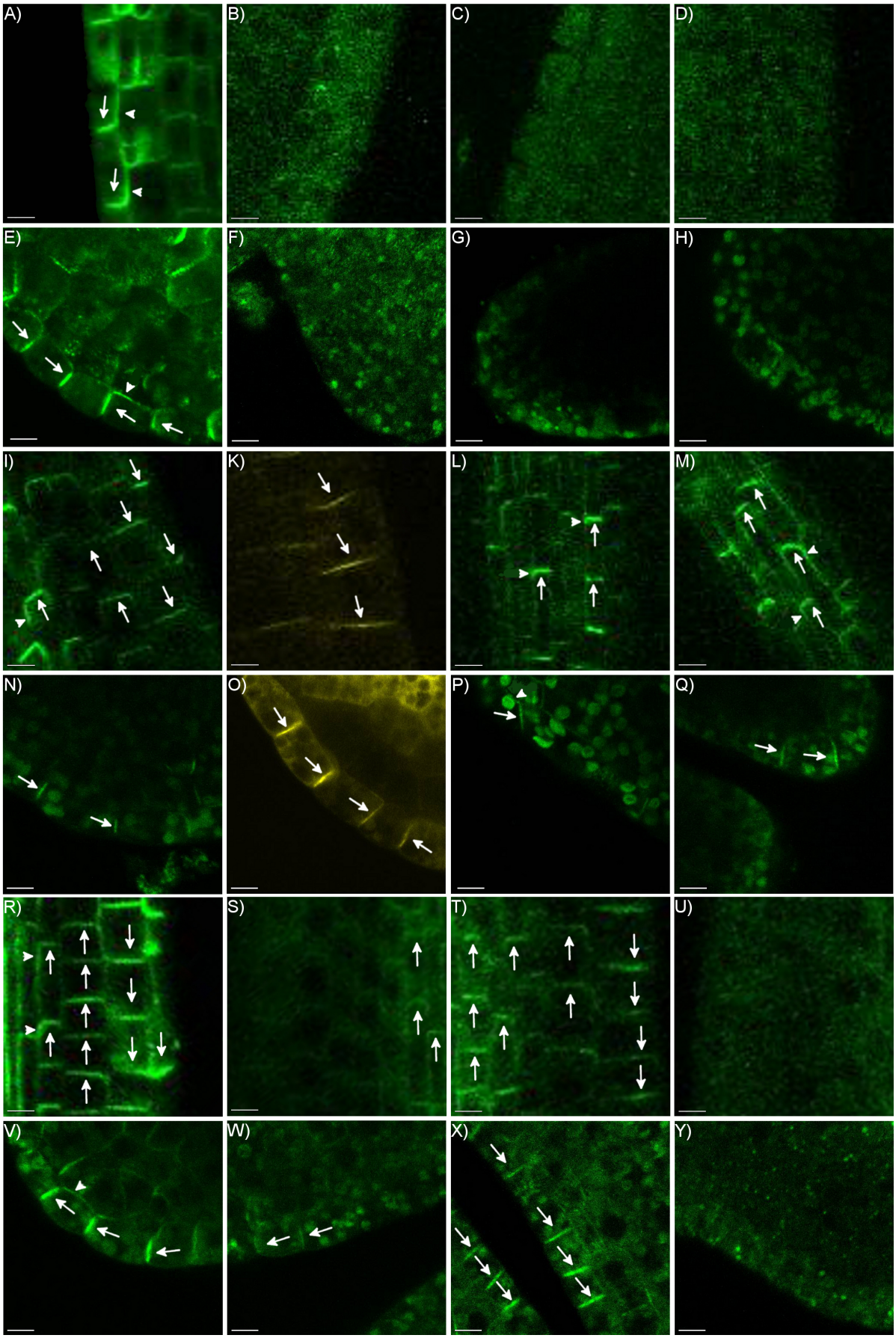

Figure 13 - *legend see next page*

Figure 13 – Localization study of GFP/YFP-tagged ENP/NPY4 derived constructs in *A.thaliana* roots of 10 days old seedlings and torpedo stage embryos. A, B, C, D, I, K, L, M, R, S, T, U depict the respective construct analysis in roots of 10 days old seedlings. E, F,G, H, N, O, P, Q, V, W, X, Y depict the respective construct analysis in torpedo stage embryos. A) and E) p35S:GFP::ENP. B) and F) p35S:ENPdeltaNPH3_All::GFP. C) and G) p35S:ENPdeltaNPH3_2+3::GFP. D) and H) p35S:ENPdeltaNPH3_3::GFP. I) and N) p35S:ENPdeltaCterm::GFP. K) and O) p35S:NPY4::YFP. L) and P) p35S:NPY4_ENPCtermShort::GFP. M) and Q) p35S:NPY4_ENPCtermLong::GFP. R) and V) p35S:ENP_P46T::GFP. S) and W) p35S:ENP_L144D::GFP. T) and X) p35S:ENP_Y409A::GFP. U) and Y) p35S:ENP_Y409E::GFP. Root tips are upwards; arrows depict localization and orientation respectively; arrowheads depict lateral localization; scale bars: 5 µm

In summary this series of experiments showed that firstly ENP's polar localization depends on the existence of specific domains. The C-terminus of ENP seems to harbour signals, which determine the targeting to the PM and more specifically allows in a tissue specific manner lateral localization. The N-terminal regions appear to refine ENP's localization to be polar at the apical site of the PM. Secondly, specific sites in the N-terminal region of ENP show a drastic influence on ENP's capability to localize correctly, as seen by the disturbed localization of the ENP_L144D construct (Fig. 13S and 13W). Thirdly, ENP's localization might depend on the phosphorylation status of Y409. At least, this is an important residue for polarization.

3.1.3 Separation of full functionality and polarity

Previous work showed that a full p35S:GFP::ENP construct could rescue the *laterne* flower phenotype (Treml, 2008; Zweigardt, 2010). The seedling phenotype could not be rescued, since the activity of p35S is too late in the embryo (Zweigardt, 2010). p35S:NPY4::YFP, although ectopically localized in the epidermis in cotyledons did not rescue the *laterne* flower phenotype (Zweigardt, 2010; this study). This suggested that ENP's correct polarity is necessary, but might not be sufficient for the flower rescue. In order to test this hypothesis the named deletion (see 3.1.2.1), domain swap (see 3.1.2.2) and point mutation constructs (see 3.1.2.3) were tested with regard to their capability to rescue the *laterne* flower phenotype. For this the p35S:X:GFP constructs were crossed in *enp pid/enp* + (see 2.2.1.4). In the T2 progeny *laterne* seedlings were selected, which proves a double mutant *enp pid/ enp pid* genotype. The localization of the respective transgene was assessed with the CLSM. The seedlings were grown and the flower phenotype scored. The development of flower organs or leaf structures on the stem proved a functional or partly functional ENP (see 2.2.1.4). In addition to the assessment of protein localization, this analysis aimed at revealing respective intrinsic functional determinants of ENP.

Construct	n	% (partial) rescue	% no rescue
ENP P46T	58	13	87
ENP L144D	9	0	100
ENP Y409A	23	4.3	95.7
ENP Y409E	7	0	100
ENP deltaNPH3_All	27	15	85
ENP deltaNPH3_3	33	0	100
ENP deltaCterm	7	0	100
NPY4	8	0	100
NPY4_ENPCtermShort	2	0	100
NPY4_ENPCtermLong	2	0	100

Table 37 – Statistics for the evaluation of rescue and non rescue of the *laterne* flower phenotype by overexpression of the generated deletion, domain swap and point mutation constructs in the *enp pid* double mutant background

3.1.3.1 Analysis of the deletion constructs

The results from this study showed the same cellular localization of the deletion constructs in the *enp pid* double mutant background as in the wild type. The ENP_deltaNPH3_ALL construct was found predominantly in the cytosol (Fig. 14A), which was also true for the ENPdeltaNPH3_3 construct (Fig. 14B). The ENPdeltaCterm construct was apically localized in epidermis cells and was basally localized in the stele cells (Fig. 14C). Only *laterne* seedlings were tested, assured by the presence of trichomes on already developed leaf structures (Fig. 14D - F; respective inset on the right; note the black arrowhead). The functionality tests of the deletion constructs revealed that the ENPdeltaNPH3_3 and the ENPdeltaCterm constructs were not able to rescue the mutant flower phenotype in *laterne* (Table 37; Fig. 14E and Fig. 14F). The ENPdeltaNPH3_All construct, which only harbors the BTB POZ domain and the large linker region (Fig. 10) developed flower structures in 15% of the analyzed plants (Table 37; Fig. 14D; note white arrowhead). This construct further showed a development of leaf structures on the stem (6 out of 27 plants analyzed), which accounts for a partial rescue.

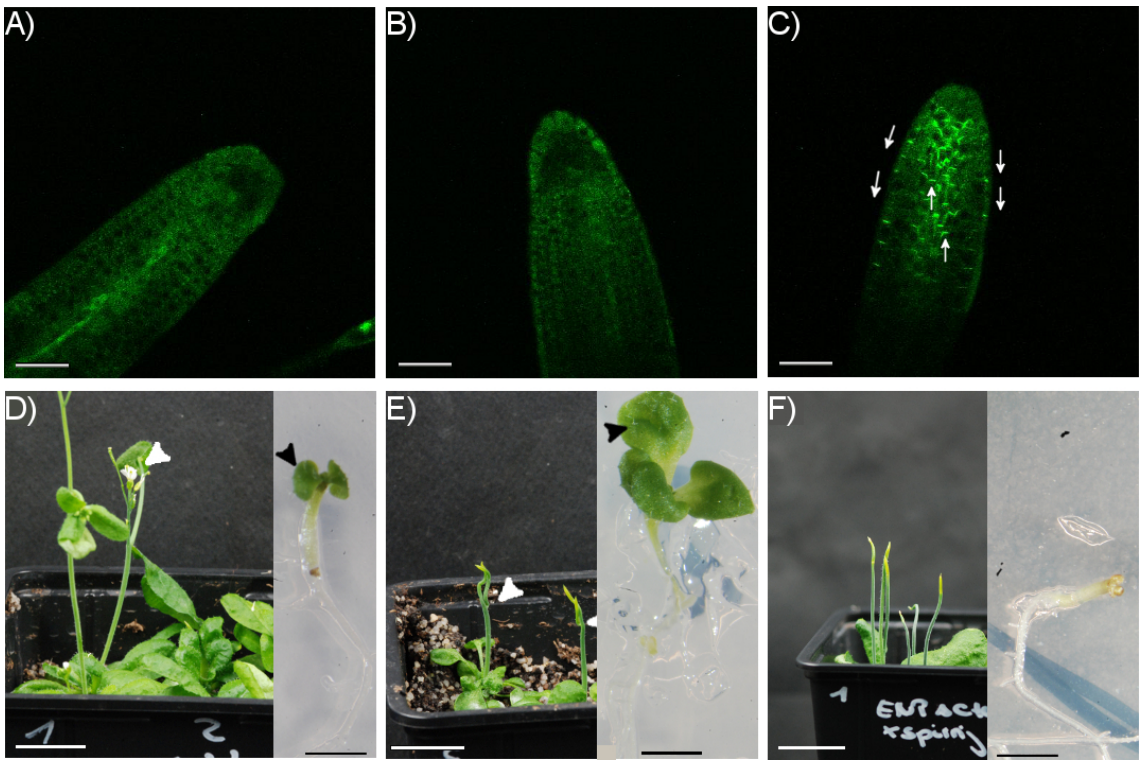

Figure 14 – Rescue experiments with the *enp pid* (= *laterne*) double mutant. Flower or stem phenotype with deletion constructs in the double mutant background. CLSM of *laterne* seedlings harboring A) p35S:ENPdeltaNPH3_All::GFP B) p35S:ENPdeltaNPH3_3::GFP C) p35S:ENPdeltaCterm::GFP. Adult and seedling phenotype of *laterne* harbouring D) p35S:ENPdeltaNPH3_All E) p35S:ENPdeltaNPH3_3::GFP F) p35S:ENPdeltaCterm::GFP. White arows depict localization and orientation respectively; white arrowheads depict in D) flower organs and E) fasciation of blind ending stem; scale bars: A)-C) 30 µm D)-E) adult phenotype: 1 cm; seedling phenotype: 0.125 cm F) adult phenotype: 2 cm; seedling phenotpye: 0.125 cm

3.1.3.2 Analysis of the domain swap constructs

The presented study suggested that the addition of the C-terminus of ENP in part (ENPCtermShort) or the full length C-terminus (ENPCtermLong) is not capable of rescuing the *enp pid* flower phenotype (Table 37 and Fig. 15). Both constructs did not develop any flower structures (Fig. 15E and Fig. 15F). The analysis of the localizations revealed that the NPY4_ENPCtermShort construct mainly localized in stele cells basally and epidermal localization was almost completely absent (Fig. 15B). The NPY4_ENPCtermLong construct displayed additionally a weak apical localization in epidermal cells (Fig. 15C).

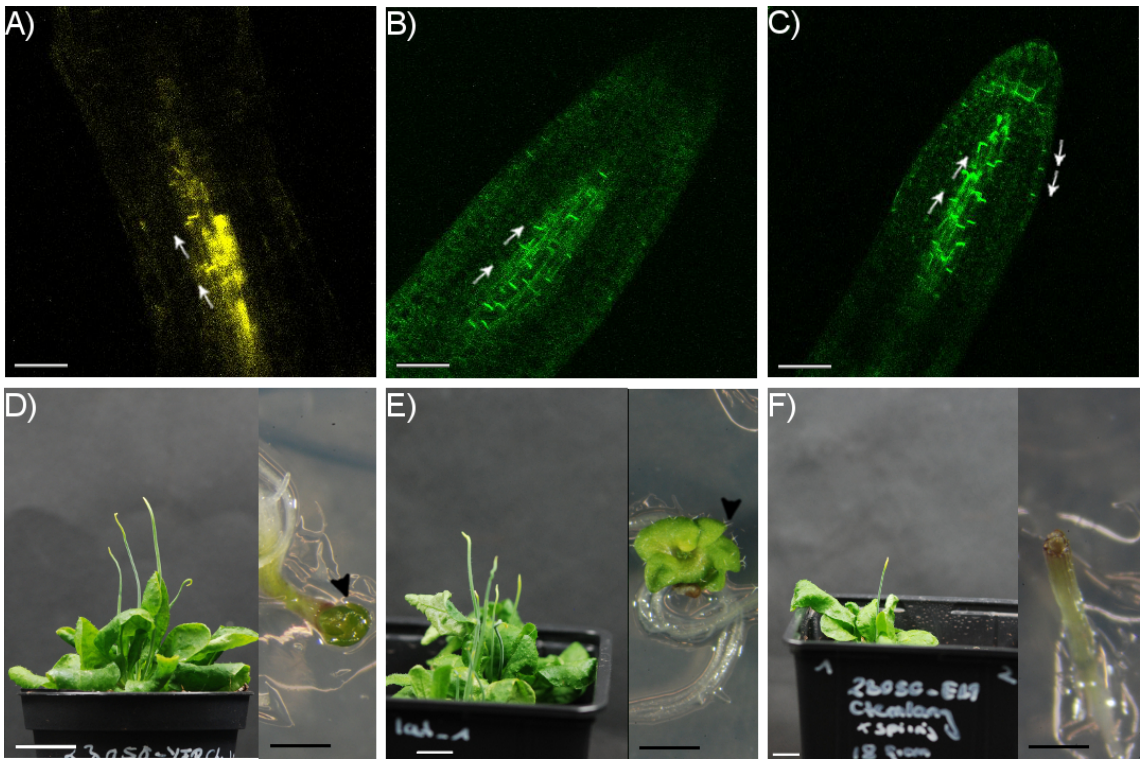

Figure 15 – Rescue experiments with the *enp pid* (= *laterne*) double mutant. Flower or stem phenotype with domain swap constructs in the double mutant background. CLSM of *laterne* seedlings harbouring A) p35S:NPY4::YFP B) p35S:NPY4_ENPCtermShort::GFP C) p35S:NPY4_ENPCtermLong::GFP. Adult and seedling phenotype of *laterne* harbouring D) p35S:NPY4::YFP E) p35S:NPY4_ENPCtermShort::GFP F) p35S:NPY4_ENPCtermLong::GFP. White arrows depict localization and orientation respectively; black arrowheads depict trichomes on developing rosette leaves; scale bars: A)-C) 30 µm D) adult phenotype: 1 cm; seedling phenotype: 0.25 cm E)-F) adult phenotype: 0.5 cm; seedling phenotype: 0.25 cm

3.1.3.3 Analysis of point mutation constructs

This series of experiments showed that the proline in the BTB POZ domain, although not being critical for ENP's localization is pivotal for its correct functioning (Fig. 16A and Fig. 16D; Table 37). The mutation in this residue (P46T) lead to a partial rescue of the *laterne* phenotype (Fig. 16D). The analyses of the mutated proline showed that in rare cases flower structures (Fig. 16C) developed and that leaf structures developed along the stem (Table 37; Fig. 16D and Fig. 16F). The highly conserved leucine in the large linker region between the BTB POZ domain and the NPH3 domains showed no rescue of the mutant flower phenotype (Fig. 16E; Table 37). The analyses of the tyrosine residue at position 409 displayed that the potential phospho-mimick (Y409E) was not able to rescue the *laterne* phenotypic defect (Table 37; Fig. 16L), which also held true for the destruction of the phosphorylation site (Y409A; Fig. 16K). The over expression of ENP_Y409A in the *laterne* background lead in rare cases to the development of fertile flowers (Table 37). While in wild type the localization of p35S:ENP_Y409A::GFP was found to be apical in the epidermal cell layer of the seedling root (Fig. 13T), in the *enp pid* double mutant the localization was sometimes reversed and detected at the basal site of the PM (Fig. 16G; surface focus).

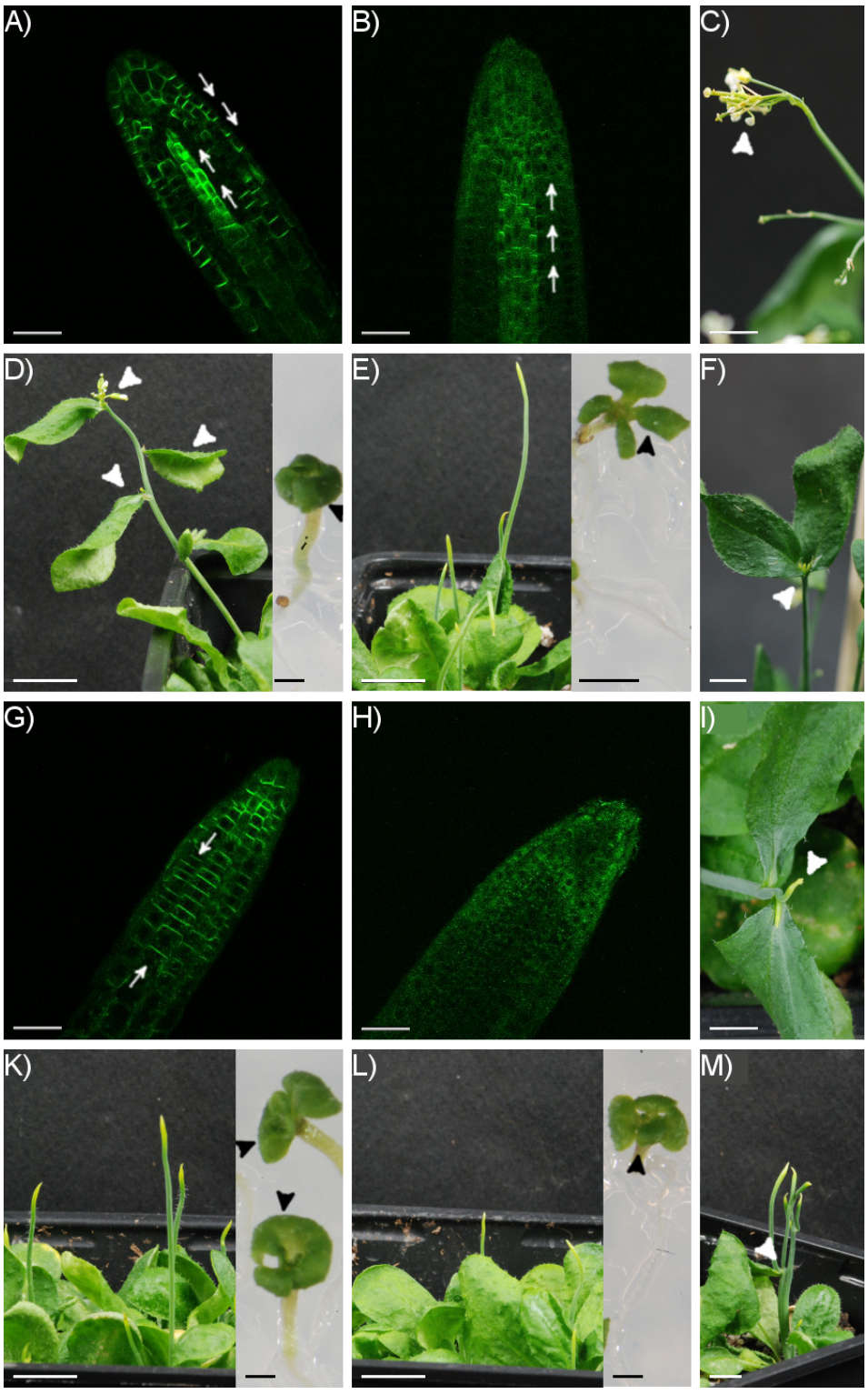

Figure 16 – Rescue experiments with the *enp pid* (= *laterne*) double mutant. Flower or stem phenotype with point mutation constructs in the double mutant background. CLSM of *laterne* seedlings harbouring A) p35S:ENP_P46T::GFP B) p35S:ENP_L144D::GFP. C) Developing flower structures indicating a (partial) rescue. Adult and seedling phenotype of *laterne* harbouring D) p35S:ENP_P46T::GFP E) p35S:ENP_L144D::GFP. F) Leaf-like structures on the stem indicating a partial rescue. CLSM of *laterne* seedlings harbouring G) p35S:ENP_Y409A::GFP H) p35S:ENP_Y409E::GFP. I) Stigmata on blind ending stem. Adult and seedling phenotype of *laterne* harbouring K) p35S:ENP_Y409A::GFP L) p35S:ENP_Y409E::GFP. M) Fasciation of the stem. White arows depict localization and orientation respectively; white arrowheads depict in C) Flower structures in D) and F) Leaf-like structures in I) stigmata on a blind ending stem and in M) Fasciation of the stem. scale bars in A)-B) and G)-H) 30 µm. In C), F), I), M) 0.5 cm. In D), K), L) adult phenotype: 1 cm; seedling phenotype: 0.125 cm. In E) adult phenotype: 1 cm; seedling phenotpye: 0.25 cm

The results from the rescue experiments with the point mutations were compared with an *in silico* analysis using the PredictProtein software toolbox (www.predictprotein.org). Snap2 out of this toolbox predicts the impact of single amino acid substitutions on protein function. For a given substitution a score ranging from -100 (strong neutral prediction= no effect) to +100 (strong effect prediction) is predicted, that reflects the likelihood of this specific mutation to alter the native protein function. The ranges are colour coded with green (neutral = no effect), white (intermediate effect) and red (severe effect). An analysis of ENP with Snap2 showed that basically any amino acid substitution in all mutagenized sites (P46, L144 and Y409) would theoretically be able to have severe effects (Fig. 17).

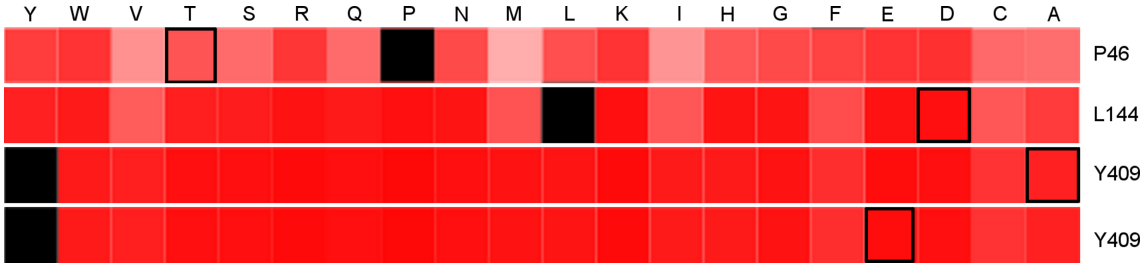

Figure 17 – Effect of point mutations in three specific residues in ENP, namely P46, L144 and Y409, as predicted by SNAP2. Dark red indicates a high score (score > 50, strong signal for effect), white indicates weak signals (-50 < score < 50) and green a low score (score < -50, strong signal for no effect); black indicates the corresponding wild type residues.

All deletion, domain swap and point mutation constructs in the *laterne* background displayed to different extents fasciation (Fig. 16M), which was not reported for the full length construct (Treml et al., 2005). In some cases pistil-like structures developed on the blind ending stems (Fig. 16I).

Taken together the rescue experiments with deletion, domain swap and point mutations of ENP and NPY4 revealed essential functional domains and sites in ENP the most promising ones being the C-terminus of ENP, the BTB POZ domain and the tyrosine site at position 409.

3.2 Global and targeted yeast two-hybrid screens to uncover ENP interactors

In order to find interaction partners with ENP, global Y2H screenings were conducted. Preceding this PhD thesis, one screen was performed in collaboration with Joachim Uhrig (University Cologne) and it revealed two possible interaction partners, namely the transcription factor VOZ1 (At1g28520) and NPY4 (At2g23050), an ENP-like protein.

These findings were assessed by directly testing the interactions between ENP and VOZ1 and between ENP and NPY4 with the ProQuest^{TM} Y2H system (see 2.2.4). In this series of experiments ENP was fused to the DNA activation domain (bait; DB clone), whereas VOZ1 and NPY4 respectively were fused to the activation domain of the GAL4 transcription factor (prey; AD clone). To test possible interactions the ProQuest^{TM} system makes use of growth on selective plates, as well as blue coloring of positively assessed interactors. Whereas the judgment

of growth on selective plates is quite subjective and prone for mistakes, a detection of a blue color is more reliable for a correct assessment. Nevertheless the success of X-gal assays strictly depends on the expression level of the fusion proteins. Both protein protein interactions (ENP-VOZ and ENP-NPY4) were confirmed on the basis of the selection plates and were determined to be weak interactions (Fig. 18). Since NPY4 like ENP contains a BTB POZ domain and this domain is known to be a versatile protein protein interaction motif able to form hetero-, but also homodimers (Stogios et al., 2005), the possibility of ENP and NPY4 to form homodimers was tested by direct interaction tests with the respective protein in the named ProQuest^{TM} System (Gateway®). According to the selective plates (compare x2 (=A2,C2, E2, G2, I2) with x4 (=A4, C4, E4, G4, I4) and x7 (A7, C7, E7, G7, I7), respectively in Fig. 18) homodimer formation of ENP or NPY4 respectively appeared to be weak, as well as heterodimer formation (compare x2 (= A2,C2, E2, G2, I2) with x5 (=A5, C5, E5, G5, I5) and x6 (=A6, C6, E6, G6, I6), respectively in Fig. 18). Additionally X-gal assays were performed, which showed a clear blue color for the interaction of VOZ1 with ENP (Fig. 18H). For the interaction of ENP with NPY4 one out of four colonies showed a slight blue color (data not shown). For the homodimerization tests no blue color could be detected in the X-gal assay. In addition to interaction tests with VOZ1 and NPY4, PDK1 found in the global Y2H screen (see below) was also confirmed to be weakly interacting with ENP in the ProQuest^{TM} assay (Fig. 18K).

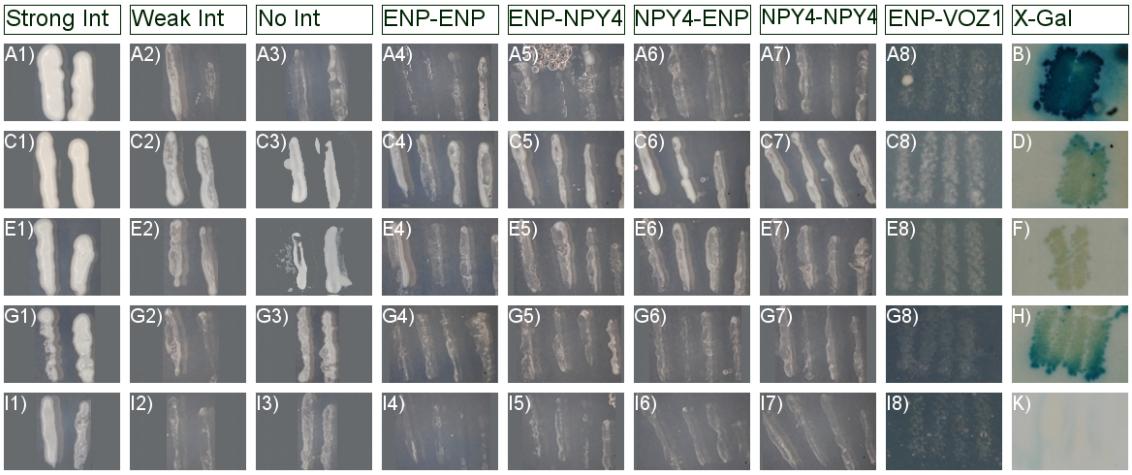

Figure 18 – Direct verification of the protein protein interactions of ENP with ENP, NPY4, VOZ1 and PDK1 with the ProQuest^{TM} System. A1)-A8) Selection on SC-Ura plates A1) strong interaction control A2) weak interaction control A3) no interaction control A4) ENP-ENP A5) ENP-NPY4 A6) NPY4-ENP A7) NPY4-NPY4 A8) ENP-VOZ1. B) X-gal assay of strong interaction control. C1)-C8) Selection on SC-His + 10 mM 3AT plates. The order of interactions: C1) strong interaction control C2) weak interaction control C3) no interaction control C4) ENP-ENP C5) ENP-NPY4 C6) NPY4-ENP C7) NPY4-NPY4 C8) ENP-VOZ1. Note that 3AT concentration is (still) not sufficient to inhibit HIS-production. D) X-gal assay of weak interaction control. E1)-E8) Selection on SC-His + 25 mM 3AT plates. The order of interactions: E1) strong interaction control E2) weak interaction control E3) no interaction control E4) ENP-ENP E5) ENP-NPY4 E6) NPY4-ENP E7) NPY4-NPY4 E8) ENP-VOZ1 F) X-gal assay of no interaction control G1)-G8) Selection on SC-His + 50 mM 3AT plates. The order of interactions G1) strong interaction control G2) weak interaction control G3) no interaction control G4) ENP-ENP G5) ENP-NPY4 G6) NPY4-ENP G7) NPY4-NPY4 G8) ENP-VOZ1. H) X-gal assay of interaction between ENP and VOZ1 I1)-I8) Selection on SC-His + 100 mM 3AT. The order of interactions: I1) strong interaction control I2) weak interaction control I3) no interaction control I4) ENP-ENP I5) ENP-NPY4 I6) NPY4-ENP I7) NPY4-NPY4 I8) ENP-VOZ1. K) X-gal assay of ENP and PDK1 (taken from Jakab, 2013).

In order to find more interaction partners, but also to confirm the ones previously found in a different system, another global yeast two-hybrid screening with ENP was performed. This time several deletion and point mutation constructs of ENP, as well as the full lenght NPY4 protein and domain swap constructs of NPY4 were included. The underlying rationale was that full length proteins can block certain interactions due to the fact that specific domains are not freely accessible for possible interaction partners (Joachim Uhrig and Pascal Braun personal communication). Full length ENP and NPY4 proteins as well as deletion, point mutation and domain swap variants were fused with the DNA binding domain of the GAL4 transcription factor. The constructs were all together four times screened against a collection of 12000 ORFs, which were fused to the activation domain of the GAL4 transcription factor. One repetition was performed with the addition of the phytohormone auxin, because the hormone itself could foster the interaction of proteins involved in its transport as for instance shown for TIR1 and Aux/IAA proteins (Calderon-Villalobos et al., 2012). Like in other studies IAA was used, since synthetic auxins like 2,4D for example were shown to be relatively poor substrates for auxin efflux carriers (Delbarre et al., 1996; Chen and Xiong, 2010; Calderon- Villalobos et al., 2012). The screen revealed all together six possible interaction candidates of ENP and NPY4. These

candidates were the GTP cyclohydrolase 1 (At3g07270), a GDSL esterase/lipase (At5g62930), PDK1 (At5g04510), NPY4 (At2g23050), At5g09770 and At4g28690 (Table 38).

	ENP	**ENP P46T**	**ENP BTB POZ**	**ENP ΔCterm**	**ENP ΔCterm P46T**	**NPY4**
GTP cyclohydrolase 1	x			x	x	x
GDSL esterase lipase	x			x		
PDK1			x			
NPY4						x
At5g09770		x				
At4g28690					x	

Table 38 – Found interaction partners in a global yeast two-hybrid screen performed in collaboration with Dr. Pascal Braun from the Chair of Systemsbiology (TU München)

The addition of auxin did not uncover further interaction partners. Notably, the screen identified an interaction partner of ENP, whose affinity was significantly reduced in the presence of auxin (Fig. 19 ; compare white arrows in Fig. 19A and in Fig. 19B). This gene is the GTP cyclohydrolase 1. The interactions with the GTP cyclohydrolase 1 and the GDSL esterase/lipase were independently verified by four researchers in direct interaction assays of bait and prey construct respectively.

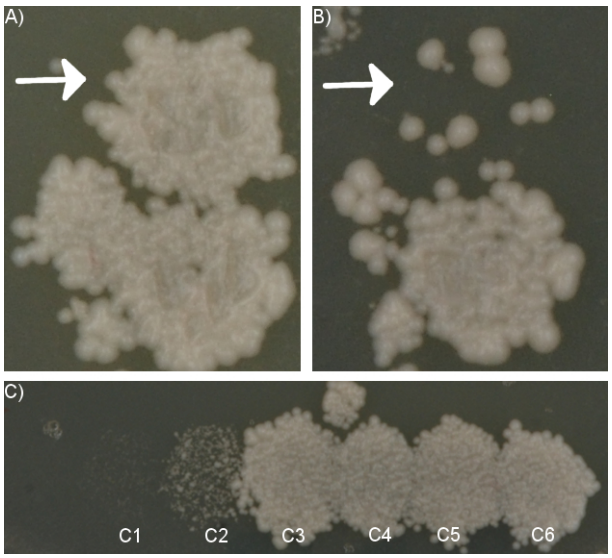

Figure 19 – Auxin effect on specific *S.cerevisiae* interactions. A) Interaction of ENP with GTP cyclohydrolase 1 (white arrow) B) Interaction as in A) with the addition of auxin C) Y2H interaction controls

3.3 The analysis of the cellular polarity of ENP and PIN1 in *rpk1-7*

In order to improve the understanding of the role of ENP with respect to its impact on the cellular polarity of PIN1, as well as cotyledon formation, *rpk1-7* mutants were analyzed (Luichtl et al., 2013).This is a rare class of mutants that specifically delete one cotyledon, such that monocotyledonous phenotypes occur. *rpk1-7* is a strong allele of the *RECEPTOR-LIKE PROTEIN KINASE 1* (*RPK1*) gene (Luichtl et al., 2013). The segregation of the mutant phenotype, however is low penetrating due to complex genetic redundancy (Luichtl et al., 2013). The rationale behind this analysis was to see, whether the loss of one cotyledon is related to the effects found in the *enp pid (= laterne)* homozygous mutant.

For the analysis monocotyledonous and anisocotyledonous heart to torpedo stage *rpk1-7* embryos harbouring transgenic p35S:GFP::ENP or pPIN1:PIN1::GFP were analysed. As control *rpk1-7* embryos with two equally sized cotyledons were analyzed, which in the following are referred to as wild type embryos. In wild type embryos PIN1 was localized on the apical side of epidermal cells oriented towards the tip of the emerging cotyledon primordia (Fig. 20C; Fig. 21D; Benková et al., 2003). The epidermal cells display a regular shape with comparable sizes between each other and the cell walls are perpendicular to the surface (Fig. 20A and Fig. 20C; Fig. 21A and Fig. 21D). The convergence point (Scarpella et al., 2006) at the tip of the primordium contains cells with PIN1 polarity pointing to at least one terminal cell. This displays a PIN1 orientation towards the sub-epidermis (Fig. 20C; Fig. 21D). Vascular precursor cells in the sub-epidermal tissue possess significant PIN1 protein concentrations and display a basal and lateral localisation such that auxin is guided towards the hypocotyl and root tip respectively (Fig. 20C; Fig. 21D). This PIN1 pattern was mostly not altered in aniso- and monocotyledonous *rpk1-7* embryos (Fig. 20D). For instance, in torpedo stage monocotyledonous embryos PIN1 arrangement can be almost wild type (compare Fig. 20C with Fig. 20D). The same held true for the localization of ENP, which in epidermal cells of cotyledons is apically localized just like PIN1 (compare Fig. 20A with Fig. 20B).

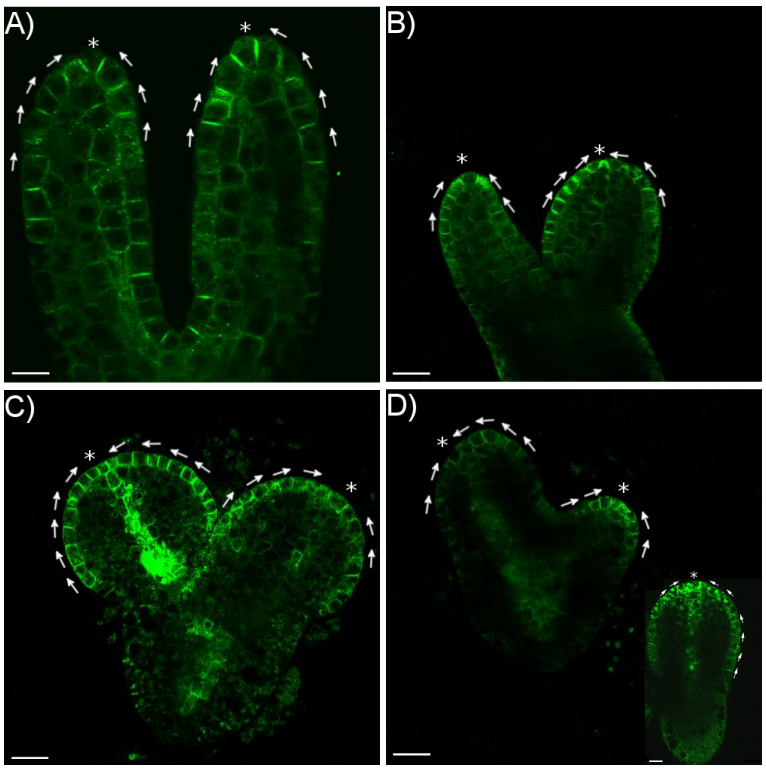

Figure 20 – Localization study of p35S:GFP::ENP and pPIN1:PIN1::GFP transgene *A.thaliana* torpedo stage embryos in *rpk1-7* background. A) p35S:GFP::ENP in wild type/dicot *rpk1-7* embryos. B) p35S:GFP::ENP in anisocotyledonous *rpk1-7* embryos C) pPIN1:PIN1::GFP in wildtype/dicot *rpk1-7* embryos D) pPIN1:PIN1::GFP in mono- and anisocotyledonous *rpk1-7* embryos. White arrows indicate localization and orientation respectively. Stars indicate convergence points. Scale bars in A) 15 µm and in B)-D) 30 µm

However, a detailed analysis revealed rare but detectable deviations in altered as well as in normal cotyledon primordia.

Firstly, epidermal cells had sometimes different or altered size proportions (Fig. 21B). Secondly, oblique cell walls were found alongside with reduced cell sizes (Fig. 21B and Fig. 21E). Thirdly, some cells displayed weak or an almost global or multipolar ("u- or n-shaped") distribution of PIN1 in the membrane, which sometimes included a localisation towards the endosperm space respectively (Fig. 21E and Fig. 21F). In case of ENP no global or multipolar distributions could be detected, but in rare cases the polar localization seemed to have extended to the basal site (Fig. 21C). Although these alterations were prominent at the tip, they were also found in more lateral primordia positions. This and their absence/occurrence in embryos of different developmental stages, indicated that these alterations occur spatially and timely in a stochastic fashion during embryogenesis.

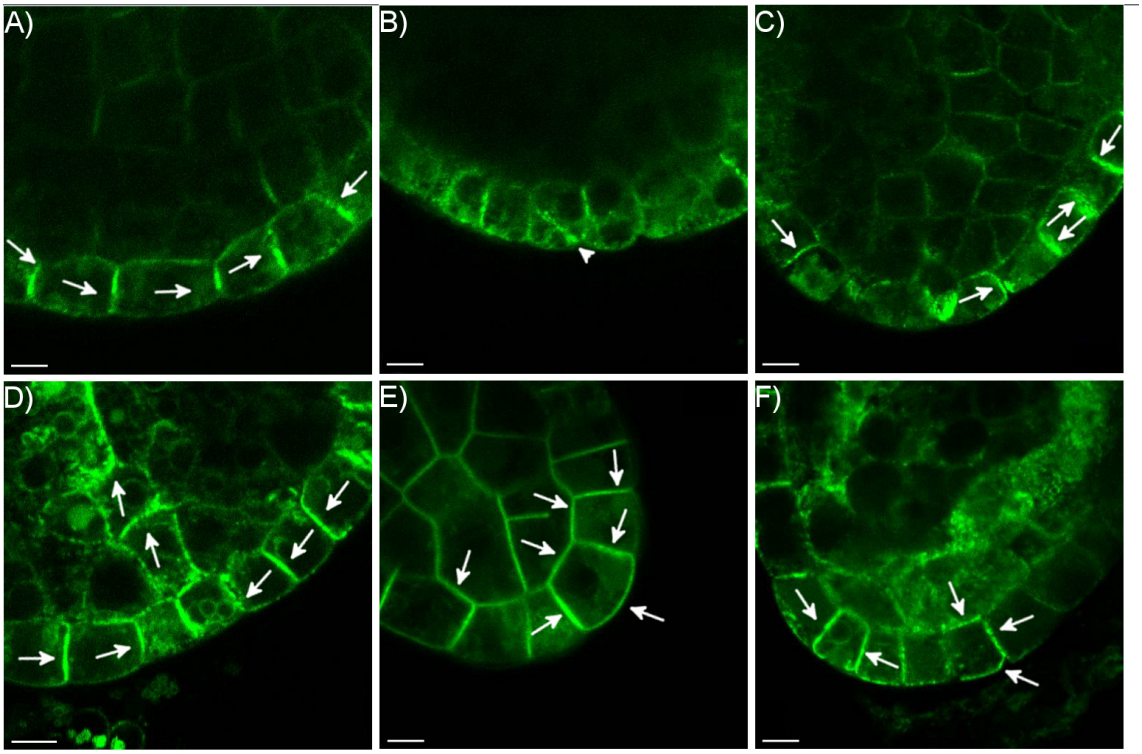

Figure 21 – Detailled analysis of p35S:GFP::ENP and pPIN1:PIN1::GFP transgene *A.thaliana* torpedo stage embryos in *rpk1-7* background. A) p35S:GFP::ENP in wild type/dicot *rpk1-7* embryos. B) and C) p35S:GFP::ENP in anisocotyledonous *rpk1-7* embryos. D) pPIN1:PIN1::GFP in wild type/dicot *rpk1-7* embryos. E) and F) pPIN1:PIN1::GFP in mono- and anisocotyledonous *rpk1-7* embryos. White arrows indicate localization and orientation respectively; white arrowheads indicate altered cell division planes. Scale bars: 5µm

It should be noted that RPK1 protein expression overlaps with PIN1 and ENP (Luichtl et al., 2013). RPK1 shows an epidermal as well as a (weak) sub-epidermal tissue localisation (Luichtl et al., 2013, Nodine et al., 2007). Its abundance is high in hypocotyls and root tip regions and low in the apical regions.

3.4 Transcriptomics of cotyledon-less seedlings

Previous work by Zweigardt (2010) had analyzed the consequences of the loss of cotyledons, caused by the *enp pid* double mutation on a transcriptomic level in the embryo. To follow up this study the work presented here aimed at analyzing the consequences of *pid enp* on the postembryonic level and should compare the obtained results with those in the embryonic stage.

To follow up the differentiation process of cotyledons into storage organs transcriptomic experiments were performed with wild type versus cotyledon-less seedlings (*enp pid*). Eight array analyses were done including four biological replicates and four technical replicates in form of a dye swap experiment. For hybridization the *Arabidopsis* (V4) Gene Expression Microarray, 4x44k (Agilent) was used. The Agilent slides were scanned by IMGM Laboratories GmbH (Martinsried, Germany) and the statistical analysis was done with the Bioconductor software (www.bioconductor.org) in collaboration with Dr. Georg Haberer from the Institute of Bioinformatics and Systemsbiology at the HelmholtzZentrum München (IBIS). Differentially expressed

genes between wild type and *laterne* (*enp pid* double mutant) seedlings were obtained by using the limma package of the Bioconductor (www.bioconductor.org). The obtained lists of differentially expressed genes from the dye swap experiments were compared with each other and with the list obtained from all eight arrays in form of a rank sum comparison. Based upon this comparison the list of differential gene expression resulting from all eight arrays was taken for further analysis. The created list is based on the loess normalization and the holm method for adjusted p-values. For further analysis the significance value threshold (p-value) was set to < 0.05 and the log FC cut off was set to be < -1 for suppressed genes and > 1 for over expressed genes. The statistical tests revealed 421 genes over expressed in the wild type tissue and 124 genes over expressed in the *laterne* seedlings. In an initial step 23 candidate genes (13 over expressed in wild type, 10 over expressed in *laterne*) were chosen and experimentally analyzed for differential expression with RT-PCR in a semi-quantitative approach (Fig. 22 and Table 39). Actin 2 was used as internal control. Out of the chosen 13 genes over expressed in wild type, eight could be repeatedly verified to be over expressed in wild type compared to *laterne* seedlings. Out of the 10 genes chosen from the list of genes over expressed in *laterne* one gene was repeatedly verified. In many cases the PCR as such failed or the expression between wild type and *laterne* tissue appeared to be equal, as judged by eye. The only case, where an opposite differential expression was repeatedly observed was for LTP2 (At2g38530).

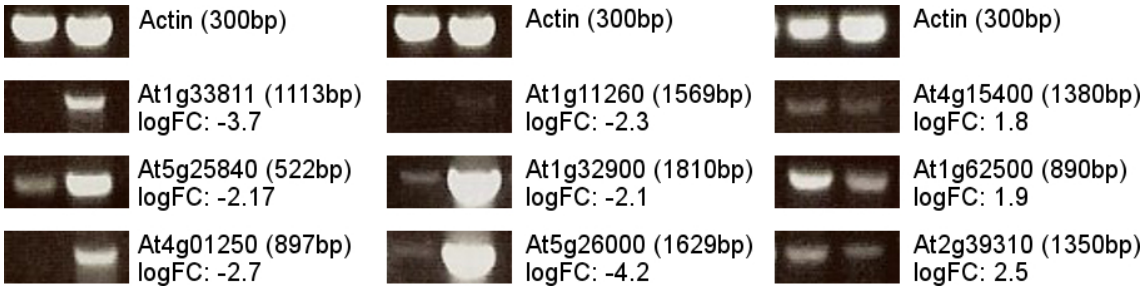

Figure 22 – Experimental validation with semi-quantitative RT-PCR of candidate genes found to be differentially expressed between *laterne* and L*er* seedlings; the first band respectively represents the specific amplification in *laterne*, the second band respectively represents the corresponding amplification in L*er*

At Number	p-value	log FC	Verification
At3g05730	0.03	-4.7	+ - -
At5g26000	0.0004	-4.2	+ +
At4g28780	0.0003	-2.4	+ +
At1g12940	0.003	-2.2	+ +
At1g32900	0.03	-2.1	+ +
At5g59750	0.002	-1.6	+ +
At4g17810	0.00000008	-2.6	- -
At1g11260	0.0000001	-2.3	- +
At4g01250	0.0000004	-2.7	- + +
At1g33811	0.000003	-3.7	+ +
At2g32500	0.000001	-3.3	- +
At5g25840	0.000007	-2.1	+ +
At4g32280	0.00001	-2-2	- +
At1g80050	0.000001	1.7	- - +
At4g15400	0.00008	1.8	- +
At2g38530	0.00006	2.0	- - - +
At1g76930	0.00008	2.0	- -
At4g37150	0.005	2.05	- -
At3g08860	0.003	2.3	- -
At2g39310	0.00001	2.5	- +
At1g62500	0.004	1.9	+ +
At2g05440	0.0001	1.8	- -
At5g42580	0.00005	1.6	- -

Table 39 – List of candidate genes chosen for the experimental validation with semi-quantitative RT-PCR

In order to detect enriched functionality modules the list of differentially expressed genes was subjected to a GO enrichment analysis using the software ClueGo (Bindea et al., 2009). The created enrichment network was visualized using Cytoscape 3.0.2 (Shannon et al., 2003). The analysis was done for all three domains of the Gene Ontology, namely biological process, cellular component and molecular function. Further, the analysis was done for the genes over expressed in wild type and for the genes over expressed in *laterne* respectively, with the significance and log FC cut offs as described above. The analysis was based on a two-sided (enrichment/depletion) test. A kappa score of 0.5, representing a medium stringency, was used. Further, the Bonferroni method for adjusted p-values was applied and the network specificity was set to be medium. The restriction on GO-terms was set to have a minimum level of three and a maximum level of eight, whereas a grouping of functional terms was made, in case at least eight genes or at least 5% of genes were represented in the group. The p-value cutoff was set to be 0.05 and the leading term of a functional group was determined to be the term with the highest percentage of genes/term. Functional modules regarding the domain biological process that are overrepresented in wild type seedlings deal among others with leaf morphogenesis, glucosinolate and unsaturated fatty acid biosynthetic process, regulation of localization, protein dephosphorylation and hydrogen peroxide metabolic process as well as with photosynthesis (Fig. 23).

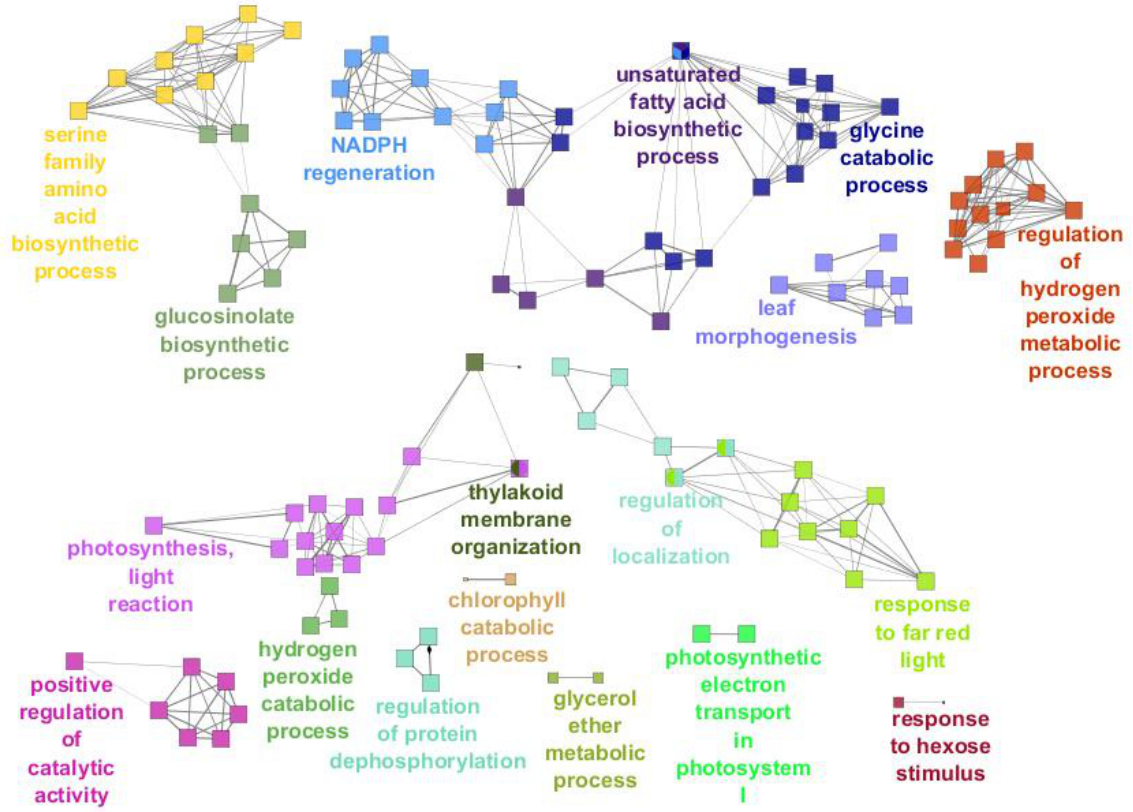

Figure 23 – Network representation of enriched GO categories among the genes (GO category: Biological Process) that were enriched in the wild type resulting from the transcriptomics analysis of *laterne* versus L*er* seedlings. The network was analysed with ClueGo (Bindea et al., 2009). GO terms are represented as nodes and the node size indicates the significance of the term's enrichment. The edges are related to the relationships between the selected terms, which are defined based on the genes that are shared in a similar way.

In comparison, the functionalities of genes over expressed in the *laterne* data set regarding the domain biological process have to do with cell wall modification involved in abscission, the polarity specification of the adaxial/abaxial axis, the positive regulation of the innate immune response and the cytokinin biosynthetic process (Fig. 24D). With respect to the GO domains cellular component and molecular function no enrichments could be detected for the *laterne* data set. In the wild type data cellular components with respect to photosystem I and II, the chloroplast, cytochrome complexes, plastids, as well as ribosome and peroxisome were enriched (Fig. 24B). When analysing the molecular function domain of GO in the gene list over expressed in wild type functions involved in photorespiration, plant stress response, plant growth and development, photsynthetic electron transport, nitrogen and sulfur assimilation. sugar transport, fatty acid desaturation, catalytic activity, chlorophyll biosynthesis, sucrose synthesis, detoxification of arsenate, amino acid metabolism, chloroplast biogenesis and response to iron deficiency stress appeared (Fig. 24A).

Next to Gene Ontology there exists the Plant Ontology (PO). This consortium similarly to GO aims at providing a common vocabulary, but in this case for describing anatomical structures as well as growth and developmental stages for all plants (www.plantontology.org). ClueGo also offers to analyze input data with a PO annotation. The results for the wild type data set showed

that genes are highly enriched, which are part of the shoot axis cortex, a portion of embryo plant tissue, the stomatal complex, the embryo root, the nucellus, the phloem, a primordium, the plant ovule, the vascular bundle, the flower bud and the cotyledon primordium (Fig. 24C).

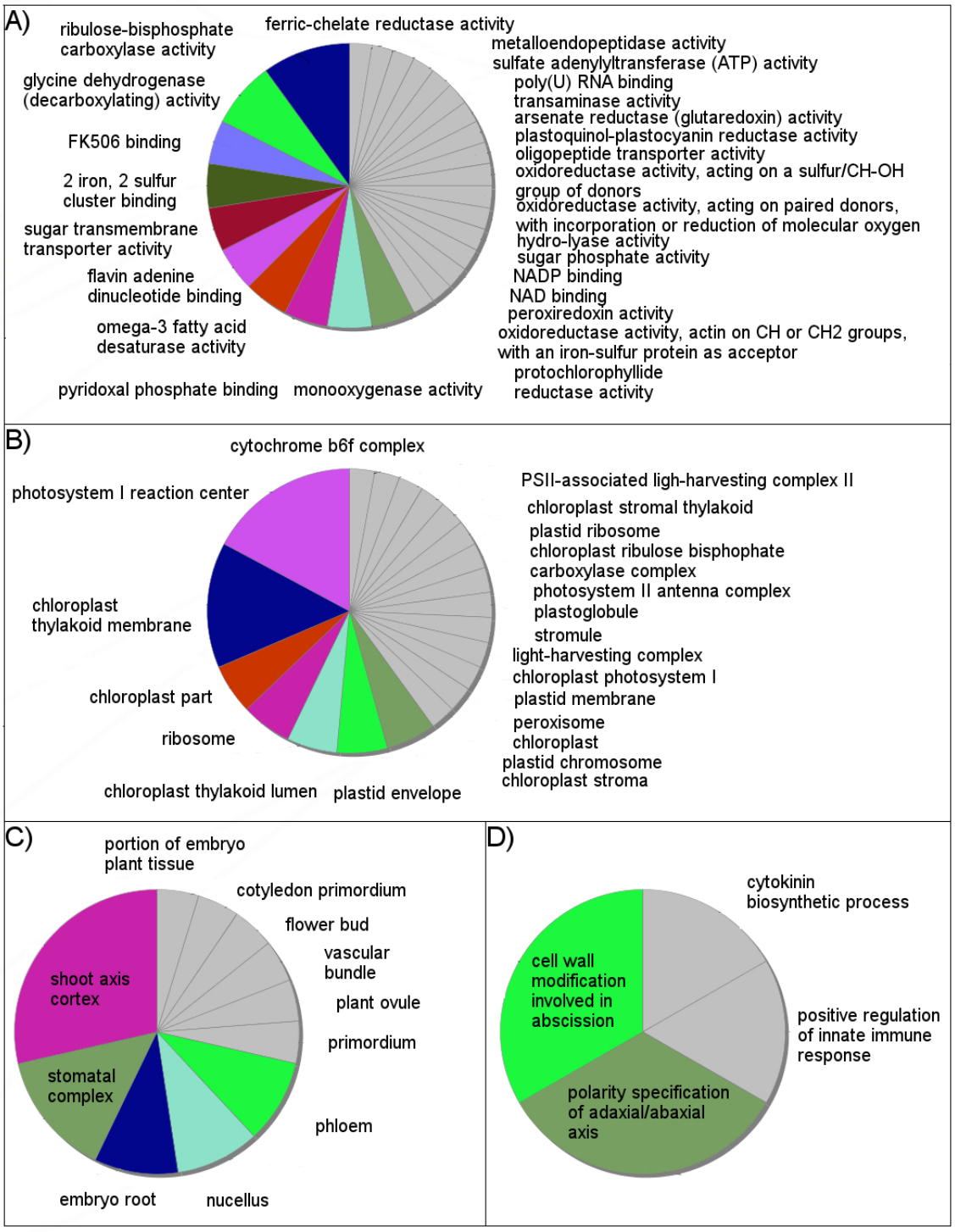

Figure 24- *legend see next page*

Figure 24 – GO and PO enrichment analysis of the transcriptomics analysis of *laterne* versus L*er* seedlings. A) Pie chart representation of enriched GO categories among the genes (GO category: Molecular function) that were over expressed in the wild type, analysed with ClueGo (Bindea et al., 2009). GO terms are represented as nodes and the node size indicates the significance of the term's enrichment. The edges are related to the relationships between the selected terms, which are defined based on the genes that are shared in a similar way. B) Pie chart representation of enriched GO categories among the genes (GO category: Cellular component) that were overexpressed in the wild type, analysed as in A). C) Pie chart representation of enriched PO categories (PO category: Plant Structure) among the genes that were over expressed in the wild type, analysed as in A). D) Pie chart representation of enriched GO categories among the genes (GO category: Biological Process) that were overexpressed in the *laterne*, analysed as in A);

In a next step the differentially expressed genes, that were obtained with the transcriptomics analysis were structured and assigned to functional categories with the help of the pathway analysis program MapMan (version 3.6.0) (Thimm et al., 2004; Usadel et al., 2005). In comparison to the GO enrichment analysis it allows the display of genomic data sets onto diagrams of metabolic pathways. As input set all statistically significant differentially expressed genes (p-value < 0.05; logFC <-1 and logFC >1) were used. The overview of the mapping of the input genes onto a metabolism diagram showed that genes over expressed in the wild type mainly control the light reactions, photorespiration and the biosynthesis of amino acids like serine, glycine or cysteine (Fig. 25; red bins). Genes over expressed in the *laterne* seedlings deal with the biosynthesis of flavonoids (Fig. 25; blue bins), mainly anthocyanins. The MapMan analysis further revealed differences in hormone signaling between the wild type and the *laterne* data set. Whereas the genes over expressed in the wild type show relation to auxin, brassinosteroid, abscisic acid (ABA) and ethylene signaling, those in *laterne* deal with jasmonic acid (JA) and gibberellic acid signalling. The wild type data set further showed an accumulation of receptor-like kinases mainly belonging to the DUF26 class and an accumulation of TCP, WRKY and basic helix-loop-helix (bHLH) transcription factors (TFs).

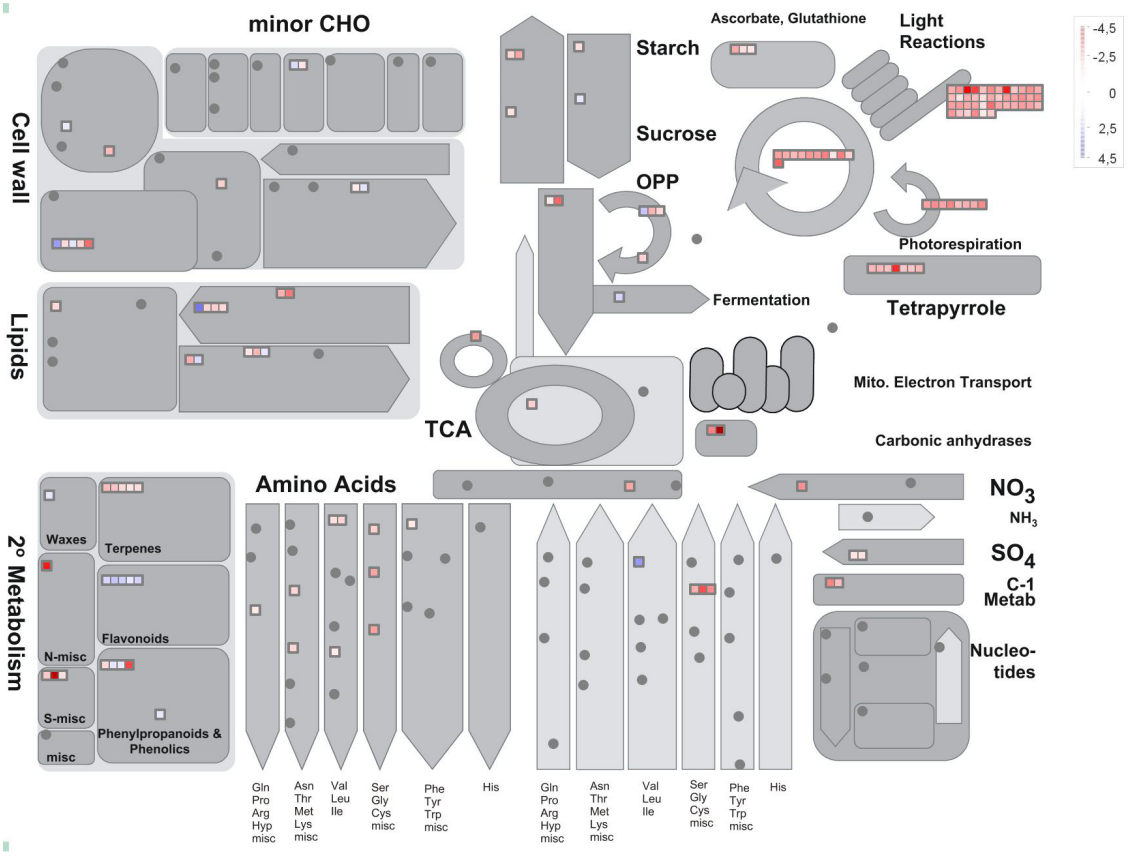

Figure 25 – Overview of the expression changes related to metabolic pathways observed in the transcriptomics data set of *laterne* versus L*er* seedlings using the MapMan software, vers.3.6.0 (Thimm et al., 2004; Usadel et al., 2005). Genes, whose expression levels were increased are indicated with an increasingly blue color (= over expressed in the *laterne*), while decreasing expression is indicated in red (= over expressed in the wild type). The graduation can be seen on the scale presented in the top right corner of the figure.

The question arose, whether the result of the embryo transcriptomics (Zweigardt, 2010) could be combined with the seedling transcriptomics done in this study. Zweigardt, 2010 showed that only a limited amount of genes is differentially expressed between wild type and *laterne* embryos. These genes fall into two functional groups. Group one consists almost exclusively of known and unknown TFs, which are normally expressed in wild type and suppressed in *laterne* embryos. Group two harbours genes coding for enzymes, that are up regulated in the cotyledon-less mutant embryos. Among them are genes, which indicate links to hormones (Zweigardt, 2010). These findings urged the question, whether the genes enriched in wild type seedlings would be direct targets of the TFs found to be over expressed in the embryo study. Therefore *in silico* promoter analyses for common transcription factor binding sites with Common TFs out of the Genomatix software suit (www.genomatix.de; version 3.0) were performed. This software allows the search for transcription factor binding sites, common to a set of promoter regions. For this the leaf morphogenesis cluster found with ClueGo was analysed further. Categories, which were functionally grouped in this cluster were stomatal complex development, shoot morphogenesis, shoot development, phyllome development, positive regulation of cellular biosynthetic process, stomatal complex morphogenesis, leaf development and leaf morphogenesis. The cluster comprised a total of 69 individual genes. All of these genes

were analyzed with Common TFs. In order to detect transcription factor binding sites common to the input set of genes the Genomatix software suit initially searches for promoter regions of the input genes. The matrix library of Common TFs offers several subsections, including plants. Further the default settings of the software were chosen for the analysis (core similarity = 0.75, matrix similarity = optimized, TFs common to 85% of input sequences). TF families were determined to be common to the input set of sequences in case they were found in at least 59 out of the 69 sequences (85%) and in case the p-value was < 0.05. The analysis revealed all together six significant transcription factor families to be common to the input set of genes (Table 40). These transcription factor matrix families were the P$IBOX family, to which the GATA transcription factors and HANABA TARANU belong, the P$DOFF family, comprising among others the OBP TFs and the DNA binding with one finger (Dof) TFs, the P$GTBX family, including 6B-INTERACTING PROTEIN 1-LIKE 1 (ASIL1) and S1F, the P$CCAF family, with the members CCA and LATE ELONGATED HYPOCOTYL (LHY), the P$MYBS family, containing SPOROCYTELESS (SPL) and PHOTOLYASE 1 (PHR1) and the P$AHBP family, comprising several members of the HB family and WUSCHEL (WUS). For the full list of the association of TFs to the matrix families used by the Genomatix software see appendix 1. Strikingly, the P$MYBS transcription factor family appeared and it was tested, whether the MYB transcription factor found in the embryo transcriptomics, namely ENHANCER OF TRY AND CPC 2 (ETC2), would fall into the same transcription factor family. The binding motif of this transcription factor is not yet described, but it is known that it is involved in trichome patterning (Kirik et al., 2004; Hilscher et al., 2009). The P$MYBS matrix family does not have a further description. The Genomatix Software suit harbors a second class of MYB TFs, namely the P$MYBL matrix family. According to the description of this transcription factor matrix family, which refers to gibberellic acid mediated signaling pathway, leaf formation, negative regulation of transcription, petal development, pollen sperm cell differentiation, proximal/distal pattern formation and most importantly trichome patterning it is more likely that ETC2 has to be subgrouped to this matrix family. Notably, when sorting the obtained matrix families common to the input sequences according to the number of genes, a specific matrix family is common to, the P$MYBL family appears to fulfill the preset 85% condition, but not statistically significant (p-value = 0.9). Another additional matrix family of TFs appears, which is the P$MADS.

Matrix Family	p-value	Common to # sequences
P$IBOX	1.25165E-005	63
P$DOFF	0.00953236	65
P$GTBX	0.013297	68
P$CCAF	0.0143515	59
P$MYBS	0.0210785	66
P$AHBP	0.0359214	66
P$MYBL	0.9	64
P$MADS	0.08	64

Table 40 – TF matrix families common to at least 85% of the individual genes grouped in the leaf morphogenesis functional unit by Cluego (Bindea et al., 2009) as found by the CommonTFs tool from the Genomatix software suit (www.genomatix.de)

3.5 The effect of boronic acids in signaling studies of different membrane proteins and in *in vivo* studies

The observation that PBA could effectively and reversibly interfere with the cellular localization of proteins, lead to an extension of these studies aiming to investigate the impact of this and related compounds on subcellular signaling. The question arose, whether boronic acids might be of general use to analyze the subcellular trafficking and the architecture of membranes and associated proteins respectively.

3.5.1 Phenylboronic acid (PBA) treatment of roots

Since usually signaling studies are done in the root, the PBA procedures established for embryos, harbouring transgenic p35S:GFP::ENP were transferred to the root tissue. As in the embryos the analysis concentrated on the epidermis by analyzing transverse optical sections or surface foci with the CLSM. The incubation of roots of 10 days old seedlings with the same concentrations as in the embryo revealed that the root system was more sensitive to the concentrations used in embryos. A series of concentrations, ranging from 50 µM to 5 mM and incubation times ranging from 15 minutes to 3 hrs revealed, that indeed in the root system PBA has the same effect on ENP as observed in the embryo. With progressing time the membrane is depleted of ENP, which accumulates in the cytosol. It further showed that the best concentration to time relation in the root is 5 mM PBA for 15minutes. Whereas in the embryo the PBA studies were done in H_2O mQ, the analysis in the root revealed, that working with 0.5 MS leads to more stable results. With this system in hand it could be shown that upon PBA incubation ENP was detached from the PM (Fig. 26B) as stated before and upon washout with 0.5 MS for 2 hrs ENP was retargeted to the PM (Fig. 26C). With this established system the effect of PBA on pPIN2:PIN2::GFP roots was tested. This protein showed an apical localization in epidermal root cells, like ENP (Fig. 26D). In the cortex cells PIN2 displays a basal localization. Treatment with 5 mM PBA for 15 minutes lead to a lateral diffusion within the membrane instead of a detachment from it (Fig. 26E). A two hour washout with 0.5 MS lead to a retargeting of

pPIN2:PIN2::GFP to the apical site of the PM (Fig. 26F).

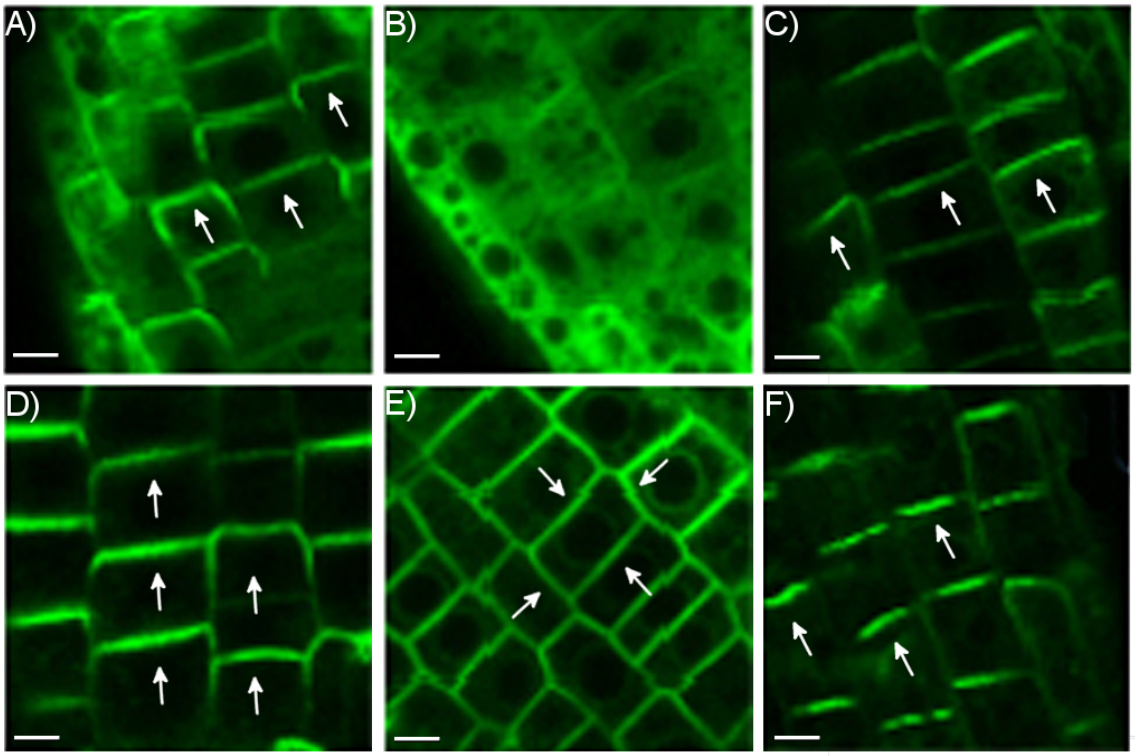

Figure 26 – Signaling studies of p35S:GFP::ENP and pPIN2:PIN2::GFP in transgenic *A.thaliana* roots. 10 days old seedlings were treated with PBA. A) p35S:GFP::ENP; 0.5 MS control, 2 hrs. B) p35S:GFP::ENP; incubation in 5 mM PBA for 15 minutes. C) p35S:GFP::ENP; 5 mM PBA for 15 min, three times washout with 0.5 MS and incubation in 0.5 MS for 2 hrs. D) pPIN2:PIN2::GFP; 0.5 MS control, 2hrs. E) pPIN2:PIN2::GFP; incubation in 5 mM PBA for 15minutes. F) pPIN2:PIN2::GFP; 5 mM PBA for 15 min, three times washout with 0.5 MS and incubation in 0.5 MS for 2hrs. White arrows depict localization; scale bars: 5 µm

PBA was shown in *Nicotiana tabacum cultivar Bright Yellow-2* (BY2) cells to destroy cytoplasmatic strands (Bassil et al., 2004). In order to test, whether the observed effect on the localization of ENP and PIN2 were due to a rupture of the membrane by PBA, transgenic p35S:GFP::ENP roots, treated with PBA were stained with the steryl dye FM4-64. This dye stains the PM (Betz et al., 1992; Betz et al., 1996). The results showed that PBA leaves the PM intact (Fig. 27).

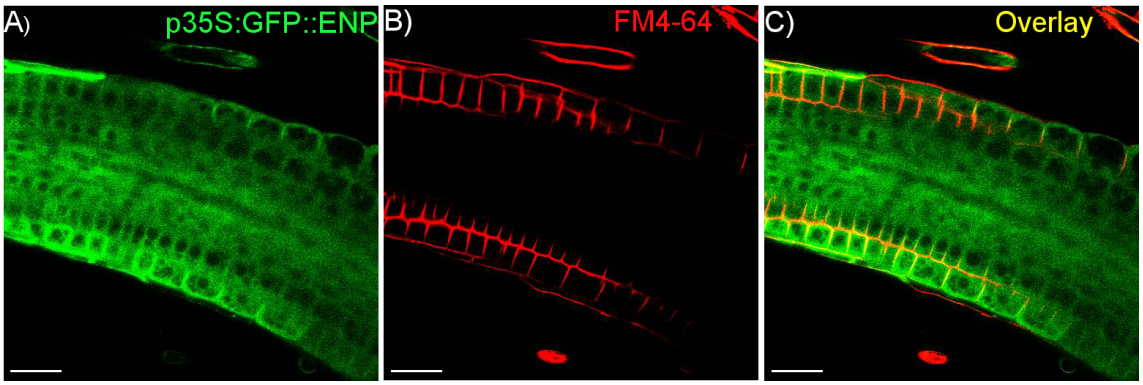

Figure 27 – FM4-64 staining of PBA treated roots harboring p35S:GFP::ENP. scale bars: 30 µm

3.5.2 *In vivo* studies

PBA is one of several boronic acids (Bassil et al., 2004). They form the same reversible bonds with *cis*-diols as the borate anion, but they cannot cross link molecules (Bassil et al., 2004). This makes them specific and effcient competitors of boron and they can be used for mimicking boron depletion.

3.5.2.1 Application of PBA onto siliques causes *mp*-like seedling phenocopies

In order to see how a transient application of PBA acts *in vivo*, this substance was applied onto siliques of *A.thaliana*. Former observations in the lab indicated a possible morphogenetic effect in *A.thaliana* seedlings (R.A.Torres-Ruiz, personal communication). Also, similar effects had been reported several decades ago with respect to PBA and *Eranthis hyemalis* (Haccius, 1960). Seedlings, germinating from young PBA-treated siliques produced with high frequency phenocopies of *A.thaliana* embryo/seedling pattern mutants lacking the embryonic root, such as *mp*, *bdl* and others (Berleth and Jürgens, 1993; Hardtke and Berleth, 1998; Hamann et al., 1999; Dharmasiri et al., 2007). For convenience the obtained phenocopies are referred to as *mp*-like (Fig. 28; Tables 41 and 42). With small frequencies lethal, developmentally defect or retarded seedlings, including cotyledon-defect seedlings germinated as well. However, these were also observed in the control treatments (see below). *Mp* mutants and the PBA-phenocopies showed no morphological differences. Both displayed the same spectrum of root-less seedlings with no or little hypocotyl development and one, two or rarely three cotyledons with more or less developed tracheary elements (Fig. 28 and Fig. 30). The induction of *mp*-like phenocopies was not ecotype specific (compare table 41 with table 42). The phenocopies developed the same transformed basal region as the *mp* mutants consisting of large (vacuolated) cells without recognizable differentiation as seen in whole mount preparations (Fig. 28 and Fig. 30). In case seedlings had developed part of the hypocotyl, epidermal cells were recognizable, but this differentiation disappeared towards the root pole and no RAM was recognisable (Fig. 30).

No of silique	% wildtype	% mp like phenocopies	% other e.g cotyledon defects	% retarded seedlings	not germinated
1	100	0	0	0	0
2	100	0	0	0	0
3	84.6	15.4	0	0	0
4	95.2	4.8	0	0	0
5	55.3	**44.7**	0	0	0
6	59.3	**40.7**	0	0	0
7	37.8	**62.2**	0	0	0
8	33.9	**66.1**	0	0	0
9	74.4	**25.6**	0	0	0
10	84.5	15.5	0	0	0
11	81.3	16.6	0	2.1	0
12	93.5	6.5	0	0	0
13	100	0	0	0	0

Table 41 – Representative example of the seedling spectrum of five independent experiments. *A.thaliana* ecotype Col-0 siliques were treated with 50 mM PBA.

No of silique	% wildtype	% mp like phenocopies	% other e.g cotyledon defects	% retarded seedlings	not germinated
1	100	0	0	0	0
2	100	0	0	0	0
3	100	0	0	0	0
4	100	0	0	0	0
5	95	5	0	0	0
6	94.7	0	0	0	5.3
7	75	5	0	20	0
8	48	**52**	0	0	0
9	51.2	**48.8**	0	0	0
10	46.6	**54.4**	0	0	0
11	/	/	/	/	/
12	96.3	3.7	0	0	0

Table 42 – Seedling spectrum that germinated from *A.thaliana* ecotype L*er* siliques treated with 50 mM PBA.

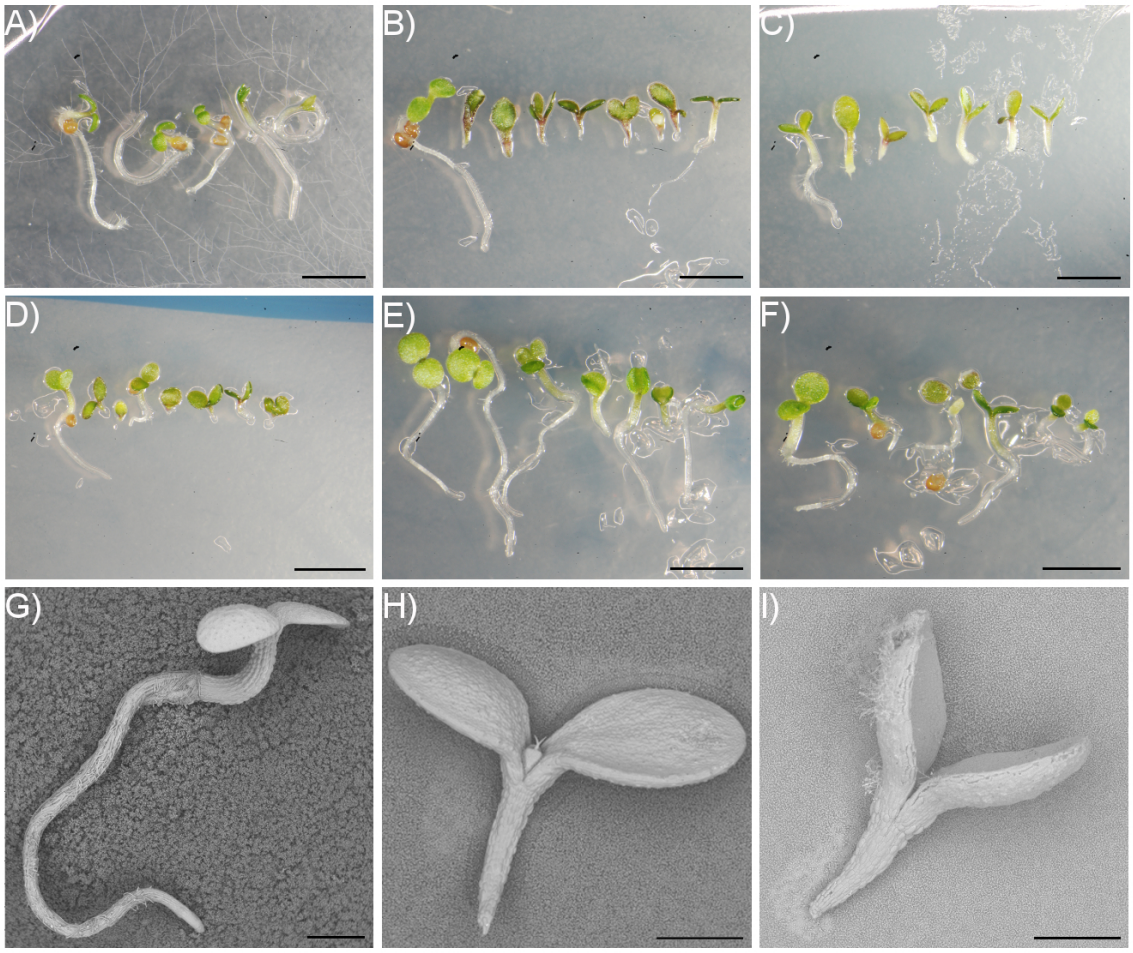

Figure 28 – Seedling phenotypes after application of boronic acids and analogs. A) Spectrum of seedlings germinating from untreated Col-0 siliques. B) Spectrum of *mp* seedlings. C) Spectrum of *bdl* seedlings. D) Spectrum of seedlings germinating from Col-0 siliques treated with 50 mM PBA. E) Spectrum of seedlings germinating from Col-0 siliques treated with 50 mM phenylacetic acid. F) Spectrum of seedlings germinating from Col-0 siliques treated with 50 mM benzoic acid. G) Scanning electron microscopic picture of a wildtype Col-0 seedling. H) Scanning electron microscopic picture of a *mp* seedling. I) Scanning electron microscopic picture of a PBA induced *mp*-like phenocopy seedling. Scale bars in A) - F) 0.5 cm; in G) 1 mm and in H) - I) 0.5 mm.

To see whether this was an effect due to the boronic acid moiety, appropriate analoga were tested (Fig. 29).

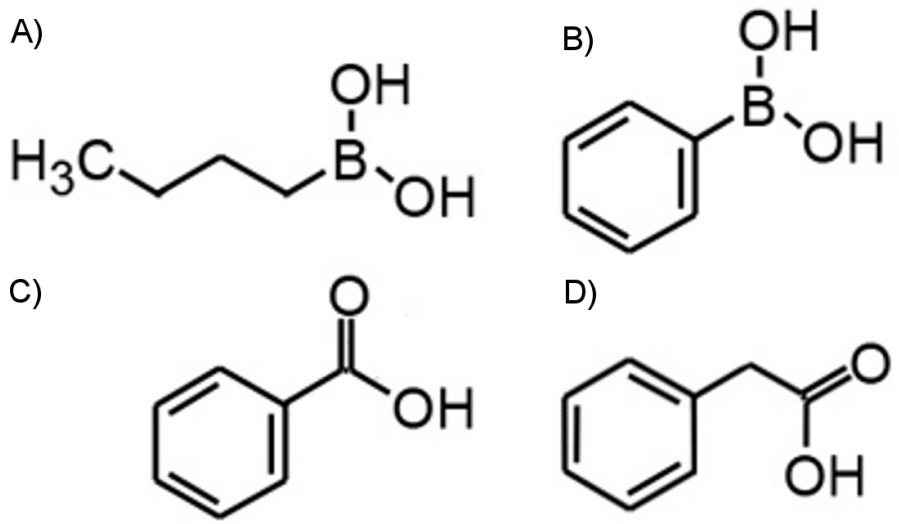

Figure 29 – Structures of applied boronic acids and analoga. A) butylboronic acid. B) phenylboronic acid. C) benzoic acid. D) phenylacetic acid.

Benzoic acid (BES) is a non-boronic analog with one carbon replacing the boron atom. The resulting seedlings were predominantly wild-type, others were retarded in growth including small seedlings with short roots, often sticking in to the seed coat and often malformed in the apex (Fig. 28F). Their root tip if stunted still had regular cell files quite different to those in the basal region of *mp*. Notably, the BES treatment produced retarded seedlings in all, i. e. not only the youngest siliques indicating some toxic, growth-inhibiting effect during germination (Tables 43 and 44). Different ecotypes revealed the same results (compare Table 43 with Table 44).

No of silique	**% wildtype**	**% mp like phenocopies**	**% other e.g cotyledon defects**	**% retarded seedlings**	**not germinated**
1	100	0	0	0	0
2	100	0	0	0	0
3	100	0	0	0	0
4	100	0	0	0	0
5	97.7	0	0	2.3	0
6	96.1	0	0	3.9	0
7	97.9	0	0	2.1	0
8	100	0	0	0	0
9	100	0	0	0	0
10	100	0	0	0	0
11	100	0	0	0	0
12	100	0	0	0	0
13	100	0	0	0	0

Table 43 – Representative example of the seedling spectrum of three independent experiments. *A.thaliana* ecotype Col-0 siliques were treated with 50 mM BES.

No of silique	% wildtype	% mp like phenocopies	% other e.g cotyledon defects	% retarded seedlings	not germinated
1	75	0	0	25	0
2	100	0	0	0	0
3	100	0	0	0	0
4	100	0	0	0	0
5	100	0	0	0	0
6	100	0	0	0	0
7	100	0	0	0	0
8	100	0	0	0	0

Table 44 – Representative example of the seedling spectrum of five independent experiments. *A.thaliana* ecotype L*er* siliques were treated with 50 mM BES.

Phenylacetic acid (PAA) is an acetic acid analog, where the boron atom is replaced by two carbon atoms. Treatments with PAA did not produce any *mp*-like phenocopies in the two ecotypes tested (Col-0, L*er*) (Tables 45 and 46). Most seedlings had a wild type appearance except rare cases in young siliques displaying a spectrum of cotyledon defects including simultaneous fusions of both cotyledons (Fig. 28E).

No of silique	% wildtype	% mp like phenocopies	% other e.g cotyledon defects	% retarded seedlings	not germinated
1	100	0	0	0	0
2	100	0	0	0	0
3	100	0	0	0	0
4	97.1	0	**2.9**	0	0
5	81.8	0	**18.2**	0	0
6	91.7	0	0	0	8.3

Table 45 – Representative example of the seedling spectrum of three independent experiments. *A.thaliana* ecotype Col-0 siliques were treated with 50 mM PAA.

No of silique	% wildtype	% mp like phenocopies	% other e.g cotyledon defects	% retarded seedlings	not germinated
1	100	0	0	0	0
2	100	0	0	0	0
3	100	0	0	0	0
4	100	0	0	0	0
5	55.6	0	**44.4**	0	0
6	69.2	0	**28.8**	0	1.9
7	100	0	0	0	0
8	100	0	0	0	0

Table 46 – Representative example of the seedling spectrum of three independent experiments. *A.thaliana* ecotype L*er* siliques were treated with 50 mM PAA.

In cooperation with Prof. Ramon Angel Torres-Ruiz further boronic acids, benzoic acids and acetic acids were tested. All boronic acids tested induced *mp*-like phenocopies, whereas the benzoic acids and the acetic acids did not.

Additionally the structurally unrelated butylboronic acid was tested to account for an effect due to the boron moiety and not due to the overall structure of the tested substances (Fig. 29). This compound when applied to siliques of Col-0 plants was only very rarely able to induce the *mp*-like phenotype (Table 47).

No of silique	**% wildtype**	**% mp like phenocopies**	**% other e.g cotyledon defects**	**% retarded seedlings**	**not germinated**
1	100	0	0	0	0
2	100	0	0	0	0
3	100	0	0	0	0
4	100	0	0	0	0
5	100	0	0	0	0
6	100	0	0	0	0
7	100	0	0	0	0
8	100	0	0	0	0
9	100	0	0	0	0
10	100	0	0	0	0
11	100	0	0	0	0
12	100	0	0	0	0
13	100	0	0	0	0
14	100	0	0	0	0
15	100	0	0	0	0
16	98.3	**1.7**	0	0	0
17	100	0	0	0	0
18	100	0	0	0	0
19	100	0	0	0	0

Table 47 – Representative example of the seedling spectrum of six independent experiments. *A.thaliana* ecotype Col-0 siliques were treated with 50 mM butylboronic acid.

The ability to compete with boron depends on different parameters and differs between boronic acids (Bassil et al., 2004). The possibility was considered, that the structure of butylboronic acid might cause a less effective penetration of tissues like siliques or ovules. To test this possibility, siliques (L*er* ecotype) were carefully opened with microsurgical forceps and butylboronic acid was applied to the artificial opening. This treatment induced a higher amount of *mp*-like phenocopies, namely up to 23.8% (Table 48).

No of silique	**% wildtype**	**% mp like phenocopies**	**% other e.g cotyledon defects**	**% retarded seedlings**	**not germinated**
1	100	0	0	0	0
2	85.7	**4.8**	0	0	9.5
3	52.4	**23.8**	0	0	23.8
4	89.5	0	0	5.3	5.2
5	91.7	0	0	0	8.3

Table 48 – Representative example the seedling spectrum of three independent experiments. *A.thaliana* ecotype L*er* siliques were opened with microsurgical forceps and treated with 50 mM butylboronic acid.

In order to understand the effect of PBA on root formation the *mp*-like phenocopies were analysed further.

3.5.3 Comparative analysis between *mp*, *bdl* and *mp*-like phenocopies

3.5.3.1 Analysis of PBA effects in early embryogenesis

The *mp*-like phenocopies were induced in young siliques (or sometimes flowers). In older branches with many siliques of different ages, their frequency declined rapidly towards older siliques (Tables 41 and 42). This excluded a late or postembryonic impact of PBA on root development and suggested that early embryo stages were competent for this induction. This is reminiscent of the effects of mutations in *MP*, which disturb embryonic root meristem specification, during early embryo stages (Hardtke and Berleth, 1998; Schlereth et al., 2010). In wild type the development of the RAM starts with the unequal horizontal division of the hypophysis, the most apical suspensor cell, into a lens shaped and basal cell (Fig. 30A and Fig. 30B). These cells continue with a series of predictable cell divisions until late heart stage to give the embryonic RAM, which is then implemented in the embryo body (Fig. 30E). To address, whether PBA interferes in the process, the substance was applied on wild type siliques and the developing embryos were microscopically analyzed 24hrs later. In fact, analyses of embryos 24 hrs after PBA application displayed defects in the same cell(s) leading to vertical and/or equal cell divisions (Fig. 30C and Fig. 30D) of the hypophysis cell very much like those observed in *mp* mutants (Fig. 30G and Fig. 30H; Schlereth et al., 2010). These abnormal cell divisions could be traced back to the early globular stages (ca. 32 cells) when the division of the hypophysis takes place (Fig. 30C and Fig. 30D). The disturbance of cell divisions could obviously happen along the complete development of the RAM, since some phenocopies developed relatively long hypocotyls ending in undifferentiated basal cells (Fig. 28D). In rare cases, unequal sized cotyledon primordia were visible before RAM defects. Both observations are compatible with late or incomplete contacts of the embryo with the boronic acids.

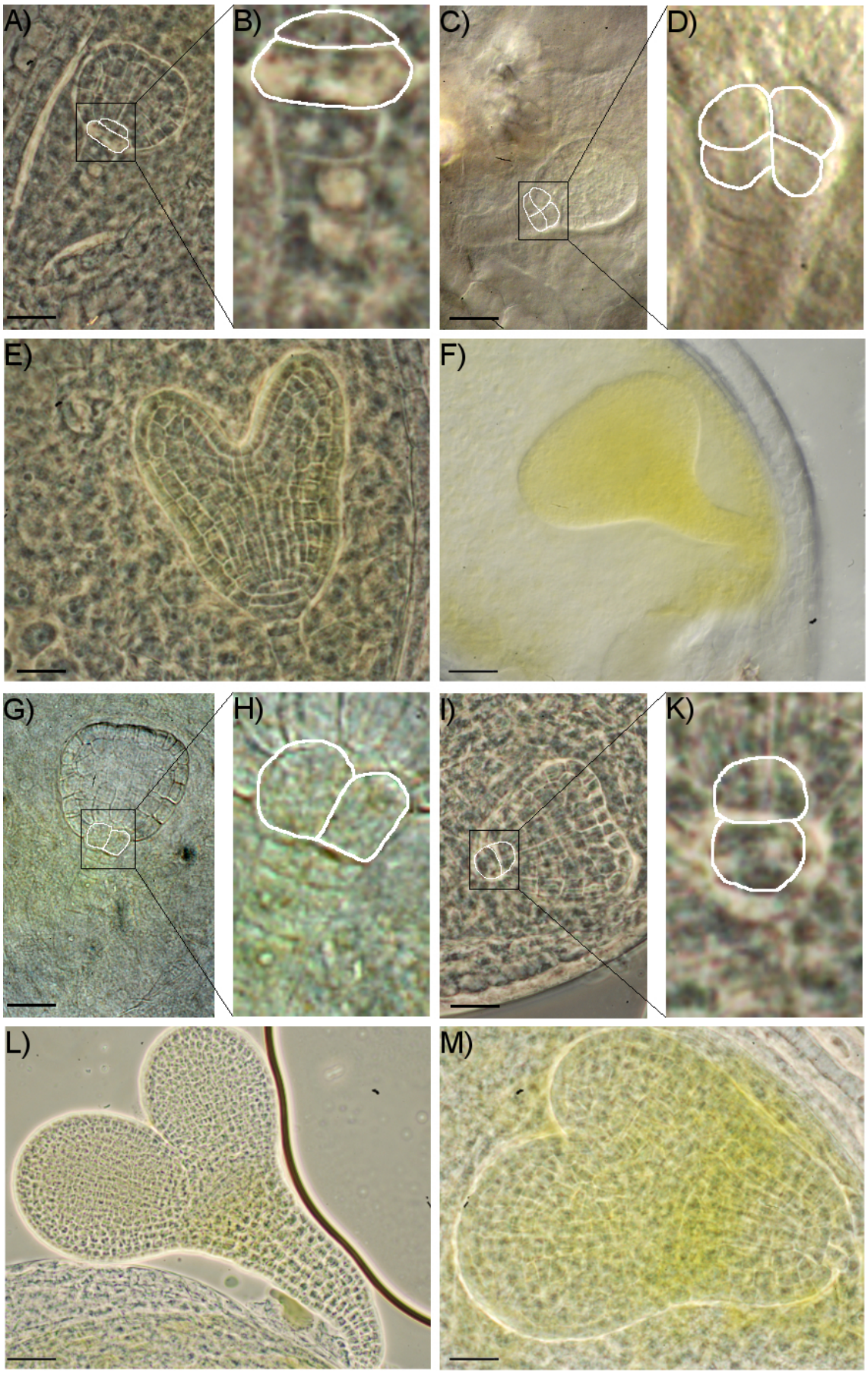

Figure 30 - *legend see next page*

Figure 30 – Comparison of boronic acid induced phenocopies with *mp* and *bdl* mutants in the course of embryogenesis. A)-D) and G)-K) globular to early heart stage embryos, focusing on the division of the hypophysis. In A) and B) wild type (Col-0). C) and D) PBA treated. G) and H) *mp.* I) and K) *bdl.* E), F), L), M) torpedo stage embryos. In E) wild type (Col-0). F) PBA treated. L) *mp.* M) *bdl.* Scale bars in A) - D) and G) - K) 22.5 µm E), F), L), M) 50 µm

3.5.3.2 Expresssion analysis of *TARGET OF MONOPTEROS* genes in *mp*, *bdl* and *mp*-like phenocopies

mp-like phenocopies and *mp* mutants were further characterized and compared according to their expression of target genes of MP, namely *TARGET OF MONOPTEROS 5* and *7* (*TMO5/7*). *TMO5* expression was completely absent in *mp* cDNA, but was detected in *bdl* weakly, in wild type seedlings, which germinated from chemical treated siliques, as well as in all treated seedlings, including those treated with boronic acids PBA (Fig. 31). This held true in both Col-0 and L*er* background. In case of *TMO7*, *mp* mutants showed a reduced expression, whereas *bdl* seedlings completely lacked any *TMO7* expression. PBA-induced phenocopy seedlings displayed a strong reduction, if not a complete absence in *TMO7* expression compared to wild type seedlings, germinating from treated siliques (Fig. 31). The PAA and BES treated seedlings did not show any difference in *TMO7* expression compared to the wild type control expression (Fig. 31).

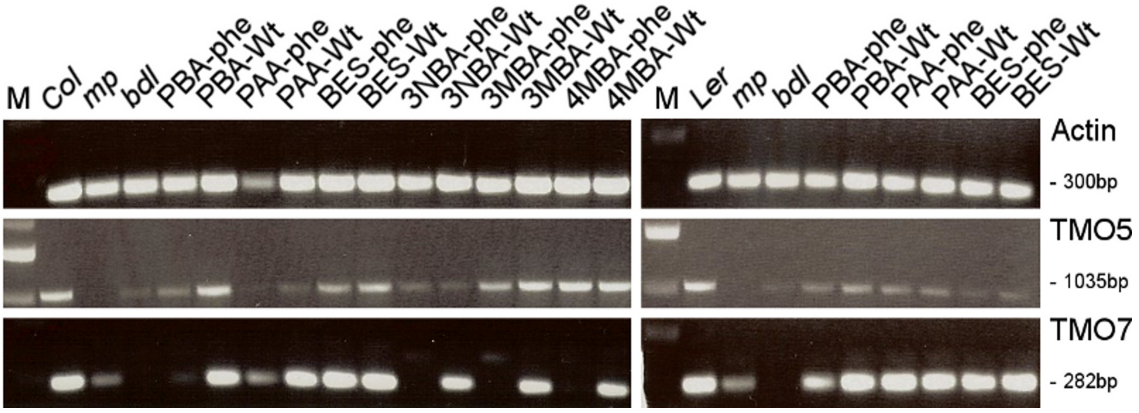

Figure 31 – Comparison of the boronic acid induced phenocopies with *mp* and *bdl* mutants according to the expression of the target genes of *mp TMO5* and *TMO7. Actin2* was chosen as control.

3.5.3.3 Analysis of auxin maxima in *mp*-like phenocopies

Since the performed expression analyses showed a reduction in *TMO7* in seedlings, it was assumed that the activity of MP with respect to *TMO7* induction cannot be resumed in the basal cells of *mp*-like phenocopies. This and the lack of the embryonic root lead to the conclusion that auxin levels must be altered upon PBA treatment.To test this, PBA was applied to siliques of transgenic DR5:GFP plants. The DR5 construct is regularly used to monitor auxin accumulation in plants (Ulmasov et al., 1997; Benková et al., 2003). The DR5 signal was analysed 24 hours after PBA treatment in embryos with a fluorescence microscope (Zeiss). The experiments

showed a clear reduction of DR5:GFP in the basal region of heart stage embryos (Fig. 32B) of PBA treated siliques. The untreated DR5:GFP control embryos on the contrary showed a strong fluorescence in the same region (Fig. 32A).

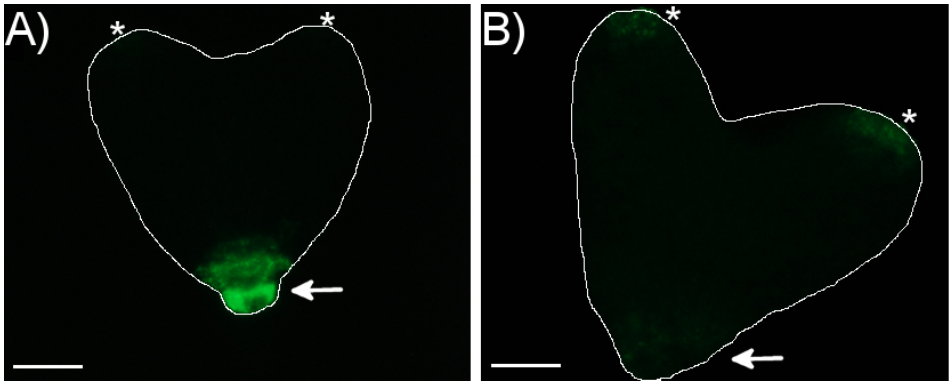

Figure 32 – Comparative analysis between auxin accumulation in PBA induced phenocopies and in wild type. A) DR5 expression in wild type (Col-0) heart stage embryos. B) DR5 expresssion in wild type (Col-0) heart stage embryos 24 hrs after PBA treatment of siliques. Scale bars: 22.5 µm.

4 Discussion

4.1 ENP's localization is dependent on extrinsic and intrinsic factors

4.1.1 Tissue specific factors determine an apical or basal localization of ENP

ENP localizes in epidermal cells of cotyledons to the apical site of the PM (Zweigardt, 2010; Furutani et al., 2011). Extrinsic and intrinsic factors that establish and maintain this polarity were elusive at the beginning of this work. The performed experiments showed that extrinsic factors are first necessary for the decision between apical and basal localization. One important extrinsic factor here is an as yet unidentified tissue dependent factor and its effect is uncovered, when ENP is ectopically expressed in stele cells. It appears as if in stele cells ENP adopts a basal localization like PIN1 (Zweigardt, 2010). However, due to difficulties in the expression of ENP by p35S in the embryo, this could not be unambigously demonstrated. By using the root system to analyze GFP fusion proteins in this work a basal localization of p35S:GFP::ENP in root stele cells could be demonstrated. This showed that ENP not only co- localizes endogenously with PIN1 in the epidermis, but also when being constitutively expressed in the root. This had the initial assumption that the mechanisms by which these two proteins establish their localization might be the same or that the localization of ENP might be due to a recruitement of ENP by PIN1. However, when being ectopically expressed in the root epidermis under the control of the PIN2 promoter, PIN1 was shown to localize to the basal site (Wiśniewska et al., 2006), whereas ENP depicted an apical localization, like the endogenous PIN2 (Fig. 33). This showed that although the localizations of both proteins are similar, the mechanisms on how these proteins establish their polar domain are at least in part different. In fact due to the similarity of localization of ectopic ENP and endogenous PIN2 in the root the question arose, whether ENP and PIN2 share a membrane targeting and maintenance mechanism. Two aspects argue against this possibility. First, PIN2 is an integral membrane proteins, whereas ENP is associated (Treml, 2008; Zweigardt, 2010). Second, PBA experiments point to significantly different responses of these proteins to this compound.

Additionally, the ENP-like protein NPY4, under the constitutive p35S, showed the same tissue specificity as ENP and PIN1. Whereas endogenous ENP in the cotyledons is restricted to the epidermis, where it is localized apically, endogenous NPY4 is predominantly found in the provascular system, where it localizes basally (Furutani et al., 2011). In case both proteins are expressed with a constitutive promoter like p35S, both proteins are additionally ectopically expressed in the endogenous domain of the other (Zweigardt, 2010; this study).

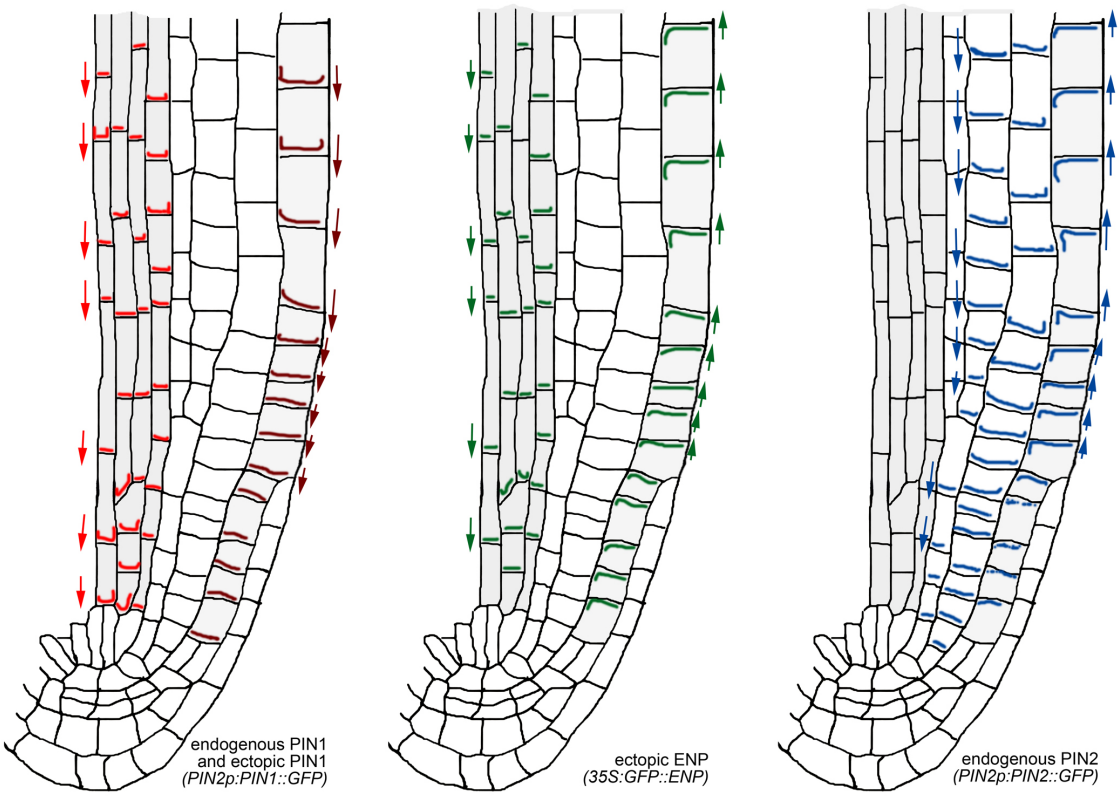

Figure 33 – Schematic representation of ectopic and endogenous PIN1,2 and ENP polar localizations in the root. Left: endogenous localization of PIN1 in the stele (light red) and ectopic localization of PIN1 (expression driven by the *PIN2* promotor) in the epidermis. Middle: ectopic localization of ENP (expression driven by the 35S promotor) is apical in the stele and in the epidermis. Right: endogenous localization of PIN2 in cortex and epidermis shows basal and apical polarity respectively. Cortex expression of ENP not shown for better comparison. Arrows indicate orientation of the proteins in the adjacent cells. Left and right after Wisniewska et al., 2006, middle this study

4.1.2 The subcellular targeting of ENP is actin, but not BFA dependent

Additional extrinsic factors, were further shown to be necessary for the polar targeting of ENP to the PM. At the beginning of this work transport routes to target ENP to its polar PM localization were elusive, since a depletion of ENP from the PM could not be achieved by applying numerous inhibitors including, NAA, 2-4D, CHX, oryzalin, CytD, wortmannin, fillipin, TIBA, NOA, NPA and BFA (Zweigardt, 2010; Furutani et al., 2011). By testing additional chemicals with respect to the capability to deplete ENP from the PM PBA was found to be effectively able to do so. With the help of this tool a procedure was established, which made it possible to study the cellular transport of ENP. It could be shown that ENP uses actin filaments to reach the PM and that this process is independent of BFA. This is in contrast to PIN1, for which it was shown to accumulate in so called BFA-vesicles after BFA treatment (Geldner et al., 2003). This in turn supports the conclusion that first, the localization of ENP, also considering the initial localization, is completely independent on the localization of PIN1 and second, that the localization of ENP is maintained through mechanisms different than those for PIN1.

These observations open the possibility for numerous future studies. For instance, analyses could include the application of diverse inhibitors after PBA-induced separation of ENP from

the PM. In case of PIN1 for example an effect on auxin transport inhibitors could only be shown for the retargeting of PIN1 to the PM after its detachment from it (Geldner et al., 2003). These analyses should use the root system rather than the embryo, because for roots conditions (and concentrations) are established.

4.1.3 Intrinsic factors determine a lateral extension of ENP's localization

Like the mechanisms for polar targeting possible sequence-based determinants for ENP's localization were unknown as well. Molecular determinants specifying the polar localization of ENP were addressed in this study and it appeared that ENP in addition to its apical localization shows an extension to lateral sites of the PM. The significance of the extension of protein localization from central to the upper lateral membrane sites/regions in cells has been pointed out for PIN1 and PIN2 recently (Klein-Vehn et al., 2011). When lacking the C-terminal region (as seen in the construct ENPdeltaCterm) ENP localizes exclusively to the apical site and any lateral extension is abolished. This allows the hypothesis that molecular determinants for lateral diffusion lie in the C-terminus of ENP. This was further addressed by an analysis of the ENP-like protein NPY4 (construct: NPY4), which shows high sequence homology with ENP, but strikingly has a much shorter C-terminus. The performed localization studies showed that NPY4 exclusively localized centrally to the apical site of the plasma membrane. However, with the addition of the full C-terminus of ENP (NPY4_ENPCtermLong), the localization domain was sometimes extended to lateral sites in epidermal cells.

The control of lateral diffusion was described in the case of PIN2 to be dependent on clathrin-mediated endocytosis, which in turn was directly coupled to the phosphorylation status of a specific tyrosine residue (Klein-Vehn et al., 2011). Upon loss of phosphorylation in this residue, PIN2 strongly localized to lateral sites (Klein-Vehn et al., 2011). In the course of the performed localization studies of ENP, one tyrosine residue was also mutated into a loss-of phosphorylation and a potential phospho-mimick version (constructs: ENP_Y409A and ENP_Y409E). In contrast to the PIN2 loss-of phosphorylation construct, ENP_Y409A did not show any lateral diffusion, but rather was restricted exclusively to the apical site of the PM. Thus the examined tyrosine residue is not necessary for clathrin-mediated endocytosis and whether clathrin-mediated endocytosis is relevant for ENP and its maintenance of polarity in general, remains to be determined.

The intrinsic factors determined to be necessary for ENP's localization depict parallels to intrinsic localization signals for BRASSINOSTEROID INSENSITIVE1 KINASE INHIBITOR (BKI). Wild type BKI is localized at the PM and in the cytosol in roots (Jallais et al., 2010). A specific subdomain in the N-terminal fraction of BKI, ranging from amino acids 149-221, is sufficient for proper membrane localization. Further, especially four internal [KR][KR] repeats are necessary for the membrane localization (Jallais et al., 2010). ENP shows six of the named [KR][KR] repeats at positions 196-197, 201-202, 235-236, 350-351, 427-429 and 437-38. How they contribute to the PM localization of ENP has been shown in this study on first approach. It is likely that the ones at positions 427-429 and at positions 437-438 are the most important for

apical localization, since all mutations deleting these repeats lead to delocalization of ENP from the PM (ENPdeltaNPH3_All, ENPdeltaNPH3_2+3, ENPdeltaNPH3_3). In the C-terminus of ENP there are four more [KR][KR] repeats, which might contribute to the lateral extension of the membrane localization of ENP. This is supported by the fact that the construct that lacks the C-terminus (construct: ENPdeltaCterm= amino acids 1-460) and therefore these additional [KR][KR] repeats is localized to the apical site.

4.2 ENP's function can be separated from its polar localization

Being polarly localized at the apical site of epidermal cells in cotyledons, ENP supports and maintains together with PID the polarity of PIN1 at the PM. This was shown in the *laterne* (= *enp pid*) mutant, which completely abolished cotyledons (Treml et al., 2005). The *laterne* seedlings continued their development normally, but failed later to initiate flower organogenesis and produced sterile blind ending stems (Treml et al., 2005). The mutation in ENP leading to this mutation is causing an early stop codon, therefore abolishing the C-terminus, like the construct ENPdeltaCterm, which allowed the conclusion that functional elements for ENP lay in the C-terminus. A fully functional ENP protein, under control of the constitutive 35S promotor, could rescue the flower phenotype (Treml, 2008). The seedling phenotype cannot be rescued since the activity of the 35S promoter is too late in the embryo (Zweigardt, 2010). This suggested that ENP's correct polarity is necessary for the flower rescue. When part of the BTB POZ domain is missing, the localization of ENP is impaired with the main part of the protein pool being found in the cytosol (Treml, 2008). This construct could not rescue the mutant flower phenotype (Treml, 2008). On the other hand, it was shown that a localization at the apical site of the PM *per se* is not sufficient to rescue the mutant *laterne* flower phenotype (Zweigardt, 2010). However this was only shown with NPY4, a homologue of ENP, which shows ectopically an apical localization in the epidermal cells of *A.thaliana* embryos (Zweigardt, 2010). Since NPY4 has also additional amino acid differences to ENP in the BTB POZ as well as NPH3 domains, the aforementioned conclusion was not fully justified.

The presented work showed that ENP's localization can be separated from its functionality. This was seen initially be analysing the ENP_deltaCterm construct. It showed an apical localization, but it could not rescue the mutant phenotype. The series of performed analyses detected additional sites, that separated full function and sole localization. One was the tyrosine residue at position Y409. Localization studies showed that a potential phospho-mimick of this residue (ENP_Y409E) leads to an accumulation of ENP in the cytosol, whereas destruction of the phosphorylation site (ENP_Y409A) maintains the localization of ENP at the PM. Both constructs were further not able to rescue the mutant flower phenotype of *enp pid* double mutants, therefore showing the functional importance of this residue in ENP.

Furthermore, the addition of the C-terminus of ENP in part (ENPCtermShort) or in full length (ENPCtermLong) to NPY4 is not capable of rescuing the *enp pid* flower phentoype, as well. At present, this was only seen in two plants and to undermine these results a higher amount of samples should be analyzed. Notably, in pools of different F2-seedlings in both lines, adult

plants developed that had flower like structures, but also blind ending stems. This requires further analysis, but might hint at possible *laterne* seedlings, since *pid-15* single mutants don't produce blind ending stems (Treml et al., 2005). In case this observation holds true, the domain swap constructs of NPY4 with the addition of the C-terminus of ENP possess a partial rescue capability.
Interestingly, the construct only harboring the BTB POZ domain and the large linker region (ENPdeltaNPH3_All) sometimes developed flower structures, which also indicates a partial rescue. This construct nevertheless is not localized and therefore seems to contradict aforegoing statements. The reason for this rescue is not clear and although the transgenes were correctly sequenced in the rescued plant it cannot be excluded that the endogenous mutant *enp* is altered. Further, this rescue might hint at a possibility of this deletion construct to interact with endogenous enp (which ich localized as ENPdeltaCterm) and with a specific interactor, thus causing a partial functionality of ENP.

4.3 ENP is a potential target for phosphorylation

Protein phosphorylation appears to be a mechanism that allows plants to developmentally adapt in response to environmental changes. There are several hints that this post transcriptional modification is also important for ENP.

4.3.1 Functional importance of Y409

ENP's localization and its functioning might be dependent on the phosphorylation state in at least one tyrosine residue, namely Y409. The obtained results nevertheless do not unambiguously show that Y409 has to be phosphorylated to be functional active, since due to high structural differences it is not possible to perfectly phospho-mimick tyrosine residues. It is also possible that the introduced site mutation destroyed the overall structure of the fusion protein. Therefore the analysis only revealed the functional importance of this residue. Notably, a small deletion mutant of *ENP/MAB4* abolishing this residue in concert with two other residues, leads with simultaneous *pid* to the *laterne* phenotype (Furutani et al., 2007). Further, this tyrosine is highly conserved between NPH3-like proteins and it suspected to be a functional site in NPH3 (Liscum and Briggs, 1995). Phosphorylation events in tyrosines are rare in plants, compared to serine or threonine phosphorylations (reviewed in de la Fuente van Bentem and Hirt, 2009), but they contribute to important signaling mechanisms as for example brassinosteroid signaling (Jallais et al., 2010).
This signaling involves two receptor-like kinases BRI1 and BRI1-ASSOCIATED RECEPTOR KINASE (BAK), as well as the inhibitor BKI. BRI1 was shown to have tyrosine kinase activity and to phosphorylate its inhibitor BKI, which is located at the PM. Upon phosphorylation this inhibitor moves to the cytosol, where it is inactive, thereby releasing the kinase activity of BRI1 (Jaillais et al., 2010). In part such a scenario might hold true for ENP as well, where unphosphorylated ENP is polarly localized at the PM, but remains inactive, explaining the non

functional Y409A mutation. For reasons stated before, the interpretation of the Y409A mutation is however limited. Nevertheless, pharmacological studies analyzing the effect of tyrosine kinase inhibitors and tyrosine phophatase inhibitors would allow a general interpretation, whether tyrosine phosphorylation as such is important for ENP's localization.

4.3.2 ENP might be substrate of AGCVIII kinases other than PID

ENP and PIN1 show a colocalization at the apical site of the PM in the epidermis of cotyledons. Whereas the apical localization of PIN1 is controlled through direct phosphorylation by PID, ENP might not be a substrate of PID due to several reasons. First, constitutive localization of ENP in the root epidermis is apical, whereas that of PIN1 is basal, due to non-expression of *PID* in this tissue. Second, in the presence of BFA ENP is apical, whereas PIN1 is cytosolic in BFA compartments. Third, ENP and PID have never been shown to interact directly. Fourth, ENP does not show the highly conserved TPRXS(N/S) motif, found in several PIN proteins as phosphorylation target for PID and other AGCVIII kinases. Fifth, the phosphorylation site detected in this study is a tyrosine and PID is known as a serine/threonine kinase. Interestingly though, PIN proteins have a conserved tyrosine motif (NPNTY) at the C-terminal end of the central hydrophilic loop, which was suggested to be important for PM localization (Mravec et al., 2009). Showing that PID and other AGC kinases could have dual specificity and also phosphorylate tyrosines would be interesting, but not new, since BRI1, initially described as serine/threonine kinase, was recently found to phosphorylate tyrosines as well (Jallais et al., 2010). Identifying the tyrosine kinase that phosphorylates PIN1-like proteins might link PIN1 and ENP.
It further cannot be ruled out that the tyrosine in ENP is not the only phosphorylation site. Recently two serines in the C-terminus of ENP were found as phosphorylated residues in ENP-related peptide fragments in a global mass spectrometry analysis (Chen et al., 2010). The first serine lies in the sequence KSTRSGGG and the second one in the sequence SSQSPPAK (underlinings indicate the phosphorylated residues). They don't resemble the aforementioned TPRXS(N/S) motif known to be a target for PID and other AGC kinases, like PID2, WAG1 and WAG2, but it was observed that triple mutations of *pid2*, *wag1*, *wag2* in a *pid* background lead to cotyledon-less seedlings just like the *enp pid* double mutant (Dhonukshe et al., 2010). Detection of these AGC kinases to be able to phosphorylate substrates different to PIN1 would have significant impact. Experimental approaches have been done to assess the role of the mentioned serines in the C-terminus of ENP. They are both part of the sequence that was added to the ENP-like NPY4 in the domain swap constructs. As mentioned before this addition so far did not result in any rescue, but more samples have to be analyzed. To specifically account for the effect of the named serines on the functioning of ENP, both serines were individually mutated into loss of phosphorylation and phospho-mimick variants, but could not be analyzed.
To account for a possible phosphorylation of ENP by the WAG kinases, in an initial step p35S:GFP::ENP was crossed into *wag1/wag2* as well as *pid2/wag1/wag3* mutants in *pid* background. If these kinases take ENP as substrate for phosphorylation and if this is necessary for targeting ENP to the apical site of the PM, a basal localization of ENP in these mutants should

be observed.

4.3.3 ENP might be linked to a PDK1 associated signaling cascade

The Y2H data showed that ENP might be involved in a PDK1 associated signaling cascade. The found interaction partner PDK1 is a highly conserved gene between animals and plants. In addition it is involved in the phosphatidylinositol signaling pathway. The phosphatidylinositol metabolism creates signaling molecules, which are pivotal for plant growth and development (Xue et al., 2009). PDK1 is known to bind to different signaling lipids in the PM (Hirt et al., 2011). It is generally known that signaling lipids arise by modification of hydrolytic enzymes, such as hydrolases, esterases or lipases. Interestingly, two enzymes of these classes were found to interact with ENP as well, namely the GTP cyclohydrolase1 and a GDSL esterase/lipase, for which not much is known. The former protein was found to mediate the first and committing step of the pterin branch of the folate-synthesis pathway (Basset et al., 2002) and is predominantly found in the cytosol. Folates are essential cofactors for one-carbon transfer reactions in all organisms and have been recently shown to act in concert with sucrose to shape auxin distribution and sensitivity (Stokes et al., 2013). Notably the interaction of the GTP cyclohydrolase with ENP was found to be auxin-sensitive in the way that the addition of auxin to the selection plates lead to a decrease in growth of *S.cerevisiae* colonies, referring to a reduction of interaction between GTP cyclohydrolase 1 and ENP. Nothing is known so far about the found GDSL esterase/lipase protein (At5g62930). The GDSL family of esterases and lipases nevertheless was described to be hydrolytic enzymes with multifunctional properties, such as broad substrate specificity and regiospecificity (Akoh et al., 2004). The found GDSL esterase therefore might mediate the substrate specificity for ENP targets. Gene Ontology further assesses it to have hydrolase activity and to be involved in a lipid metabolic process. To account for the roles of these two hydrolases in plant organogenesis and specifically cotyledon and flower development T-DNA insertion lines should be analyzed in a first step. Interestingly to note is that generally hydrolases are involved in lipid signaling and membrane signaling. This might hint at a connection of these two proteins to ENP via a PDK1-associated signaling cascade. Most notably, it has been demonstrated, that PDK1 phosphorylates PID in plants (Zegzouti et al., 2006), which in turn cooperates with ENP to polarize PIN1. The finding of PDK1 as interaction partner of ENP, links for the first time the players of the ENP/PID/PIN1 chain on a molecular level, suggesting that ENP itself might be a phophorylation target of PDK1. It should be further noted though, that PDK1 was also reported to bind to different proteins, such as 14-3-3 in order to target them to specific cellular locations and to bring them in close contact to their functional interaction partners (Weckermann et al., 2010). Therefore it might also be possible that PDK1 functions as a membrane anchor for ENP. This in turn might enable ENP's real interaction at the PM with its thematic players PID and PIN1 and at least fits with the fact that ENP has no obvious PM targeting signals like myristoylation and palmitoylation. The interaction between ENP and PDK1 was directly tested with the ProQuest^{TM} system (Gateway®) and was assessed to be weak (Jakab, 2013). To account for the detection of a weak interaction it should be noted

that this was tested with the full length ENP protein, whereas the global Y2H screen revealed the interaction between PDK1 and ENP with the construct only harboring the BTB POZ domain of ENP.

The findings from the experimental work are unified in the working model depicted in figure 34.

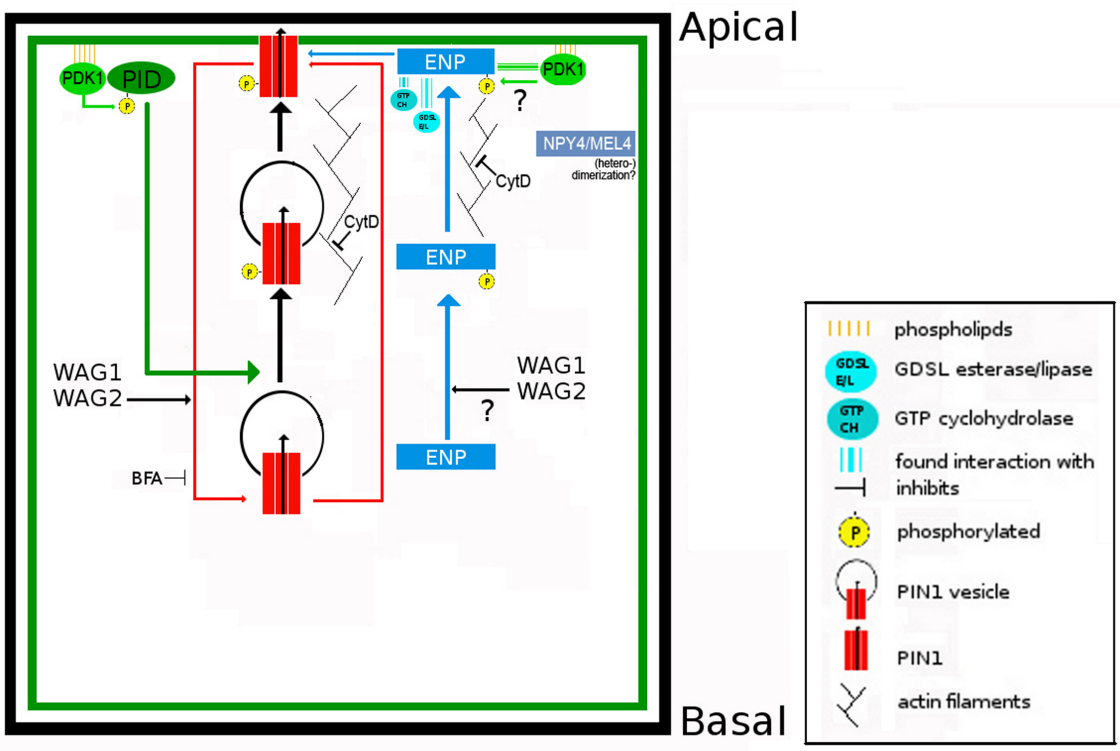

Figure 34 – Working model integrating the most important findings of the presented work concerning ENP's function and polarity in epidermal cells of *A.thaliana.* For details see text.

4.4 The function of ENP with respect to its BTB POZ domain

The function of ENP also has to be discussed with respect to its N-terminal BTB POZ domain. The BTB POZ domain was identified in the *Drosophila melanogaster* brac-a-brac, tramtrack and broad complex transcription regulators and in many pox virus zinc finger proteins (Stogios et al., 2005). Among involvement in different cellular processes, BTB proteins were shown to be interaction partners of the Cullin3 Skp1-Cullin-F-Box (SCF)-like E3 ubiquitin ligase complex (reviewed in Genschik et al., 2013). The BTB domain mediates the recruitement of the substrate recognition modules to the Cul3 component of the SCF-like complex, therefore acting as protein-protein interaction module that is able to self-associate and interact with non-BTB proteins. A plant specific architecture is the combination of the BTB POZ domain with the functionally unknown NPH3 domain. In total, 21 BTB-NPH3 proteins exist in *A.thaliana* (Stogios et al., 2005), one of which is ENP. For this class of BTB proteins it was initially shown that NPH3 is involved in phototropism as adapter protein that connects modules of the light signal transduction pathway, which is initiated by the light activated serin/threonine kinase PHOTOTROPIN1 (PHOT1) (Motchoulski and Liscum, 1999). Further it was observed that these

BTB POZ domains show heteromerization as in case of NPH3 and ROOT PHOTOTROPISM2 (RPT2), but they can also bind non-BTB binding proteins. A similar observation was found in this study as well. Repeatedly, interactions between full length ENP and full length NPY4, which is also a BTB-NPH3 protein were observed in Y2H experiments. That hints that ENP and NPY4 both show hetero- and possibly homomerization. Nevertheless the detected interactions were assessed to be weak. The weakness of the interactions were found for the full length as well as for constructs only harboring the respective BTB POZ domain. Additional confirmation might come from co-immunoprecipitation experiments, which have been initiated for ENP. Important to note here is that the interactions between ENP and NPY4 *in vivo* will be restricted to early embryonic stages, since in later stages both proteins reside in different tissues. A possible *in vivo* interaction might also be possible in the root, since promoter GUS fusions just recently showed an overlapping appearance of both proteins in root tissue (Li et al., 2011).
Non-BTB interaction partners of ENP (PDK1, VOZ1, GTP cyclohydrolase1, GDSL esterase/lipase) were detected, showing that the BTB POZ domain of ENP behaves like that in other BTB-NPH3 containing proteins, meaning that various interactions can be observed. An important role of BTB-containing proteins appears to emerge in its ability to bind Cul3 (reviewed in Genschik et al., 2013), which in turn regulates various signaling processes. A mapping of the experimentally obtained results onto recent literature descriptions allow the hypothetical assumption that ENP might be involved in a Cul3-BTB complex as well, although all performed interaction assays so far have not revealed such an interaction. First, ENP was repeatedly shown to interact with its close homolog NPY4 and further *in silico* analysis done with the *A.thaliana* protein interaction network suggest interactions of ENP with further *NPY* genes (Brandao et al., 2009). Interactions with close homologs have been reported to recruit one specific member to Cul3 (Fu et al., 2012). Second, a global screen with ENP detected an interaction of ENP with the transcription factor VOZ1. This interaction was directly verified in *S.cerevisiae* with the ProQuest^{TM} System (Gateway®). VOZ1 in turn was shown to be degraded in a 26S proteasom dependent manner in the nucleus. This in turn is phytochrome B dependent, which is translocated into the nucleus upon far red light (Yasui et al., 2012). Whether this might be a translocation signal for ENP into the nucleus as well, remains to be tested. With respect to the VOZ1 ENP interaction, leading to a degradation of VOZ1 it is interesting to note, that VOZ1 was shown to actively control the expression of *FLOWERING LOCUS T* (*FT*) (Yasui et al., 2012). An over expression construct of FT in turn lead to the development of leaf like structures at the apex of the stem, similar to those observed in the ENP_P46T and ENP_Y409A rescue experiments, suggesting an over expression of FT through reduced degradation of VOZ1.

4.5 PIN1 polarity changes in *rpk1* are different to those in *pid enp*

Mutations in the *RPK1* gene lead to a monocotyledonous phenotype with a low penetrance of 4.8% (Nodine et al., 2007; Nodine and Tax, 2008). RPK1 acts redundantly with its homolog RPK2/TOAD2 and double mutations lead to a higher penetrance of the monocotyledonous phenotype (Nodine and Tax, 2008). Both genes were further shown to be important for proper embryo development, since mutations in both genes lead to abnormal embryos described as "defective half" and "toadstool" (Nodine et al., 2007). Pleiotropic defects of the analyzed double mutants lead Nodine et al. (2007) to conclude that RPK1 and 2 are required for central domain pattern formation, as well as basal pole differentiation during globular stages of embryogenesis and that signaling mediated by RPK1/2 is dependent on a critical threshold. However, the pleiotropic effects made it difficult to disentangle cotyledon-specific from more general pattern functions.

In order to understand the cotyledon-specific defects of RPK1, the recently identified *rpk1-7* single mutant (Luichtl et al., 2013) was analysed with respect to the cellular localization of ENP and PIN1. The *rpk1* monocotyledonous phenotype raised the question, whether PIN1 would be basally localized in the region lacking the cotyledon and whether this could be compared to the overall basal localization of PIN1 in *pid enp* (= *laterne*) (Fig. 35). Moreover, this raised the question, whether RPK1 could be an integral element in the PID/ENP/PIN1 network.

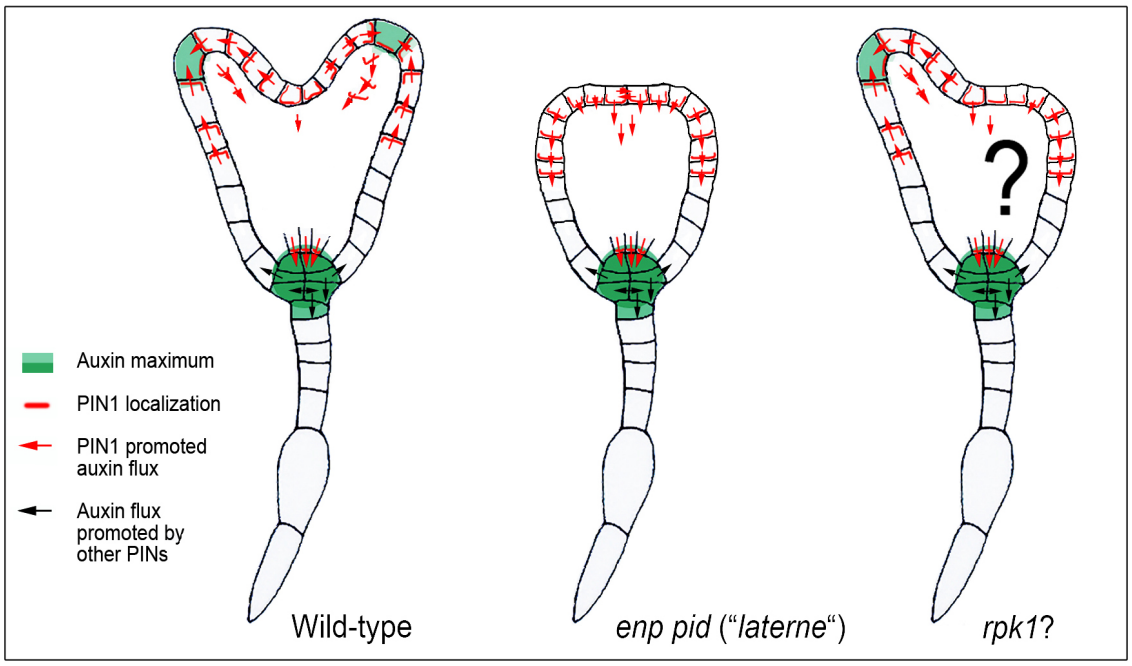

Figure 35 – Working model on PIN1 polarization in monocotyledonous *rpk1-7* mutants. (left) PIN1 localization in wild type, (middle) PIN1 localization in *enp pid*, (right) initially assumed PIN1 localization in *rpk1-7*

Thus, ENP and PIN1 localizations were analyzed in the mutant *rpk1* background in order to see how these localizations are altered in mono and anisocotyledonous embryos in comparison

to cotyledon-less embryos of *pid enp*. It was shown that *rpk1* specifically, but in a stochastic manner, altered cell divisions and the cellular polarity of PIN1 (and ENP) in different ways. Whether RPK1 directly or indirectly links these two processes is not clear, but it has been shown that polarity of PIN proteins is a post-cytokinesis event, which results from an initially non-polar arrangement (Boutté et al., 2006; Men et al., 2008). Both effects lead to a stochastic alteration of position and number of auxin maxima and a concerted alteration or ablation of one cotyledon (Luichtl et al., 2013). The observed defects depend on the time point and the position of the lapse of *RPK1* function (Fig. 36).

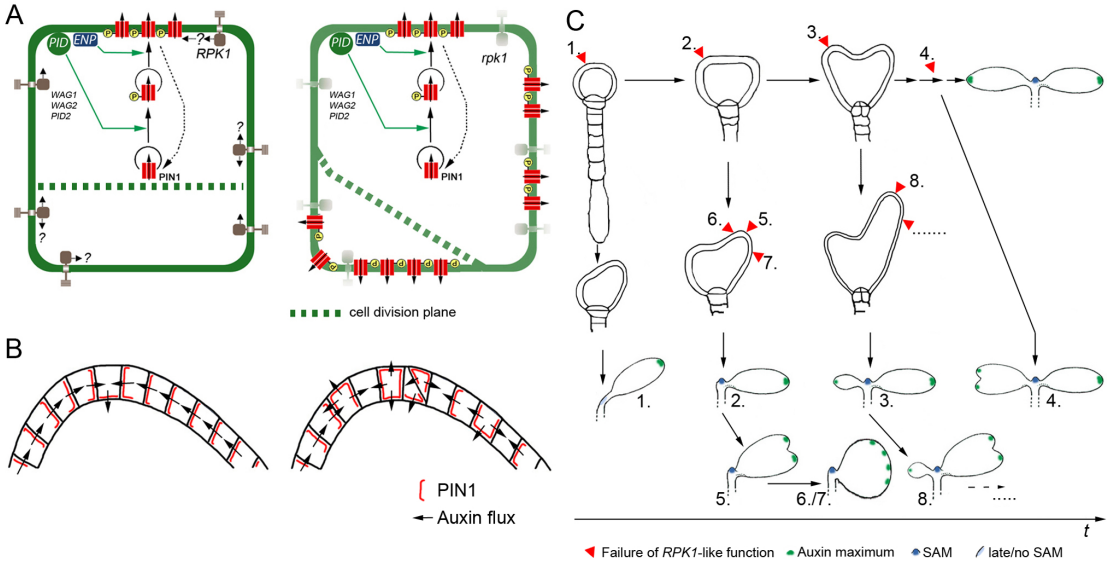

Figure 36 – Stochastic disturbance of cell shape and PIN1 polarity in *rpk1* cells. The model illustrates the consequences of stochastic *RPK1* dysfunction during embryo development, at different levels. A) On a cellular level: wildt type (left) compared to *rpk1* (left). RPK1 stabilizes cell wall orientation and PIN1 position in the wild type, in an as yet unknown fashion. In *rpk1*, in spite of a correct function of PID, ENP (and others WAG1 etc.), cell division and PIN1 localization are perturbed when the treshold of required *RPK1* function is not reached. B) On a tissue level (the epidermal layer): wild-type (left) compared to *rpk1* (right). Patterns of cell wall and PIN1 localization , respectively, and the deduced auxin flux are shown. C) On an organ level: The *rpk1* effect has different outcomes depending on its manifestation along the developmental time axis. Numbers in panel C link the time and region of stochastic alteration of cell division and PIN1 polarity with the corresponding seedling morphology. Taken from Luichtl et al., 2013.

These findings were summarized in a recent publication (Luichtl et al., 2013). The observed defects are in clear contrast to *enp pid* (=*laterne*) mutants. PIN1 localization in the *laterne* phenotype is always reverted and mutants depict normal cell shapes (Treml et al., 2005). Thus, the alteration in *rpk1* are independent from PID/ENP pathways. However, *rpk1* effects can only manifest, when PID and ENP are functional. In *pid enp* background RPK1 cannot contribute to a correction of PIN1 polarity. This implies that PID and ENP act before RPK1. Therefore future studies should not only analyze whether RPK1 links the processes of altered cell division and altered polarity, but also what the ligand(s) of RPK1 are. The former question might be adressed with the analysis of Rho-GTPase signaling in *rpk1-7*, which was recently shown to be important in establishing PIN1 polarity in leaf pavement cells by altering the actin cytoskeleton

and inhibiting endocytosis (Xu et al., 2011; Nagawa et al., 2012).
In this respect it is interesting to add, that RPK1 was initally shown to be activated by endogenous and exogenous abscisic acid (ABA) (Hong et al., 1997; Osakabe et al., 2005), that it positively regulates many ABA-inducible genes and that its leucine-rich repeat domain is important for the reception of an ABA signal (Osakabe et al., 2005). In this ABA context, RPK1 was shown to regulate senescence in conjunction with other age-related factors (Lee et al., 2011). Whether there is a link between auxin-related and the ABA-related RPK1 functions during early- and post embryogenesis remains to be determined. Notably, auxin and ABA are connected through FUSCA3 (FUS3) activity in late embryo development (Gazzarini et al., 2004). Interestingly, recent work has demonstrated a link of embryo- and cotyledon development respectively to GA, the main antagonist of ABA, through cotyledon-defect phenotypes of the mutant *GA requiring 1 (ga1)* (Willige et al., 2011).

4.6 Transcriptomics of cotyledon-less seedlings

To follow up the transcriptomics approach done by Zweigardt (2010) with cotyledon-less embryos, the presented study performed transcriptomics of cotyledon-less seedlings (*enp pid* = *laterne*). The rationale was to see the consequences resulting from the deletion of cotyledons in *laterne* in the seedling stage and to compare them with those in the embryo stage. Cotyledons are major storage organs of developing plants and understanding their genetic factors could also be of agricultural importance.

The major storage compounds in mature *A.thaliana* seeds are storage lipids and proteins, each accounting for 30%-45% of the seed dry weight (Baud and Lepiniec, 2009). Genes involved in the accumulation of seed storage reserve have been shown to be involved in *de novo* fatty acid biosynthesis and in the triacylglycerol assembly pathways (Peng and Weselake, 2011). The analysis of enriched GO functionalities in the list of over expressed genes in the wild type detected genes to be over represented that refer to unsaturated fatty acid biosynthesis. This finding indicates that the *laterne* mutant was restricted in the expression of genes leading to seed storage proteins. Next to the accumulation of seed storage proteins, the cotyledon in the seedling stage harbored quite different functional modules compared to the embryo. It is important to have photosynthesis working, to account for leaf morphogenesis, to show a response to different stimuli, like hexose for example and to have enough genes for glucosinolate biosynthetic processes. In comparison to that, the wild type embryo cotyledon mainly displayed expression of transcription factors, primarily responsible for primordia growth and cell differentiation, eventually leading to seed storage accumulation.

In order to understand the genetic control working in the cotyledon a promoter analysis with a subset of genes, enriched in wild type seedlings was performed. The subset comprised genes, which formed the leaf morphogenesis cluster from the Gene Ontology enrichment analysis. This subset of genes appeared to be regulated by various transcription factor families involved in epidermal patterning, root hair and leaf trichome formation, circadian clock machinery, the

regulation of meristem development, the regulation of reproductive and vegetative development, as well as seed storage protein production and the establishment of cotyledon identity. Most notably, the DOF transcription factors and the GATA transcription factor families were detected. They have been shown to regulate light-induced genes (Jiao et al., 2005) and their motifs were just recently found to be overrepresented in the promoters of FA biosynthetic genes (Peng and Weselake, 2011). Whereas the DOF transcription factor family represents a plant specific transcription factor family involved in the development of the vasculature (Le Hir and Bellini, 2013), the GATA transcription factors are thought to be involved in the stable establishment of cotyledon identity, as it is the case for the transcription factor HANABA TARANU (Kanei et al., 2012). With respect to seed storage proteins, GLABRA2 was also detected, which was shown to regulate the accumulation of seed storage reserves (Peng and Weselake, 2011).

In the seedling cotyledon therefore not only factors for seed storage accumulate, but also those for establishing a cotyledon identity, as well as for the control of the circadian clock and for the development of flowers and leaves. This shows that the transcriptome of the seedling cotyledon is in part, but not exclusively controlled by transcription factors already found in the embryo.

The transcriptomics data between wildtype and *laterne* also revealed about a hundred genes, which were enriched in the *laterne* data set (~ a 1/3 of the number of genes found to be enriched in the wild type). Genes found to be over represented in *laterne* corresponded to the GO categories cell wall modifications involved in abscission and polarity specification of the adaxial/abaxial axis. For the specification of the adaxial/abaxial sites a signal from the shoot meristem is necessary (Yamaguchi et al., 2012). The functioning of the SAM is unaffected in the *laterne,* as can be concluded by the observation that rosette leaves developed normally. The question nevertheless arose, why this group of genes is over expressed in *laterne*. As shown by Treml et al., 2005 *laterne* has an extended embryonic SAM, shown by the expression of STM. Strinkingly STM also appeared to be over expressed in the *laterne* seedling. Since signals from the SAM lead to polarity specifications of adaxial and abaxial sites, they might be enriched as well, as compared to the wild type.

An additional point to discuss is the different hormone signaling distribution between wild type and *laterne* seedlings. Whereas in the wild type auxin, ABA, brassinosteroid and ethylene signalling were important, in the *laterne* jasmonic and GA signaling processes were accumulated. In order to explain this, the *enp pid* double mutant (= *laterne*) has to be further seen as mutant, which interferes with the polar auxin transport by reversing the polar localization of PIN1 (Treml et al., 2005). Auxin was shown to be correlated with ABA and GA by the transcription factor FUS 3 (Gazzarini et al., 2004). In wild type embryos auxin triggers the expression of FUS3, which in turn inhibits GA and promotes ABA, which in concert with factors such as ABA INSENSITIVE3 leads to the production and accumulation of seed storage proteins (Gazzarini et al., 2004). This could explain an increased GA signaling upon reduction of the auxin flux, with simultaneous decrease in ABA and auxin signaling. This feedback is also discussed in recent findings, where auxin and GA pathways converge on the transcription factors GNC (GATA TRANSCRIPTION FACTOR 21) and GNL (GATA TRANSCRIPTION FACTOR 22)

(Richter et al., 2013).

To understand a whole system, future research should aim at the integration of different -omics approaches since an organism or an organ cannot be simply seen as the sum of its genes. By having performed also metabolomics analyses between wildtype and cotyledonless seedlings in collaboration with Dr. Lilla Römisch-Margl and Dr. Rafał Jończyk (Chair of Genetics, TU München) the obtained transcriptomics data set is aimed at being integrated with the metabolomics data set in order to get an understanding on a systems level about the molecular make up of cotyledons.

4.7 Boronic acids in signaling studies

PBA was shown to induce monocotyledonous seedlings, when applied to undifferentiated *E.hyemalis* embryos (Haccius, 1960). In fact, as shown in this thesis PBA did not generally disturb embryogenesis, since application on *A.thaliana* siliques specifically induced *mp*-like phenocopies. In different plant species PBA was further shown to induce a reduction of petals in *Cucumis sativus* (Haccius and Massfeller, 1959) and to inhibit the formation of individual leaves in a whorl, when being applied to seeds of different caryophyllacea (Haccius and Massfeller, 1961). At that times it could be only speculated about the biochemical effect of PBA. It was suggested that this increased boron effect was due to the phenylgroup (Torssell, 1956). In the last decades, accumulated data nevertheless showed that PBA competes with boron for *cis*-diols, the binding of which is the key for boron function (reviewed in Bolaños et al., 2004). Therefore PBA and other boronic acids are increasingly used to mimick boron depletion in plants and fungi (Bassil et al., 2004). Indeed, the *mp*-like phenocopies in this study, were only induced with the application of boronic acids and never with any analoga missing the boron group.

As suspected already by Haccius (1960) the effect of PBA has inhibitory effects on specific developmental processes. Even earlier it was described that the first effects on boron deficiency appear in meristems (Sommer and Sorokin, 1928, cited in Bonilla et al., 2009) and since then it was looked for proof that boron has a role in signaling mechanisms during embryogenesis. Next to a localization of boron in the membrane (Pollard et al., 1977; Tanada 1983) and showing that there are rapid changes in membrane function, which are induced by boron deficiency (Robertson and Loughmann, 1974; Pollard et al., 1977; Goldbach, 1984; Goldbach, 1990; Schon et al., 1990; Barr et al., 1993; Barr and Crane, 1991) the closest hints for boron functions in the plasma membrane came from studies with growing pollen tubes for which rapid membrane formation is necessary (Jackson, 1989). Further boron was shown to be essential in organisms without cell wall (Bennet et al., 1999) for instance, and in animal embryo development (Lanoue et al., 2000; Rowe and Eckkert, 1999).

As could be shown in this study the main effect of PBA is a direct or indirect, reversible interference with membrane trafficking mechanisms. By using PAA, BES, the unrelated butylboronic acid, which lacks the phenylgroup, and PBA, this work points to the boronic acid moiety as the sole part responsible for the observed effect. The PBA effect was shown by detachment

and dispersal of different membrane and membrane associated proteins from and in the plasma membrane, while keeping the PM intact. This study therefore displayed not only a functional role of boron in endocytotic processes and/or in membrane structure, but further showed that boron indirectly has a role in signaling processes, since competing with boron in a particular developmental stage leads to a specific morphogenetic defect, namely *mp*-like phenocopies. In early embryogenesis (~32 cell-stage) this leads to a stop in auxin flux in direction of the hypophysis cell, presumably caused by a depletion of the PM of PIN1. At this early stage PIN1 is the main contributor to the auxin accumulation in the hypophysis cell. It is also possible, that the reduction of auxin is also significant in the neighbouring cells above the hypophysis. This could cause a feed-back impact on the repression of BDL on MP, such that it resumes or continues its repression. This in turn would not only affect MP's positive induction of *PIN1*, but also *TMO7*. The expression analysis of *mp*-like phenocopy seedlings at least suggest, that such an inhibition extends to this later stage. In this scenario, both, a missing auxin maximum and a missing TMO7 protein cause a breakdown of any specification signal for the hypophysis. The hypophysis in turn divides incorrectly leading to the disruption and malformation of the root meristem, eventually leading to *mp*-like phenocopies (Fig. 37).

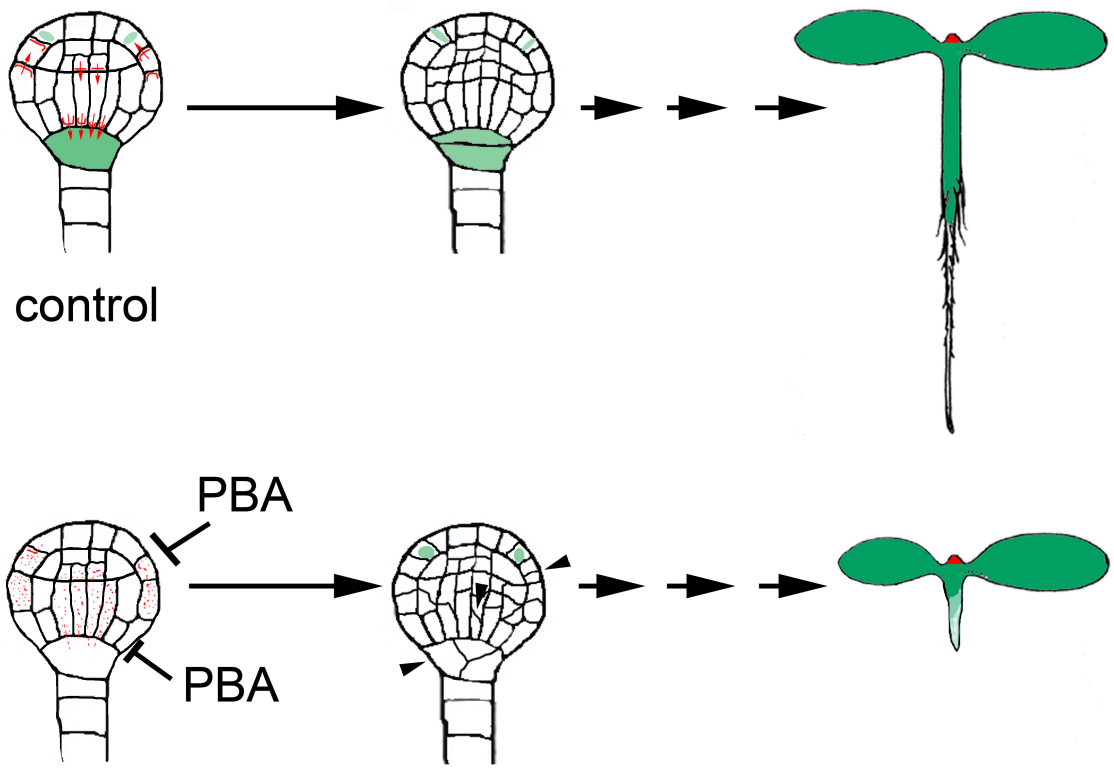

Figure 37 - *legend see next page*

Figure 37 – Scheme illustrating the early effects of PBA. Shown are globular embryos with incipient organization of the major efflux carrier in stele cell precursors PIN1 (red lines). Other PINs, as for instance PIN7 in the suspensor, are not shown. Before formative cell division of the hypophysis into a lens shaped and a larger basal cell, auxin is polarly transported (red arrows) by PIN1. At this stage, auxin begins to accumulate in the hypophysis and very slightly in the cotyledon anlagen. In the hypophysis, the auxin maximum (together with the TMO7 protein) is required for correct cell divisions ultimately leading to a wild type root apical meristem allowing correct root growth. Upon transient application of PBA, the membrane is depleted of integrated and associated proteins, such as PIN1 (and PIN2, ENP). The disturbed auxin flux blocks the generation of auxin maxima. This causes abnormal cell divisions in the basal pole as well as in other embryo regions (arrowheads). The transient application of PBA is sufficient to induce root-less phenocopies reminiscent of *A.thaliana* root pattern mutants such as *mp* and *bdl*.

The example of the induction of *mp*-like phenocopies due to a mislocalization of PM proteins showed that boronic acids and especially PBA can be used as novel compounds for disturbing membrane trafficking and in turn also suggests a role of boron in membrane trafficking.
Since PBA was shown to interrupt cytoplasmic strands in tobacco BY2 cells (Bassil et al., 2004) it could be argued that the observed effects are due to a general disruption of cells and membranes, respectively. Several observations in this work argue against such an effect. First, the PBA effect is reversible. Second, counterstaining with FM4-64 showed that the PM was intact after PBA treatment. Third, no cellular lethality occurred in embryos. Fourth, no seedling lethality could be detected. And fifth, the PBA effect was observed in specific cell groups, namely the RAM and/or at the cotyledon tip.
As could be shown in this study, in the embryo tissue higher concentrations fro the same effect had to be applied (5 mM PBA in root in comparison to 25 mM PBA in embryos). This might be due to attenuated pervasion of the applied chemicals through the ovules. Additionally, embryos appeared to be highly sensitive to the isolation from the ovules and successful experiments strictly were dependent on the elapsed time between separating embryos from the ovule and microscopic analysis. Therefore pharmacological studies in the root might give more reliable results and faster.

There are additional aspects considering the induced phenocopies that should be discussed as well. Although seedling phenotypes were assessed to be *mp*-like phenocopies, embryos growing in PBA treated siliques displayed often strong cotyledon defects, like fused cotyledons or completely deformed cotyledons. It is likely that the caused defects in cell division observed in the hypophysis also occur at a second specific cell group in the embryo. This is the dividing cell group in the epidermis, at the tip of cotyledon primordia. This effect is very likely explained by the membrane's depletion of proteins like PIN1 and ENP in the PM upon PBA application. However, it seems that these organs are more tolerant to transient disturbance of cell division. This is reminiscent of reports on *yoda* embryos in *A.thaliana*, which often lack a well-formed suspensor, but occasionally develop into relatively normal seedlings (Jeong et al., 2011 and references therein). An enhanced recovery of cotyledon primordia from an initial cell polarity and cell division defect was also observed in *rpk1-7* mutants (Luichtl et al., 2013). It should be further noted, that the observed cotyledon defects, induced in young embryos, could

not be induced in later stages, as shown by long term treatments of PBA, where the substance was applied daily for one week (unpublished observation).
Further, the DR5 signal in PBA treated embryos was stunning. Whereas the root maxima was almost completely missing, the maxima in the cotyledons often seemed to be larger compared to the wild type. This DR5 pattern is known from mutants interfering with the Rab5-mediated endocytotic pathway (Dhonukshe et al., 2008). There it is shown that interference with endocytosis keeps PIN proteins in a non-polar way at the PM, thereby disrupting auxin flux from the cotyledons to the root pole. This in turn leads to an increase in auxin levels, which establishes ectopic auxin response maxima at cotyledon positions. Interestingly, in endocytosis mutants these pervasive ectopic auxin maxima are interpreted by the embryo as a positional signal for root formation. Notably in these mutants root structures develop at the tips of cotyledons (Dhonukshe et al., 2008). However, these ectopic roots were never observed for seedlings germinating from PBA treated siliques, which further fosters the statement that the PBA effect is reversible.

5 References

Abas L., Benjamins R., Malenica N., Paciorek T., Wisniewska J., Moulinier-Anzola JC, Sieberer T., Friml J. and Luschnig C. (2006) Intracellular trafficking and proteolysis of the *Arabidopsis* auxin-efflux facilitator PIN2 are involved in root gravitropism; ***Nat. Cell Biol.***, 8(3), 249-256

Aida M., Ishida T., Fukaki H., Fujisawa J. and Tasaka M. (1997) Genes involved in organ separation in *Arabidopsis*: an analysis of the *cup-shaped cotyledon* mutant; ***Plant Cell***, 9, 841-857

Aida M., Ishida T. and Tasaka M. (1999) Shoot apical meristem and cotyledon formation during *Arabidopsis* embryogenesis: interaction among the *CUP-SHAPED COTYLEDON* and *SHOOT MERISTEMLESS* genes; ***Development***, 126, 1563-1570

Altschul SF, Gish W., Miller W., Myers EW and Lipman DJ (1990) Basic local alignment search tool; ***J. Mol. Biol***., 215, 403-410

Akoh CC, Lee GC, Liaw YC, Huang TH and Shaw JF (2004) GDSL family of serine esterases/lipases; ***Prog. Lipid Res.***, 43(6), 534-552

Bainbridge K., Guyomarch S., Bayer E., Swarup R., Bennet M., Mandel T., Kuhlemeier C. (2008) Auxin influx carriers stabilize phyllotactic patterning. ***Genes Dev***, 22, 810-823

Balla J., Kalousek P., Reinöhl V. Friml J. and Procházka S. (2011) Competitive canalization of PIN-dependent auxin flow from axillary buds controls pea bud outgrowth, ***Plant J.***, 65, 571-577

Barr R. and Crane FL (1991) Boron stimulates NADH oxidase activity of cultured carrot cells; ***Current Topics in Plant Biochemistry***, Vol. 10, p. 290, Univ. Missouri Press

Barr R., Bottger M. and Crane FL (1993) The effect of boron on plasma membrane electron transport and associated proton secretion by cultured carrot cells; ***Biochem. Mol. Biol. Int.***, 31, 31-39.

Barton MK and Poethig RS (1993) Formation of the shoot apical meristem in *Arabidopsis thaliana*: an analysis of development in the wild type and in the *shoot meristemless* mutant; ***Development***, 119, 823-831

Basset G., Quinlivan EP, Ziemak MK, de la Garza RD, Fischer M, Schiffmann, S., Bacher A., Ill JFG and Hanson AD (2002) Folate synthesis in plants: The first step of the pterin branch is mediated by a unique bimodular GTP cyclohydrolase I; ***PNAS***, 99(19), 12489-12494

Bassil E., Hu HN and Brown PH (2004) Use of phenylboronic acids to investigate boron functions in plants. Possible role of boron in transvacuolar cytoplasmic strands and cell-to-wall adhesion; ***Plant Physiology***, 136(2), 3383-3395

Baud S. and Lepiniec L. (2009) Regulation of de novo fatty acid synthesis in maturing oilseeds of *Arabidopsis*; ***Plant Physiol. Biochem.***, 47(6), 448-455

Benjamins R., Quint A., Weijers D., Hooykaas PJJ and Offringa R (2001) The PINOID protein kinase regulates organ development in *Arabidopsis* by enhancing polar auxin transport; ***Development***,128, 4057– 4067

Benková E., Michniewicz M., Sauer M., Teichmann T., Seifertová D., Jürgens G. and Friml J (2003) Local, efflux dependent auxin gradients as a common module for plant organ formation; ***Cell***, 115, 591-602

Benková E., Ivanchenko MG, Friml J., Shishkova S. and Dubrovsky JG (2009) A morphogenetic trigger: Is there an emerging concept in plant developmental biology?; ***Trends Plant Sci.***, 14, 189-193

Bennet SRM, Alvarez J., Bossinger G. and Smyth DR (1995) Morphogenesis in *pinoid* mutants of *Arabidopsis thaliana*; ***Plant J.***, 8, 505-520

Bennet MJ, Marchant A., Green HG, May ST, Ward SP, Milner PA, Walker AR, Schulz B, Feldmann KA (1996) *Arabidopsis AUX1* gene: a permease-like regulator of root gravitropism. ***Science***, 273, 948-950

Bennett A., Rowe RI, Soch N. and Eckhert CD (1999) Boron stimulates yeast (*Saccharomyces cerevisiae*) growth; ***J. Nutr.***, 129, 2236-2238

Berleth T. and Jürgens G. (1993) The role of the MONOPTEROS gene in organising the basal body region of the *Arabidopsis* embryo; ***Development***, 118, 575-587

Bernard P. and Couturier M. (1992) Cell killing by the F plasmid CcdB protein involves poisoning of DNA-topoisomerase II complexes; ***J Mol Biol,*** 226, 735–745

Betz WJ, Mao F. and Bewick GS (1992) Activity-dependent fluorescent staining and destaining of living vertebrate motor nerve terminals; ***J. Neurosci.***, 12, 363–375

Betz WJ, Mao F. and Smith CB (1996) Imaging exocytosis and endocytosis; ***Curr. Opin. Neurobiol.***, 6, 365–371

Bindea G, Mlecnik B, Hackl H, Charoentong P, Tosolini M, Kirilovsky A., Fridman WH, Pagès F., Trajanoski Z. and Galon J. (2009) ClueGO: a Cytoscape plug-in to decipher functionally grouped gene ontology and pathway annotation networks; ***Bioinformatics***, 25(8), 1091-1093

Blakeslee JJ, Bandyopadhyay A., Lee OR, Mravec J., Titapiwatanakun B., Sauer M., Makam SN, Cheng Y., Bouchard R., Adamec J., Geisler M., Nagashima A., Sakai T., Martinoia E., Friml J., Peer WA and Murphy AS. (2007) Interactions among PIN-FORMED and P-glycoprotein auxin transporters in Arabidopsis; ***Plant Cell***, 19, 131-147

Blilou I., Xu J., Wildwater M., Willemsen V., Paponov I., Friml J., Heidstra R., Aida M., Palme K. and Scheres B. (2005) The PIN auxin efflux facilitator network controls growth and patterning in *Arabidopsis* roots; ***Nature***, 433, 39-44

Blumenthal (1989) Blumenthal, R. M. (1989). Cloning and Restriction of Methylated DNA in *Escherichia coli*; ***Focus***, 11, 41-46

Boeke JD, Trueheart J., Natsoulis G. and Fink GR (1987) 5-Fluoroorotic Acid as a Selective Agent in Yeast Molecular Genetics; ***Methods in Enzymology***, 154, 164-175

Bolaños L., Lukaszewski K., Bonilla I. and Blevins, D. (2004) Why boron? ***Plant Physiol and Biochem***, 42, 907–912

Bonilla I., Blevins D. and Bolaños L. (2009) Essay 5.1: Boron Functions in Plants: Looking Beyond the Cell Wall; ***Plant Physiol***, Fifth Edition Online, <http://www.plantphys.net>, Accessed 30.09.2013

Boutté Y., Crosnier MT, Carraro N., Traas J., and Satiat-Jeunemaitre B. (2006) The plasma membrane recycling pathway and cell polarity in plants: studies on PIN proteins; ***J.Cell Sci.***, 119, 1255-1265

Brandao MM, Dantas LL and Silva-Filho MC (2009) AtPIN: *Arabidopsis* thaliana Protein Interaction Network; ***BMC Bioinformatics***, 10:454, DOI:1471-2105/10/454

Bullock WO, Fernandez JM and Short JM (1987) XL1-Blue: A high efficiency plasmid transforming rec A *Escherichia coli* strain with beta- galactosidase selection; ***Biotechniques***, 5, 376-379

Calderon-Villalobos LI, Lee S., De Oliveira C., Ivetac A., Brandt W., Armitage L., Sheard LB, Tan X., Parry G., Mao H., Zheng N., Napier R., Kepinski S., Estelle M. (2012) A combinatorial TIR1/AFB-AUX/IAA co-receptor system for differential sensing in auxin; ***Nat Chem Biol.***, 8 (5), 477-485

Chen RJ, Hilson P., Sedbrook J., Rosen E., Caspar T. and Masson PH (1998) The *Arabidopsis thaliana* AGRAVITROPIC1 gene encodes a component of the polar-auxin-transport efflux carrier; ***PNAS***, 95, 15112-15117

Chen H. and Xiong L. (2010) Myo-Inositol-1-phosphate synthase is required for polar auxin transport and organ development; ***J Biol Chem***, 285(31), 24238- 24247

Chen Y., Hoehenwarter W. and Weckwert W. (2010) Comparative analysis of phytohormone-responsive phosphoproteins in *Arabidopsis thaliana* using TiO2-phosphopeptide enrichment and mass accuarcy precursor alignment; ***The Plant Journal***, 63, 1-17

Cheng Y., Qin G., Dai X, and Zhao Y. (2007a) NPY1, a BTB-NPH3-like protein, plays a critical role in auxin-regulated organogenesis in *Arabidopsis*; ***PNAS***, 104(47), 18825-18829

Cheng Y., Dai X. and Zhao Y. (2007b) Auxin synthesized by tge YUCCA flavin monooxygenases is essential for embryogenesis and leaf formation in *Arabidopsis*; ***Plant Cell***, 19, 2430-2439

Cheng Y., Qin G., Dai X. and Zhao Y (2008) *NPY* genes and AGC kinases define two key steps in auxin-mediated organogenesis in *Arabidopsis*; ***PNAS***, 105 (52), 21017-21022

Cho M., Lee Sh and Cho HT (2007) P-Glycoprotein4 displays auxin efflux transporter like action in *Arabidopsis* root hair cells and tobacco cells; ***Plant Cell***, 19, 3930-3943

Christensen SK, Dagenais N., Chory J. and Weigel D. (2000) Regulation of auxin response by the protein kinase PINOID; ***Cell*** ,100, 469–478

Christie JM, Yang H., Richter GL, Sullivan S., Thomson CE, Lin J., Titapiwatanakun B., Ennis M., Kaiserli E., Lee OR, Adamec J., Peer WA and Murphy AS (2006) phot1 inhibition of ABCB19 primes lateral auxin fluxes in the shoot apex required for phototropism; ***PLoS Biol.***, 9, e1001076

Clough SJ and Bent AF (1998). Floral dip: a simplified method for *Agrobacterium* mediated transformation of *Arabidopsis thaliana*, ***Plant J***, 16, 735-743

Collings DA, Lill AW, Himmelspach R. and Wasteneys GO (2006) Hypersensitivity to cytoskeletal antagonists demonstrates microtubule–microfilament cross-talk in the control of root elongation in *Arabidopsis thaliana*; ***New Phytol***.,170, 275-290

Craddock C., Lavagi I. and Yang Z. (2012) New insights into Rho signaling from plant ROP/RAC GTPases; ***Trends Cell Biol.***, 22(9), 492-501

de la Fuente van Bentem S. and Hirt H. (2009) Protein tyrosine phosphorylation in plants: more abundant than expected?; ***Trends in Plant Science***, 14(2), 71-76

Delbarre A., Muller P., Imhoff V. and Gruen J. (1996) Comparison of mechanisms controlling uptake and accumulation of 2,4-dichlorophenoxy acetic acid, naphtalene-1-acetic acid, and indole-3-acetic acid in suspension-cultured tobacco cells; ***Planta***, 198, 532-541

Dettmer J. and Friml J. (2011) Cell polarity in plants:when two do the same, it is not the same...; ***Curr. Opin. Cell Biol.***, 23, 686-696

Dharmasiri S., Dharmasiri N., Hellmann H. and Estelle M. (2003) The RUB/Nedd8 conjugation pathway is required for early development in *Arabidopsis*; ***EMBO J.***, 22, 1762-1770

Dharmasiri N., Dharmasiri S., Weijers D., Lechner E., Yamada M., Hobbie L., Ehrismann JS, Jürgens G. and Estelle M. (2005) Plant development is regulated by a family of auxin receptor F box proteins; ***Dev. Cell***, 9, 109-119

Dharmasiri N., Dharmasiri S., Weijers D., Karunarathna N., Jürgens G. and Estelle M. (2007) *AXL* and *AXR1* have redundant functions in RUB conjugation and growth and development in *Arabidopsis*; ***Plant J.***, 52, 114-123

Dhonukshe P., Tanaka H., Goh T., Ebine K., Mahonen AP, Prasak K., Blilou I., Geldner N., Xu J., Uemura T., Chory J., Ueda T., Nakano A., Scheres B. and Friml J. (2008) Generation of cell polarity in plants links endocytosis, auxin distribution and cell fate decisions; ***Nature***, 456, 962-966

Dhonukshe P, Huang F, Galván-Ampudia CS, Mähönen AP, Kleine-Vehn J, Xu J, Qint A, Prasad K, Friml J, Offringa R (2010) Plasma membrane-bound AGC3 kinases phosphorylate PIN auxin carriers at TPRXS(N/S) motifs to direct apical PIN recycling; ***Development***,137, 3245-3255

Ding Z., Galván-Ampudia CS, Demarsy E., Łangowski Ł., Kleine-Vehn J., Fan Y., Morita MT, Tasaka M., Fankhauser C., Offringa R. and Friml J. (2011) Light-mediated polarization of the PIN3 auxin transporter for the phototropic response; ***Cell Biol.***, 13, 447-452

Dreze M., Monachello D., Lurin C., Cusick ME, Hill DE, Vidal M., Braun P. (2010) High-quality binary interactome mapping; ***Methods in Enzymology***, Vol. 470, Chapter 12

Dubrovsky JG, Sauer M., Napsucialy- Mendivil S., Ivanchenko MG, Friml J., Shishkova S., Celenza J. and Benková E. (2008) Auxin acts as a local morphogenetic trigger to specify lateral root founder cells; ***PNAS***, 105, 8790-8794

Friml J., Benková E., Blilou I., Wisniewska J., Hamann T., Ljung K., Woody S., Sandberg G., Scheres B., Jürgens G. and Palme K.(2002a) AtPIN4 mediates sink-driven auxin gradients and root patterning in Arabidopsis; ***Cell***, 108, 661-673

Friml J., Wisniewska J., Benková E., Mendgen K. and Palme K. (2002b) Lateral relocation of auxin efflux regulator PIN3 mediates tropism in *Arabidopsis*; ***Nature***, 415, 806-809

Friml J., Vieten A., Sauer M., Weijers D., Schwarz J., Hamann T., Offringa R. and Jürgens G. (2003) Efflux dependent auxin gradients establish the apical-basal axis of *Arabidopsis*; ***Nature***, 426, 147-153

Friml J., Yang X., Michniewicz M., Weijers D., Quint A., Tietz O., Benjamins R., Ouwerkerk PBF., Ljung K., Sandberg G., Hooykaas PJJ, Palme K., Offringa R. (2004) A PINOID-Dependent Binary Switch in Apical-Basal PIN Polar Targeting Directs Auxin Efflux; ***Science***, 306, 862

Friml J., Benfey P., Benkova E., Bennett M., Berleth T., Geldner N., Grebe M., Heisler M., Hejatko J., Jürgens G., Laux T., Lindsey K., Lukowitz W., Luschnig C., Offringa R., Scheres B., Swarup R., Torres-Ruiz R., Weijers D. and Zazímalová E. (2006) Apical-basal polarity: Why plants don't stand on their heads; ***Trends Plant Sci***., 11,12-14

Fu ZQ, Yan S., Saleh A.,Wang W., Ruble J., Oka N., Mohan R., Spoel SH, Tada Y., Zheng N. and Dong X. (2012) NPR3 and NPR4 are receptors for the immune signal salicylic acid in plants; ***Nature***, 486, 228-232

Furutani M., Vernoux T., Traas J., Kato T., Tasaka M. and Aida M. (2004) *PIN-FORMED1* and *PINOID* regulate boundary formation and cotyledon devlopment in *Arabidopsis* embryogenesis; ***Development***, 131, 5021-5030

Furutani M., Kajiwara T., Kato T., Treml BS, Stockum C., Torres-Ruiz RA, Tasaka M. (2007) The gene MACCHI-BOU4/ENHANCER OF PINOID encodes a NPH3-like protein and reveals similarities between organogenesis and phototropism at the molecular level; ***Development***, 134, 3849-3859

Furutani M., Sakamoto N., Yoshida S., Kajiwara T., Robert HS, Friml J. and Tasaka M. (2011) Polar localized NPH3-like proteins regulate polarity and endocytosis of PIN-FORMED auxin efflux carriers; ***Development***, 138, 2069-2078

Gälweiler L., Guan CH, Muller A., Wisman E., Mendgen K., Yephremov A. and Palme K. (1998) Regulation of polar auxin transport by AtPIN1 in *Arabidopsis* vascular tissue; ***Science***, 282, 2226-2230

Gazzarini S., Tsuchiya Y., Lumba S., Okamoto M. and McCourt P (2004) The transcription facto FUSCA3 controls developmental timing in *Arabidopsis* through the hormones gibberellin and abscisic acid; ***Developmental Cell***, 7, 373-385

Geisler M., Blakeslee JJ, Bouchard R., Lee OR, Vincenzetti V., Bandyopadhyay A., Titapiwatanakun B., Peer WA, Bailly A., Richards EL, Ejendal KF, Smith AP, Baroux C., Grossniklaus U., Müller A., Hrycyna CA, Dudler R., Murphy AS and Martinoia E. (2005) Cellular efflux of auxin catalyzed by the *Arabidopsis* MDR/PGP transporter AtPGP1; ***Plant J.***, 44, 179-194

Geisler M. and Murphy AS (2006) The ABC of auxin transport: the role p-glycoproteins in plant development; ***FEBS Lett***., 580, 1094-1102

Geldner N., Friml J., Stierhof YD, Jürgens G., Palme K. (2001) Auxin transport inhibitors block PIN1 cycling and vesicle trafficking; ***Nature***, 413, 425-428

Geldner N., Anders N., Wolters H., Keicher J., Kornberger W., Muller P., Delbarre A., Ueda T., Nakano A. and Jürgens G. (2003) The *Arabidopsis* GNOM ARF-GEF mediates endosomal recycling, auxin transport, and auxin-dependent plant growth; ***Cell***, 112 (2), 219-230

Genschik P., Sumara I. and Lechner E. (2013) The emerging role of CULLIN3-RING ubiquitin ligases (CRL3s): cellular functions and disease implications; ***The EMBO Journal***, 32, 2307-2320

Goldbach HE (1984) Influence of boron nutrition on net uptake and efflux of ^{32}P and ^{14}C-glucose in *Helianthus annuus* root and cell cultures of *Daucus carota*; ***J. Plant Physiol.***, 118, 431-438

Goldbach HE, Harmann D. and Rötzer T. (1990) Boron is required for the ferricyanide-induced proton release by auxins in suspension-cultured cells of *Daucus carota* and *Lycopersicon esculentum*; ***Physiol. Plant***, 80, 114-118

Grebe M., Xu J. and Scheres B. (2001) Cell axiality and polarity in plants-adding pieces to the puzzle; ***Curr. Opin. Plant Biol.***, 4, 520-526

Grebe M. (2010) Cell polarity: lateral perspectives; ***Curr. Biol.***, 20, 446-448

Gülersönmez M.C. (2011) Stage-specific metabolomics of mutant and polyploid *Arabidopsis thaliana*, MSc thesis, Technische Universität München

Haccius B. and Massfeller D. (1959) Durch Phenylborsäure induzierte Reduktion der Petalen von *Cucumis sativus*; ***Naturwissenschaften***, 46, 585-586

Haccius B. (1960) Experimentell induzierte Einkeimblättrigkeit bei *Eranthis hiemalis*; ***Planta***, 54, 482-497

Haccius B. and Massfeller D. (1961) Über die Hemmung einzelner Blattanlagen an Caryohyllaceen-Sämlingen durch Phenylborsäure; ***Naturwissenschaften***, 17, 577-578

Hamann T., Mayer U. and Jürgens G. (1999) The auxin-insensitive bodenlos mutation affects primary root formation and apical-basal patterning in the Arabidopsis embryo; ***Development***, 126, 1387-1395

Hamann T., Benkova E., Bäurle I., Kientz M. and Jürgens G. (2002) The Arabidopsis BODENLOS gene encodes an auxin response protein inhibiting MONPTEROS-mediated embryo patterning; ***Genes & Development***, 16, 1610-1615

Hardtke CS and Berleth T. (1998) The Arabidopsis gene MONOPTEROS encodes a transcription factor mediating embryo axis formation and vascular development; ***EMBO Journal***, 17, 1405-1411

Harrison BR and Masson PH (2008) ARL2, ARG1 and PIN3 define a gravity signal transduction pathway in root statocytes; ***Plant J.***, 53, 380-392

Heisler MG, Hamant O., Krupinski P., Uyttewaal M., Ohno C., Jönsson H., Traas J. and Meyerowitz EM (2010) Alignment between PIN1 polarity and microtubule orientation in the shoot apical meristem reveals a tight coupling between morphogenesis and auxin transport; ***PLoS Biol.***, 8, e1000516

Hibara K., Karim MR., Takada S., Taoka K., Furutani M., Aida M. and Tasaka M. (2006) *Arabidopsis CUP-SHAPED COTYLEDON3* regulates postembryonic shoot meristem and organ boundary formation; ***Plant Cell***, 18, 2946-2957

Hilscher J., Schlötterer C. and Hauser MT (2009) A single amino acid replacement in ETC2 shapes trichome patterning in natural Arabidopsis populations; ***Curr. Biol.***, 19(20), 1747- 1751

Hirt H., Garcia AV, Oelmüller R. (2011) AGC kinases in plant development and defense; ***Plant Signaling and Behaviour***, 6:7

Hobbie L., McGovern M., Hurwitz LR, Pierro A., Liu NY, Bandyopadhyay A. and Estelle M. (2000) The *axr6* mutants of *Arabidopsis thaliana* define a gene involved in auxin response and early development; ***Development***, 127, 23-32

Hong SW, Jon JH, Kwak JM and Nam HG (1997) Identification of a Receptor-like protein kinase gene rapidly induced by abscisic acid, dehydration, high salt and cold treatments in *Arabidopis thaliana*; ***Plant Physiology***, 113, 1203-1212

Huang F., Zago MK, Abas L., von Marion A., Galván-Ampudia CS and Offringa R. (2010) Phosphorylation of conserved PIN motifs directs Arabidopsis PIN1 polarity and auxin transport; ***The Plant Cell***, 22, 1129-1142

Invitrogen Instruction Manual (2002) ProQuest^{TM} Two-Hybrid System with Gateway Technology.

Jackson JF (1989) Borate control of protein secretion for Petunia pollen exhibits critical temperature discontinuities; ***Sex. Plant Reprod.***, 2, 11-14

Jaillais Y., Hothorn M., Belkadir Y., Dabi T., Nimchuk Z., Meyerowitz EM and Chory J. (2010) Tyrosine phosphorylation controls brassinosteroid receptor activation by triggering membrane release of its kinase inhibitor; ***Genes & Development***, 25, 232-237

Jakab M. (2013) Analysis of cell polarity and protein interaction of variants of the NPH3-like protein ENHANCER OF PINOID; Bachelor's Thesis, TU München

Jeong S., Bayer M. and Lukowitz W. (2011) Taking the very first steps: from polarity to axial domains in the early *Arabidopsis* embryo; ***Journal of Experimental Botany***, 62 (5), 1687-1697

Jiao Y., Ma L., Strickland E. and Deng XW (2005) Conservation and divergence of light-regulated genome expression patterns during seedling development in rice and *Arabidopsis*; ***Plant Cell***, 17(12), 3239-3256

Jurado S., Abraham Z., Manzano C., Lopez-Torrejon G., Pacios LF and del Pozo JC (2010) The *Arabidopsis cell* cycle F-box protein SKP2A binds to auxin; ***Plant Cell***, 22, 3891-3904

Jürgens G., Mayer U., Torres-Ruiz RA, Berleth T. and Miséra S. (1991) Genetic analysis of pattern formation in the *Arabidopsis* embryo; ***Development***, 113, 27-38

Kanei M., Horiguchi G. and Tsukaya H. (2012) Stable establishment of cotyledon identity during embryogenesis in *Arabidopsis* by ANGUSTIFOLIA 3 and HANABA TARANU; ***Development***, 139 (13), 2436-2446

Kirik V., Simon M., Wester K., Schiefelbein J. and Hulskamp M. (2004) ENHANCER of TRY and CPC 2 (ETC2) reveals redundancy in the region-specific control of trichome development of *Arabidopsis*; ***Plant Mol. Biol.***, 55(3), 389-398

Kleine-Vehn J. and Friml J. (2008) Polar targeting and endocytic recycling in auxin-dependent plant development; ***Annu. Rev. Cell Dev. Biol.***, 24, 447-473

Kleine- Vehn J., Ding Z., Jones AR, Tasaka M., Morita MT and Friml J. (2010) Gravity-induced PIN transcytosis for polarization of auxin fluxes in gravity-sensing root cells; ***PNAS***, 107, 22344-22349

Kleine-Vehn J., Wabnik K., Martiniere A., Langowski L., Willig K., Naramoto S., Leitner J., Tanaka H., Jakobs S., Robert S., Luschnig C., Govaerts W., Hell SW., Runions J., Friml J. (2011) Recycling, clustering, and endocytosis jointly maintain PIN auxin carrier polarity at the plasma membrane; ***Molecular Systems Biology***, 7, 540

Koncz C. and Schell J. (1986). The promoter of TL-DNA gene 5 controls the tissue-specific expression of chimaeric genes carried by a novel type of *Agrobacterium* binary vector; ***Mol Gen Genet***, 204, 383-396

Lanoue L., Trollinger DR, Strong PL and Keen CL (2000) Functional impairments in preimplantation mouse embryos following boron deficiency; ***FASEB J.***, 14A, 539

Lau S., Slane D., Herud O., Kong J. and Jürgens G. (2012) Early embryogenesis in flowering plants: setting up the basic body pattern; ***Annu. Rev. Plant Biol.***, 63, 483-506

Lee IC, Hong SW, Whang SS, Lim PO, Nam HG and Koo JC (2011) Age-dependent action of an ABA-inducible receptor kinase, RPK1, as a positive regulatora of senescence in Arabidopsis leaves; ***Plant Cell Physiol.***, 52(4), 651-662

Le Hir R. and Bellini C (2013) The plant-specific Dof transcription factors family: new players involved in vascular system development and functioning in *Arabidopsis*; ***Frontiers in Plant Science***, 4, Article 164

Lenhard M., Jürgens G. and Laux T. (2002) The *WUSCHEL* and *SHOOTMERISTEMLESS* genes fulfil complementary roles in *Arabidopsis* shoot meristem regulation; ***Development***, 129, 3195-3206

Lewis DR, Miller ND, Splitt BL, Wu GS and Spalding EP (2007) Separating the roles of acropetal and basipetal auxin transport on gravitropism with mutations in two *Arabidopsis* Multidrug Resistance-Like ABC transporter genes; ***Plant Cell***, 19, 1838-1850

Li Y., Dai X., Cheng Y. and Zhao Y. (2011) NPY genes play an essential role in root gravitropic reponses in *Arabidopsis*; ***Molecular Plant***, 4(1), 171-179

Lin D., Nagawa S., Chen J., Cao L., Chen X., Xu T., Li H., Shonukshe P., Yamamura C., Friml J., Scheres B., Fu Y. and Yang Z. (2012) A ROP GTPase-dependent auxin signaling pathway regulates the subcellular distribution of PIN2 in *Arabidopsis* roots; ***Curr. Biol.***, 22, 1319-1325

Liscum E. and Briggs WR (1995) Mutations in the NPH1 Locus of *Arabidopsis* disrupt the perception of phototropic stimuli; ***The Plant Cell***, 7, 473-485

Ljung K,. Hull AK, Kowalczyk M., Marchant A., Celenza J., Cohen JD and Sandberg G. (2002) Biosynthesis, conjugation, catabolism and homeostasis of indole-3-acetic acid in *Arabidopsis thaliana*; ***Plant Mol. Biol.***, 49, 249-272

Ljung K. Hull AK, Celenza J., Yamada M., Estelle M., Normanly J. and Sandberg G. (2005) Sites and regulation of auxin biosynthesis in *Arabidopsis* roots; ***Plant Cell***, 17, 1090-1104

Long JA, Moan EI, Medford JI and Barton MK (1996) A member of the KNOTTED class of homeodomain proteins encoded by the *STM* gene of *Arabidopsis*; ***Nature***, 379, 66-69

Luichtl M., Fiesselmann B., Matthes M., Yang X., Peis O., Brunner A., Torres Ruiz RA (2013) Mutations in RPK1 uncouple cotyledon anlagen and primordia by modulating epidermal cell shape and polarity; ***Biology Open***, 2(11), 1093-1102, doi: 10.1242/bio.20135991

Marchant A, Kargul J., May ST, Muller P., Delbarre A.,Perrot -Rechenmann C., Bennet MJ (1999) AUX1 regulates root gravitropism in *Arabidopsis* by facilitating auxin uptake within root apical tissues; ***EMBO J*** ,18, 2066-2073

Matthes M. and Torres-Ruiz RA (2012) Initiation und Etablierung von Keimblättern im *Arabidopsis*-Embryo; ***BIOspektrum***, 07.12, 717-720

Men S., Boutte Y., Ikeda X., Li X., Palme K., Stierhof YD, Hartmann MA, Moritz T. and Grebe M. (2008) Sterol- dependent endocytosis mediates postcytokinetic acquisition of PIN2 auxin efflux carrier polarity; ***Nat. Cell Biol.***, 10, 237-244

Michniewicz M., Zago MK, Abas L., Weijers D., Schweighofer A., Meskiene I., Heisler MG, Ohno C., Zhang J., Huang F., Schwab R., Weigel D., Meyerowitz EM, Luschnig C., Offringa R. and Friml J. (2007) Antagonistic regulation of PIN phosphorylation by PP2A and PINOID directs auxin flux; ***Cell***, 130, 1044-1056

Motchoulski A. and Liscum E. (1999) Arabidopsis NPH3: A NPH1 Photoreceptor-Interacting Protein essential for Phototropism, ***Science***, 286, 961-964

Mravec J., Kubes M., Bielach A., Gaykova V., Petrasek J., Skupa P., Chand S., Benková E., Zazimalova E. and Friml J. (2008) Interaction of PIN and PGP transport mechansism in auxin distribution-dependent development; ***Development***, 135, 2245-3354

Mravec J., Skůpa P., Bailly A., Hoyerová K., Krecek P., Bielach A., Petrásek J., Zhang J., Gaykova V., Stierhof YD, Dobrev PI, Schwarzerová K., Rolcík J., Seifertová D., Luschnig C., Benková E., Zazímalová E., Geisler M. and Friml J. (2009) Subcellular homeostasis of

phytohormone auxin is mediated by the ER-localized PIN5 transporter; ***Nature***, 459, 1136-1140

Murphy AS and Peer WA (2012) Vesicle trafficking: ROP-RIC roundabout; ***Curr. Biol.***, 22, R567-R578

Nagawa S., Xu T., Lin D., Dhonukshe P., Zhang X., Friml J., Scheres B., Fu Y. and Yang Z. (2012) ROP GTPase-dependent actin microfilaments promote PIN1 polarization by localized inhibition of clathrin-dependent endocytosis; ***PLoS Biol.***, 10(4), e1001299

Nebenführ A., Ritzenthaler C. and Robinson DG (2002) Brefeldin A: Deciphering an Enigmatic Inhibitor of Secretion; ***Plant Physiology***, 130, 1102-1108

Nodine MD, Yadegari R. and Tax FE (2007) RPK1 and TOAD2 are two receptor-like kinases redundantly required for *Arabidopsis* embryonic pattern formation; ***Developmental Cell***, 12, 943-956

Nodine MD and Tax FE (2008) Two receptor-like kinases required together for the establishment of *Arabidopsis* cotyledon primordia; ***Developmental Biology***, 314, 161-170

Osakabe Y., Maruyama K., Seki M., Satou M., Shinozaki K. and Yamaguchi-Shinozaki K. (2005) Leucine -Rich Repeat Receptor-Like Kinase 1 is a key membrane-bound regulator of abscisic acid early signaling in Arabidopsis; ***The Plant Cell***, 17, 1105 - 1119

Peng FY and Weselake RJ (2011) Gene expression clusters and putative regulatory elements underlying seed storage reserve accumulation in *Arabidopsis*; ***BMC Genomics***, 12, 286

Perrot-Rechenmann C. (2010) Cellular responses to auxin: division versus expansion; ***Cold Spring Harb. Perspec. Biol.***, 2, a001446

Perry G., Calderon-Villalobos LI, Prigge M., Peret B., Dharmasiri S., Itoh H., Lechner E., Gray WM, Bennet M. and Estelle M. (2009) Complex regulation of the TIR1/AFB family of auxin receptors; ***PNAS***, 106, 22540-22545

Petrásek J., Mravec J., Bouchard R., Blakeslee JJ, Abas M., Seifertová D., Wisniewska J., Tadele Z., Kubes M., Covanová M., Dhonukshe P., Skupa P., Benková E., Perry L., Krecek P., Lee OR, Fink GR, Geisler M., Murphy AS, Luschnig C., Zazímalová E. and Friml J. (2006) PIN proteins perform a rate-limiting function in cellular auxin efflux; ***Science***, 312, 914-918

Pollard AS, Parr AJ and Loughman BC (1977) Boron in relation to membrane function in higher plants; ***J. Exp. Bot.***, 28, 831-841

Rakusová H., Gallego-Bartolomé J., Vanstraelen M., Robert HS, Alabadi D., Blázquez MA, Benková E. and Friml J. (2011) Polarization of PIN3-dependent auxin transport for hyocotyol gravitropic response in *Arabidopsis thaliana*; ***Plant J.***, 67(5), 817-826

Raven JA (1975) Transport of indoleacetic acid in plant cells in relation to pH and electrical potential gradients, and its significance for polar IAA transport; ***New Phytol.***, 74, 163-172

Richter R., Behringer C., Zourelidou M. and Schwechheimer C. (2013) Convergence of auxin and gibberellin signaling on the regulation of the GATA transcription factors GNC and GNL in *Arabidopsis thaliana*; ***PNAS***, 110 (32), 13192-13197

Robert S., Kleine-Vehn J., Barbez E., Sauer M., Paciorek T., Baster P., Vanneste S., Zhang J., Simon S.,Čovanová M., Hayashi K., Dhonukshe P., Yang Z., Bednarek SY, Jones AM, Luschnig C., Aniento F., Zažimalová E. and Friml J. (2010) ABP1 mediates auxin inhibition of clathrin-dependent endocytosis in *Arabidopsis*; ***Cell***, 143, 111-121

Robertson GA and Loughman BC (1974) Reversible effects of boron on the absorption and incorporation of phosphate in *Vicia faba L.*; ***New Phytol.***, 73, 291-298

Rowe RI and Eckhert CD (1999) Boron is required for zebrafish embryogenesis; ***J Exp Biol.***, 202, 1649–1654

Rubery PH and Sheldrake AR (1974) Carrier-mediated auxin transport; ***Planta***, 188, 101-121

Sachs T. (1981) The control of the patterned differentiation of vascular tissues; ***Adv. Bot. Res.***, 9, 151-262

Sambrook J, Russell DW Molecular Cloning (2001) A Laboratory Manual, Third Edition, Cold Spring Harbor Laboratory Press, Cold Spring Harbor, New York

Santelia D., Fukao Y., Martinoia E. and Geisler M. (2005) MDR-like ABC transporter AtPGP4 is involved in auxin-mediated lateral root and root hair development; ***Plant Cell Physiol.***, 47, S184-S184

Santner A. and Estelle M. (2010) The ubiquitin-proteasome system regulates plant homone signaling; ***Plant J.***, 61, 1029-1040

Scarpella E., Marcos D., Friml J., and Berleth T. (2006) Control of leaf vascular patterning by polar auxin transport; ***Genes Dev***, 20, 1015-1027

Schlereth A., Moller B., Liu W., Kientz M., Flipse J., Rademacher EH, Schmid M., Jürgens G. and Weijers D. (2010) MONOPTEROS controls embryonic root initiation by regulating a mobile transcription factor; ***Nature***, 464, 913-916

Schon MK, Novacky A. and Blevins DG (1990) Boron induces hyperpolarization of sunflower root cell membranes and increases membrane permeability to K+; ***Plant Physiol.***, 93, 566-571

Shannon P., Markiel A., Ozier O., Baliga NS, Wang JT, Ramage D., Amin N., Schwikowski B. and Ideker T. (2003) Cytoscape: a software environment for integrated models of biomolecular interaction networks; ***Genome Res.***, 13(11), 2498-2504

Shi JH and Yang ZB (2011) Is ABP1 an auxin receptor yet? ***Mol Plant***, 4, 635-640

Simon S. and Petrášek J. (2010) Why plants need more than one type of auxin; ***Plant Science***, 180, 454-460

Smyth GK (2004) Linear models and empirical Bayes methods for assessing differential expression in microarray experiments; ***Statistical Applications in Genetics and Molecular Biology***, Vol. 3, No 1., Article 3

Steinmann T., Geldner N., Grebe M., Mangold S., Jackson C., Paris S., Gälweiler L., Palme K. and Jürgens G. (1999) Coordinated polar localization of auxin efflux carrier PIN1 by GNOM ARF GEF; ***Science***, 286, 316-318

Stepanova AN, Roberston -Hoyt J., Yun J., Benavente LM, Xie DY, Dolezal K., Schlereth A., Jürgens G. and Alonso JM (2008) TAA1-mediated auxisn biosynthesis is essential for hormone crosstalk and plant development; ***Cell***, 133, 177-191

Stogios PJ, Downs GS, Jauhal JJ, Nandra SK and Prive GG (2005) Sequence and structural analysis of BTB domain proteins; ***Genome Biol.***, 6, R82

Stokes ME, Chattopadhyay A., Wilkins O., Nambara E. and Campbell MM (2013) Interplay between sucrose and folate modulates auxin signaling in *Arabidopsis*; ***Plant Physiol.***, 162(3), 1552-1565

Swarup K., Benková E., Swarup R., Casimiro I., Peret B., Yang Y., Parry G., Nielsen E., De Smet I., Vanneste S., Levesque MP, Carrier D., James N., Calvo V., Ljung K., Kramer E., Roberts R., Graham, N., Marillonnet S., Patel K., Jones JD, Taylor CG, Schachtman DP, May S., Sandberg G., Benfey P., Friml J., Kerr I., Beeckman T., Laplaze L., und Bennett M.J. (2008) The auxin influx carrier LAX3 promotes lateral root emergence; ***Nat Cell Biol*** ,10, 946-954

Szemenyei H., Hannon M. and Long JA (2008) TOPLESS mediates auxin-dependent transcriptional repression during *Arabidopsis* embryogenesis; ***Science***, 319, 1384-1386

Takada S., Hibara K., Hishida T. and Tasaka M. (2001) The *CUP-SHAPED COTYLEDON1* gene of *Arabidopsis* regulates shoot apical meristem formation, ***Development***, 128, 1127-1135

Takano J., Noguchi K., Yasumori M., Kobayashi M., Gajdos Z., Miwa K., Hayashi H., Yoneyama T. and Fujiwara T. (2002) *Arabidopsis* boron transporter for xylem loading; ***Nature***, 420, 337-340

Takano J., Miwa K., Yuan L., von Wirén N. and Fujiwara T. (2005) Endocytosis and degradation of BOR1, a boron transporter of *Arabidopsis thaliana*, regulated by boron availability; ***PNAS***, 102, 12276-12281

Takano J., Wada M., Ludewig U., Schaaf G., von Wirén N. and Fujiwara T. (2006) The *Arabidopsis* major intrinsic protein NIP5;1 is essential for efficient boron uptake and plant development under boron limitation; ***Plant Cell***, 18, 1498-1509

Takano J., Tanaka M., Toyoda A., Miwa K., Kasai K., Fuji K., Onouchi H., Naito S. and Fujiwara T. (2010) Polar localization and degradation of *Arabidopsis* boron transporters through distinct trafficking pathways; ***PNAS***, 107, 5220-5225

Tanada T. (1983) Localization of boron in membranes; ***J. Plant Nutr.***, 6, 743-749

Tanaka H., Dhonukshe P., Brewer PB and Friml J. (2006) Spatiotemporal asymmetric auxin distribution: a means to coordinate plant development; ***Cell Mol. Life Sci.***, 63, 2738-2754

Tao L., Cheung AY and Wu H. (2002) Plant Rac-like GTPases are activated by auxin and mediate auxin- responsive gene expression; ***Plant Cell***, 14, 2745-2760

Terasaka K., Blakeslee JJ, Titapiwatanakun B., Peer WA, Bandyopadhyay A., Makam SN, Lee OR, Richards EL, Murphy AS, Sato F. and Yazaki K. (2005) PGP4, an ATP binding cassette P-glycoprotein, catalyzes auxin transport in *Arabidopsis thaliana* roots; ***Plant Cell***, 17, 2922-2939

Thimm O., Bläsing O., Gibon Y., Nagel A., Meyer S., Krüger P., Selbig J., Müller LA, Rhee SY and Stitt M. (2004) MAPMAN: a user-driven tool to display genomics data sets onto diagrams of metabolic pathways and other biological processes; ***Plant J***., 37, 914-39

Torres-Ruiz RA (2004) Polarity in *Arabidopsis* embryogenesis" in "Polarity in plants" (K. Lindsey ed.); ***Annual Plant Reviews***, Blackwell Publishing, Oxford, 12, 223-261

Torssell K. (1956) Chemistry of arylboric acids. VI. Effects of arylboric acids on wheat roots and the role of boron in plants; ***Physiol Plant***, 9, 652-664

Treml BS (2008) Die Rolle des Gens ENHANCER OF PINOID in der Keimblattentwicklung und dem gerichteten Auxintransport in *Arabidopsis thaliana*; Dissertation, TU München

Treml BS, Winderl S., Radykewicz R., Herz M., Schweizer G., Hutzler P., Glawischnig E., Torres-Ruiz RA (2005) The gene ENHANCER OF PINOID controls cotyledon development in the *Arabidopsis* embryo; ***Development***, 132, 4063-4074

Ulmasov T., Murfett J., Hagen G., and Guilfoyle T. (1997) Aux/IAA proteins repress expression of reporter genes containin natural and highly active synthetic auxin response elements; ***Plant Cell***, 9, 1963-1971

Usadel B., Nagel A., Thimm O., Redestig H., Bläsing OE, Palacios-Rojas N., Selbig J., Hannemann J., Piques MC, Steinhauser D., Scheible WR, Gibon Y., Morcuende R., Weicht D., Meyer S. and Stitt M (2005) Extension of the Visualization Tool MapMan to Allow Statistical Analysis of Arrays, Display of Coresponding Genes, and Comparison with Known Responses; ***Plant Physiology***, 138, 1195-1204

Vanneste S. and Friml J. (2009) Auxin: a trigger for change in plant development; ***Cell***, 136, 1005-116

Vroemen CW, Mordhorst AP, Albrecht C., Kwaaitaal MA and de Vries SC (2003) The *CUP-SHAPED COTYLEDON3* gene is required for boundary and shoot meristem formation in *Arabidopsis*; ***Plant Cell***, 15, 1563-1577

Weckermann K., Jaspert N., Möller C. and Oecking C. (2010) 14-3-3 epsilon group members are essential for plant growth and development; Talk at Tri-National Arabidopsis Meeting, Salzburg, Austria

Weijers D., Schlereth A., Ehrismann JS, Schwank G., Kientz M. and Jürgens G. (2006) Auxin triggers transient local signaling for cell specification in *Arabidopsis* embryogenesis; ***Developmental Cell***, 10, 265-270

Wendrich J. and Weijers D. (2013) The *Arabidopsis* embryo as a miniature morphogenesis model; ***New Phytologist***, 199, 14-25

Willemsen V., Friml J., Grebe M., van den Toorn A., Palme K. and Scheres B. (2003) Cell polarity and PIN protein positioning in *Arabidopsis* require STEROL METHYLTRANSFERASE1 function; ***Plant Cell***, 15, 612-625

Willige BC, Isono E., Richter R., Zourelidou M. and Schwechheimer C. (2011) Gibberellin regulates PIN-FORMED abundance and is required for auxin transport-dependent growth and development in *Arabidopsis thaliana;* ***Plant Cell,*** 23(6), 2184-2195

Wisniewska J., Xu J., Seifertova D., Brewer PB, Ruzicka K., Blilou K., Rouquie D., Benkova E., Scheres B. and Friml J. (2006) Polar PIN Localization directs auxin flow in plants; ***Science***, 312, 883

Woodward AW and Bartel B. (2005) Auxin: regulation, action and interaction; ***Ann. Bot.***, 95, 707-735

Wu G., Lewis DR and Spalding EP (2007) Mutations in *Arabidopsis* multidrug resistance-like ABC transporters separate the roles of acropetal and basipetal auxin transport in lateral root development; ***Plant Cell***, 19, 1826-1837

Xue HW, Chen X. and Mei J (2009) Function and regulation of phospholipid signalling in plants; ***Biochem J.***, 421(2), 145-156

Xu T., Wen M., Nagawa S., Fu Y., Chen JG, Wu MJ, Perrot-Rechenmann C., Friml J., Jones AM and Yang Z. (2010) Cell surface-and Rho GTPase-based auxin signaling controls cellular interdigitation in Arabidopsis; ***Cell***, 143(1), 99-110

Xu T., Nagawa S. and Yang Z (2011) Uniform auxin triggers the Rho GTPase-dependent formation of interdigitation patterns in pavement cells; ***SmallGTPases***, 2(4), 227-232

Yamaguchi T., Nukazuka A. and Tsukaja H. (2012) Lead adaxial-abaxial polarity specification and lamina outgrowth: evolution and development; ***Plant and Cell Physiology***, 53 (7), 1180-1194

Yang Y., Hammes UZ, Taylor CG, Schachtmann DP, Nielsen E. (2006) Highaffinity auxin transport by the AUX1 influx carrier protein; ***Curr Biol*** ,16, 1123-1127

Yang H. and Murphy AS (2009) Functional expression and characterization of *Arabidopsis* ABCB, AUX1 and PIN auxin transporters in *Schizosaccharomyces pombe*; ***Plant J.***, 59, 179-191

Yasui Y., Mukougawa K., Uemoto M., Yokofuji A., Suzuri R., Nishitani A. and Kohchi T (2012) The phytochrome-interacting vascular plant one-zinc finger1 and VOZ2 redundantly regulate flowering in *Arabidopsis*; ***Plant Cell***, 24(8), 3248-3263

Zazímalová E., Murphy AS, Yang H., Hoyerova K. and Hosek P (2010) Auxin transporters-why so many?; ***Cold Spring Harp. Perspect. Biol***., 2, a001552

Zegzouti H., Anthony RG, Jahchan N., Bögre L., Christensen SK (2006) Phosphorylation and activation of PINOID by the phospholipid signaling kinase 3-phosphoinositide-dependent protein kinase 1 (PDK1) in *Arabidopsis*; ***PNAS***, 103:16, 6404-6409

Zweigardt M. (2010) Molekularbiologische Analyse relevanter Keimblattgene der Pflanze *Arabidopsis thaliana*; Dissertation, TU München

Acknowledgments

My friend Sean once pointed out that doing a PhD is pervasive unhappiness. This held true to some extent and I am grateful for quite a lot of people, who helped me make it through.

I'd like to thank Prof. Dr. Alfons Gierl for giving me the opportunity to do my PhD research at the Lehrstuhl für Genetik. I further thank him for his continuous doubt in my reserach and his productive criticism, which I think will help to become a better scientist in the end.

I am further much obliged to Prof. Dr. Erwin Grill and Prof. Dr. Brigitte Poppenberger-Sieberer, who constituted my comission.

My extremest gratitude goes to my supervisor Prof. Dr. Ramon Angel Torres Ruiz. Not only for trusting in my work and always finding the patience to give life and personal advices, but also for his huge knowledge, creativity and preciseness in science, which I will always aim at.

I also like to thank the group leaders of the Lehrstuhl für Genetik, especially Dr. Monika Frey and PD Dr. Erich Glawischnig for useful advices regarding scientific problems.

To my fellow PhD colleagues, thank you very much for the nice working atmosphere. Specifically, Stefan Lenk, Linlin Zheng and Kamil Bąkowski helped to cheer up the days.

I am further deeply grateful for the extraordinary technical assistance of Otti Peis and Nicole Däschlein. Especially Otti did not only help in whatever work I had to do, but also sacrificed her free days to push science forward. I further don't want to miss out on saying thank you to Heidi Miller-Mommerskamp, Peter Dobos, Carolin Ziegler, Petra Wick and Regina Hüttl for administrative support and creating a good mood in the daily routine.

My thanks also go to Dr. Pascal Falter-Braun and his group who helped with the yeast screen and to Dr. Erika Isono, for tremendous support with the initial Co- IP studies.

I further am indepted to my bachelor students, who helped with various aspects of my project, especially Xiaomeng Yang, Steffen Fabian and Moritz Jakab.

I deeply appreciate the patience, mental, scientific and psychological support as well as the friendship of Dr. Rafał Jończyk. There is no way I can make up for everything he did for me.

My biggest appreciation and deepest thanks go to my parents. They had to absorb all my moods and supported me whenever, wherever they could. I owe you deeply and I truly thank you that you are always there for me.

Last, but not least I'd like to thank my brothers Robert and Patrick, his wife Ireen and my niece Franziska, as well as my closest friends, Can, Lisi, Barbara, Agnes, Darcie and Sean for their various supports during this hard time.

Appendix

1. Matrix Families and their transcription factors as used by the genomatix software

Matrix family	Genes
P$DOFF	At2g34140, DAG2, DOF2, OBP1, OBP3, DAG1,
	At4g21050,OBP4, CDF1, HCA2, At5g65590, OBP2, DOF1
P$IBOX	GATA1, GATA2, GATA3, GATA4, GATA5, HAN
P$GTBX	GT-1a, S1F, S1FA, At3g25990, At5g01380, At1g13450, ASIL1
P$MYBL	AS1, AS2, AtMYB0, AtMYB66, DUO1, GaMYB, MYB101
	MYB23, MYB30, MYB33, MYB65, MYB77, MYB96,TT2
P$CCAF	CCA1, At3g09600, RVE1, LHY
P$MYBS	SPL, PHR1, At5g29000
P$AHBP	HB1, HB2, HB5, HB8,HB17, GL2
	WUS, HAT3, RPL, PHV, ATHB-15
P$MADS	SEP4, SVP, SHP2, AGL20, SEP2, AP3,
	SHP1, AG, AGL24, FLC, AGL15, SEP1,PI, AGL62,SEP3,CAL, AP1

Table 49 – Matrix families and their transcription factors as used by the genomatix software

2. Differentially expressed genes obtained in the performed transcriptomics study

Gene	logFold	pValue	Gene	logFold	pValue
AT3G05730	-4.70154059720238	0.034	DRT112	-2.30567477195231	0.015
CA1	-4.40638217714651	0.024	LHB1B2	-2.29359139707847	0.000
TGG1	-4.26804756859975	0.000	AT4G39970	-2.29157548653901	0.008
LHB1B1	-3.67411400547254	0.001	PMDH2	-2.26692773126943	0.027
AT3G16660	-3.60687547840423	0.000	SCRM2	-2.26581191436842	0.008
AT1G11850	-3.50543052591839	0.000	AT1G15330	-2.26375275658060	0.023
AT2G29290	-3.43968267278609	0.000	PTAC16	-2.25167505708502	0.002
CAB2	-3.43611412640084	0.005	NDF2	-2.24670701940895	0.001
PORA	-3.29846673402426	0.000	PSAF	-2.24324475100819	0.004
AT1G23130	-3.23285219324075	0.000	AT4G18810	-2.24308859095420	0.001
LHCB2.3	-3.12520307489527	0.005	EFE	-2.23399047731989	0.000
AT5G18600	-3.10070244907181	0.005	FBA2	-2.23328724319088	0.007
ELI3-1	-3.07637169616105	0.000	CSP41A	-2.23259275069060	0.007
THA1	-3.00087857660239	0.000	PETC	-2.23129345130302	0.000
FSD1	-2.86674466982927	0.030	NCED4	-2.21836556113265	0.000
RCA	-2.83429068826522	0.004	PSBR	-2.21800576264728	0.046
AT1G70820	-2.79469026495926	0.000	AT1G32080	-2.21657674079312	0.021
XTH6	-2.74558557819541	0.026	RBCS1A	-2.20691860287903	0.000
PSAD-2	-2.71375649404792	0.018	AT5G38990	-2.20682450635911	0.003
AT1G21130	-2.64936245684715	0.001	LHCA2	-2.20260891937839	0.000
KCS12	-2.62617763399279	0.011	LHCA4	-2.19440691261848	0.006
HCEF1	-2.59123652074292	0.001	DES1	-2.19161406290256	0.001

AT5G12050	-2.57477797224064	0.000	NRT2.5	-2.18726436421649	0.003
AT5G44680	-2.57475202329901	0.007	AT2G26500	-2.18688174899772	0.021
AT4G26530	-2.53959511541406	0.000	TC406655	-2.18460123332147	0.011
CYCP2;1	-2.53707262349424	0.002	PGLP1	-2.17278494681656	0.004
GLDP1	-2.50222361985962	0.001	NDF6	-2.17232001581	0.014
CA2	-2.49401244004171	0.007	CRK22	-2.16907975286282	0.005
AT1G76110	-2.48594939201319	0.002	CDSP32	-2.16138852242315	0.038
TMM	-2.4813159890773	0.000	AT1G68520	-2.15735088595592	0.001
AT3G62820	-2.47868187315394	0.000	PSI-P	-2.1543713706675	0.022
AT5G54710	-2.46722780973288	0.022	AT5G55570	-2.15250768187102	0.029
AT5G58260	-2.43620172891166	0.006	AT3G63160	-2.14315731098771	0.001
HPR	-2.42455360360295	0.034	AGT	-2.14255603400920	0.007
CAB3	-2.42187272641163	0.001	LHCA3	-2.13984072384966	0.000
LHCA1	-2.41324204827588	0.009	AT1G32900	-2.12326193664486	0.032
AT4G28780	-2.41022637180745	0.000	AT3G47070	-2.12302473417630	0.011
AT2G20835	-2.40996435127142	0.000	PSAG	-2.12185905539868	0.000
AT3G14420	-2.40502999584544	0.000	AT1G21500	-2.10959356063645	0.000
CRB	-2.40364210527529	0.004	LHCB6	-2.10340692008147	0.001
AT5G58770	-2.39366697898741	0.001	PSAE-1	-2.09867323809977	0.040
PPL2	-2.38064104160196	0.041	sks9	-2.09866403100513	0.000
AT1G21460	-2.37817531985371	0.000	SBP2	-2.09132467478010	0.000
GS2	-2.36352466938007	0.000	AT5G47610	-2.08200076062315	0.007
AT5G16030	-2.36312785838851	0.028	PSBO1	-2.08157484816146	0.001
CRK21	-2.35591905915719	0.011	AT5G02160	-2.07873000206467	0.020
FMA	-2.34855535798213	0.000	TAPX	-2.07643789279221	0.003
LHCA6	-2.34458611792429	0.002	AT5G38430	-2.07309465966750	0.046
AT5G21430	-2.32858801369205	0.000	AT3G47250	-2.07104291544482	0.000
AT1G54820	-2.32411716513118	0.000	LHCB5	-2.07079803312604	0.013
GPRI1	-2.31669037557784	0.000	GDCH	-2.06871791438632	0.030
FBA1	-2.31279728468911	0.000	FRO8	-2.06730181108805	0.030
AT3G50560	-2.30713920718568	0.002	LHCB3	-2.05511729057818	0.000
PSBQA	-2.03604910403366	0.029	UGT85A1	-1.74760466531585	0.020
GAPA	-2.03354913500767	0.010	STOMAGEN	-1.74500735566596	0.001
PSAD-1	-2.03202197751879	0.001	CLA1	-1.74332481019264	0.007
AT4G01460	-2.03174490846092	0.007	CRK18	-1.73898319356142	0.002
AT5G24210	-2.0141756706154	0.009	AT5G35970	-1.73028403089430	0.000
AT1G11860	-2.00597650154828	0.004	TRX-M4	-1.72207889212166	0.003
AT2G47880	-1.99182578098926	0.022	NDH18	-1.72058428182562	0.024
PSAO	-1.98202175268603	0.015	FRO6	-1.71042041224678	0.001
AT5G51720	-1.97675531844558	0.004	CAO	-1.70280729157889	0.002
ProT3	-1.96324450565113	0.004	KAT1	-1.70055452022606	0.033
PGL5	-1.96145219164626	0.000	emb2394	-1.69705807626394	0.011
AT1G21540	-1.95572541678380	0.000	AT4G01150	-1.69194228607086	0.023
DR368472	-1.93417744821183	0.021	AT2G30170	-1.69095331108841	0.042
AT1G73870	-1.92075909587104	0.001	HCF136	-1.68932330235844	0.000
SNC4	-1.91704597165929	0.022	LHCB2.2	-1.67644012919958	0.015
CRD1	-1.91701210812886	0.001	AT3G59780	-1.67456139226328	0.0128
2-Oct	-1.90853377473078	0.003	AT1G04660	-1.66886264905886	0.007
AT5G57760	-1.90563961383342	0.003	PORB	-1.66578021985624	0.000

GUN5	-1.89994648528532	0.039	AT2G33800	-1.66429229303155	0.000
GUN4	-1.89577920529872	0.004	VAR1	-1.66222029110546	0.022
SIG4	-1.89055611961178	0.009	PDX1.1	-1.65933035575995	0.013
AT1G51400	-1.88969461110277	0.002	AT2G35260	-1.65744865070536	0.000
CaS	-1.87125769856014	0.045	BOU	-1.64869745762288	0.002
PGK1	-1.87025320111481	0.043	PGR5	-1.64722300154315	0.000
AT4G32260	-1.86902745168514	0.00	AT2G32880	-1.64574712925128	0.000
PSBY	-1.85462716602422	0.00	AT2G35390	-1.64241872986826	0.004
AT1G23740	-1.85024896864539	0.000	NPQ4	-1.64182203067225	0.035
FKBP16-2	-1.8468437176417	0.000	AT5G59750	-1.64016735886498	0.002
PRP2	-1.84427418124581	0.013	ESM1	-1.61622577730052	0.001
AT5G44580	-1.83520635434494	0.004	IQD24	-1.60269296215092	0.028
CRK40	-1.83058053386190	0.002	GER3	-1.59822469352669	0.042
AT1G68190	-1.83035084069016	0.000	TCP3	-1.59438352365930	0.000
TCH3	-1.82534496556523	0.030	FAD7	-1.58342306681481	0.001
TI2	-1.82497792706361	0.008	AT3G53960	-1.57075099928969	0.000
AT1G74470	-1.82295036464094	0.000	AT3G10060	-1.56991416885015	0.033
PTF1	-1.81788647364795	0.003	AT5G43450	-1.56875622392020	0.000
LHCB2.1	-1.81737271861287	0.030	AT3G19480	-1.56361651749800	0.000
GLDP2	-1.81636757582804	0.005	AT1G16080	-1.55865282768298	0.015
AT2G15020	-1.81213038502596	0.023	AT1G21550	-1.55374958934147	0.000
AT5G44260	-1.80857132561941	0.003	TAP38	-1.54677897595334	0.018
RAV2	-1.80563831896880	0.007	RPL4	-1.54548571878015	0.002
NAP	-1.78990064715057	0.0123	AT3G06080	-1.54239368377766	0.001
PETE1	-1.7771352199582	0.017	YUC5	-1.54130067723502	0.000
CYP71B4	-1.77673082985459	0.000	YAB5	-1.53565742363165	0.003
MYB16	-1.77632184295280	0.036	AT3G14760	-1.53255676822918	0.010
OFP16	-1.77432156083765	0.000	CSLB04	-1.53104708254097	0.000
POR C	-1.77344032911954	0.030	AT2G13610	-1.52921116815759	0.000
AT1G52990	-1.77232734354100	0.021	AT2G43560	-1.52873616510672	0.033
RBP31	-1.77216401970606	0.002	ALMT12	-1.52782573236794	0.000
AT1G32780	-1.52539545368158	0.000	YUC2	-1.51867501685322	0.001
AT5G01740	-1.51925296199020	0.001	AT5G47110	-1.51793696151867	0.001
AT1G71500	-1.51445230704571	0.001	AT1G49000	-1.36141774870698	0.012
AT4G32590	-1.51349456501741	0.000	RPB5D	-1.35983296869182	0.003
AT3G60750	-1.50982921635666	0.002	NAP8	-1.35782956495728	0.002
THIC	-1.50576983228200	0.045	AT2G36145	-1.35439888517860	0.000
SZF1	-1.50404727623351	0.000	EXPA1	-1.35366593507866	0.027
PSRP6	-1.50265150467003	0.000	AT1G04620	-1.35215123942487	0.014
AT4G24930	-1.49761344030895	0.001	PHT2;1	-1.35107209129196	0.005
AT3G50685	-1.49420219919642	0.047	PSRP5	-1.34527893306164	0.004
TCH4	-1.49366755223348	0.043	AT4G11570	-1.34489862654284	0.017
AT5G08650	-1.49012050647051	0.025	AT5G57170	-1.34100698925479	0.000
HCF173	-1.48589535206170	0.016	TIFY7	-1.34042649874635	0.016
AT1G03440	-1.48307869539175	0.004	APG2	-1.33970852621806	0.001
AT5G06530	-1.48216071115815	0.001	AT3G15190	-1.33522184853234	0.003
AT2G21530	-1.47918518164113	0.027	ACS11	-1.33279311879027	0.007
AT1G14345	-1.47329915366952	0.000	AT1G29070	-1.33255964100898	0.000
AT2G17880	-1.47254061338005	0.007	TROL	-1.33033762182330	0.012

WRKY40	-1.47199203215239	0.001	AT3G54210	-1.32957062896892	0.000
FAD5	-1.47189574759739	0.001	AT5G28500	-1.32630292950197	0.000
AT2G44920	-1.4699674858734	0.003	AT5G37360	-1.32371024187363	0.015
WRKY49	-1.46701313269399	0.023	AT1G22330	-1.32217626774997	0.002
AT3G14820	-1.45289224346664	0.000	AT3G23840	-1.32011793044184	0.004
AT1G11340	-1.45210342892084	0.021	TPD1	-1.31699109543579	0.000
BCAT-1	-1.44341349942188	0.000	AT1G68400	-1.31428841100631	0.009
emb1473	-1.44313966493668	0.011	AT3G56140	-1.31306118970860	0.009
crr1	-1.44277736146400	0.005	AT5G13410	-1.31195809819764	0.002
BLH4	-1.44032606449451	0.017	HCF101	-1.31029993163356	0.022
TCP5	-1.43998211472160	0.000	LUT2	-1.31015597111651	0.020
AT5G52780	-1.43667538042883	0.000	APE1	-1.30292524900173	0.000
AT4G23890	-1.43270105555400	0.002	AT2G29170	-1.30245410567200	0.008
AT3G48390	-1.43043367314717	0.046	AT5G11950	-1.30047407487191	0.000
FTSH1	-1.42992018247943	0.000	TCP24	-1.29967638329880	0.0001
CIL	-1.42594896537748	0.002	GME	-1.29655516733187	0.015
RPS9	-1.42211294685071	0.000	BEH1	-1.29498334970618	0.004
AT4G12980	-1.41771788993562	0.030	AT3G01670	-1.29239759899332	0.010
GATA6	-1.41296784643029	0.018	AT3G18890	-1.29007228520677	0.011
ADG1	-1.41240320761746	0.001	LPA3	-1.28956483639277	0.012
AT1G69523	-1.40770073096082	0.036	APE2	-1.28771038538114	0.006
MPK12	-1.40750014490548	0.000	WOX1	-1.27643607144931	0.020
AT1G69160	-1.40184681870785	0.049	AT5G07020	-1.27381334494094	0.007
SULTR2;1	-1.38685521226302	0.000	PSAE-2	-1.2657427165482	0.007
AT3G54500	-1.38514626200363	0.001	ENP	-1.26013635843114	0.037
THM1	-1.38407116336093	0.044	ELIP2	-1.25911231683982	0.000
GLYR2	-1.38281612840939	0.001	AT5G54600	-1.25801583854174	0.022
AT2G42975	-1.38060792977497	0.002	AT3G22150	-1.25696235533876	0.000
AT3G50270	-1.37582271925465	0.018	DEG8	-1.25651926923968	0.016
HDS	-1.37524760392746	0.006	LCL1	-1.25591867463341	0.025
AT5G14970	-1.37516398612751	0.004	AT2G37030	-1.25320588834925	0.004
ATS1	-1.37270320208813	0.000	THX	-1.24195366067328	0.016
HDG2	-1.36701556827887	0.000	NGA2	-1.23951240649787	0.000
FAD6	-1.36691682978035	0.039	AT4G31390	-1.23744568339423	0.006
AT1G75460	-1.36198755910099	0.009	AT5G58660	-1.23726562240804	0.000
AT4G21570	1.06374364218224	0.002	SNRK2.9	1.06298141578633	0.015
AT3G15110	-1.2364228740401	0.004	AT2G35830	-1.08615428085277	0.031
AT3G05160	-1.23191567464967	0.001	AT5G56850	-1.08489924683431	0.033
AT2G34170	-1.23190128494481	0.002	AT3G01660	-1.08386458415268	0.006
PSB28	-1.22876035634258	0.007	LAX1	-1.07473001484149	0.000
AGL87	-1.22868007225339	0.009	UGT85A3	-1.07468423104795	0.005
emb1513	-1.22797906416610	0.000	AT5G59250	-1.07459618897666	0.010
AT1G20470	-1.22640207583947	0.000	AT5G42070	-1.07458311775982	0.004
AT3G26580	-1.22590348245331	0.031	AT4G01330	-1.07387352975211	0.001
RPL27	-1.21593309722954	0.00	SKL1	-1.07341313698486	0.005
NIT4	-1.21567881245128	0.00	CRR6	-1.07309349269646	0.000
AT1G33440	-1.20025651930055	0.031	AT3G11630	-1.06881535322443	0.029
AT4G09160	-1.19542258113482	0.001	AT5G41050	-1.06766726623534	0.045
AT4G27700	-1.19403974374121	0.026	AT4G14890	-1.06661617637549	0.033

CSR1	-1.19392663908707	0.001	AT2G44230	-1.06594575979327	0.018
AT4G17740	-1.18694306660221	0.007	AT1G29020	-1.06442109173762	0.021
AT1G64150	-1.18572238952468	0.004	AT1G18810	-1.06308942752231	0.037
AT1G74070	-1.17920888616662	0.000	AT5G08460	-1.06081033023978	0.000
AT5G02890	-1.17829607829443	0.003	AT3G10420	-1.05848972681744	0.000
APS3	-1.17650683770357	0.01	AT5G08050	-1.05596307474694	0.004
NP2699781	-1.17604516424295	0.001	BEH2	-1.05436627324618	0.000
SPP2	-1.17388836549991	0.035	PPC2	-1.05392214841239	0.002
AT5G19940	-1.1658295768688	0.001	SPCH	-1.05151046013410	0.030
AT1G03620	-1.16480429770697	0.004	GSTL2	-1.05109414550027	0.007
VTE1	-1.16427596240824	0.022	AT5G52960	-1.05071123622383	0.010
AT5G64380	-1.15890652533082	0.0001	OFP5	-1.04947714962828	0.039
MIPS1	-1.14855980737792	0.000	LON2	-1.04737315888203	0.044
GR	-1.14755469693905	0.047	IAA5	-1.04447851439714	0.000
ATAB2	-1.14495864617251	0.013	AT1G11300	-1.03831258687875	0.001
AT1G44000	-1.14076346580031	0.018	AT2G34060	-1.03562443182070	0.005
AT3G51760	-1.13796785232759	0.002	AT1G15410	-1.0340194182803	0.000
AT3G10840	-1.13227135897886	0.003	AT3G17930	-1.02322906900545	0.015
AT2G28605	-1.12835699710446	0.006	DWF4	-1.02164658380647	0.028
APS1	-1.1276928053302	0.000	AT5G06790	-1.02129573488204	0.002
AT5G13510	-1.12456448530657	0.002	IMD1	-1.02086252724307	0.013
ICE1	-1.12169869144947	0.037	SOB5	-1.01726520681662	0.003
AT1G66130	-1.12070798495529	0.014	Fes1B	-1.01383104874932	0.014
AT4G29020	-1.11968224720488	0.000	EGY2	-1.01283490899697	0.040
AT5G43870	-1.11933005031707	0.000	AT2G35800	-1.01077718779396	0.000
AT1G33600	-1.10817550814754	0.046	AT5G43190	-1.01019107186414	0.022
YSL1	-1.10789566021309	0.004	AT4G33440	-1.00809530980202	0.008
AT1G35420	-1.10773619692431	0.001	AT4G38650	-1.00668155550859	0.002
AT4G16410	-1.10657683509325	0.000	AT1G12440	-1.00302326384625	0.000
DEGP1	-1.10357342687238	0.001	TC369552	-1.00287959502738	0.004
AT2G45850	-1.1020294733018	0.000	AT5G46960	2.65709927635129	0.000
AT1G29450	-1.09968169775651	0.026	AT1G06350	2.64076829117203	0.000
AT3G01060	-1.09653119633463	0.000	CYP96A12	2.59875315781246	0.000
AT5G14260	-1.09503154860809	0.042	SAG29	2.58304782475721	0.009
NFU3	-1.09422786856035	0.000	JAL22	2.46621599167462	0.000
AT1G19620	-1.08743848098699	0.000	AT3G29970	2.36346721113405	0.033
AT4G38690	-1.08675445292401	0.003	PYD4	2.29581751215532	0.003
JAL31	1.06525841221900	0.007	AT2G38920	1.06391391764761	0.005
AT4G12170	2.28924687245237	0.000	AT3G46410	1.44229151814714	0.005
XTH32	2.24565877434863	0.000	AT2G37130	1.43826593157297	0.002
LTP6	2.21722950288237	0.015	AT2G38380	1.43768020518481	0.001
AT5G53730	2.18326692186964	0.000	AT2G22590	1.39755126856262	0.000
AT4G31330	2.17733395674527	0.0002	AT4G15680	1.3847312970471	0.029
AT4G29030	2.14551153983529	0.000	AT4G02740	1.38162725666760	0.02
MES9	2.05250646841616	0.005	AT1G66800	1.37123061417043	0.039
LOX1	2.04179661908042	0.000	CYP735A2	1.37049174397468	0.014
MES1	2.02765355447686	0.00	TLL1	1.36366073974158	0.045
MLP168	2.02330680124127	0.001	LEA14	1.34022804231225	0.024
AT1G29090	2.00742482756657	0.002	AT3G22550	1.33348082171433	0.004

AT4G33560	1.96143983496628	0.000	OFP7	1.31946203193387	0.026
AT4G10265	1.94100396298784	0.022	IQD25	1.31687190308517	0.036
AT1G70880	1.93723239430791	0.015	AT4G01700	1.31414736768744	0.016
AT1G62500	1.87739883871926	0.004	MIPS3	1.31029616641257	0.042
MES10	1.87137481735072	0.004	MYB7	1.30849618525718	0.006
MLP43	1.84808532244116	0.003	AT3G32980	1.29787053711813	0.002
GRP9	1.80405975772294	0.000	AT3G61930	1.29310138153593	0.015
scpl20	1.80178129879143	0.003	AT1G27030	1.29299787982552	0.001
AT4G16260	1.79790739021768	0.035	NAC003	1.28671806002612	0.0001
AT4G10270	1.79719730494135	0.003	AT3G57780	1.28238158303844	0.000
AT1G80160	1.78826525543889	0.002	LSH4	1.28100869756288	0.005
PRXCB	1.76902909181852	0.000	SAH7	1.27352005965750	0.01
AT2G14247	1.76900627482398	0.000	AT3G13175	1.27066764920076	0.003
AT3G18280	1.71657871276649	0.001	AT3G61900	1.26361856658903	0.000
AT1G52000	1.71075265943403	0.000	NP10421331	1.25312427300831	0.005
PGL2	1.70675496677298	0.000	AT4G16670	1.24982999874337	0.018
AT4G22870	1.70492407317320	0.005	NIP1;2	1.23921782693664	0.002
GSTF12	1.70378832697344	0.00	AT4G28040	1.22259191247054	0.003
AT5G22460	1.69879013230686	0.033	AT5G03230	1.21753028556427	0.018
AT5G14920	1.67433653690751	0.034	FRD3	1.19925594333165	0.021
E13L3	1.67398878926565	0.017	GSTU8	1.19115784847910	0.008
CYP705A12	1.62722910663151	0.000	AT5G44730	1.18530634814970	0.002
SPL8	1.61467114768336	0.005	CIPK16	1.18202524735423	0.005
AT2G14900	1.60916837494258	0.013	LCR69	1.15025600348762	0.027
KTI1	1.60428106818257	0.000	AT5G48480	1.14748753934927	0.034
AT3G10040	1.60018504909652	0.004	AT4G10260	1.14686017841507	0.001
LSH3	1.59519304093837	0.002	EXLB1	1.14020815985476	0.022
AT5G47600	1.592992927988	0.009	AT4G35060	1.14012393318913	0.029
AT3G22570	1.56960846989503	0.000	AT3G30390	1.13841521055643	0.007
CYP705A19	1.55341104040207	0.000	ARR6	1.13764743433700	0.026
LTI30	1.55217181697785	0.019	AT2G28680	1.13239347883993	0.028
AT2G28790	1.54086052746404	0.000	JR1	1.12483821976832	0.000
SRO5	1.54079056901517	0.024	NIC3	1.12458475732366	0.004
LDOX	1.53622528455626	0.036	PLA2-ALPHA	1.11495927905818	0.000
ETC1	1.53504445822455	0.035	POP1	1.09865398225797	0.012
PEL3	1.51780573857544	0.032	AT1G76790	1.09202149416592	0.015
AT3G19660	1.51738511464568	0.036	AT5G16360	1.08634700796474	0.006
SRG1	1.49623915672031	0.001	AT5MAT	1.08466288517525	0.046
AT2G47050	1.47325256511464	0.000	STM	1.08359667418676	0.010
ALDH2B7	1.45916542590620	0.038	AT5G05420	1.07306170419828	0.000
SULTR3;2	1.45130474612207	0.002	CYP81F4	1.06810505629059	0.024

Table 50 - List of differentially expressed genes as obtained by a comparative transcriptomics analysis between cotyledon-less (= *enp pid*) and wild type (L*er*) seedlings of *A.thaliana*